博士論文

Synthesis and Properties of Push-Pull Type Dipyrrins and Subporphyrazines

(Push-Pull 置換基を有するジピリンと
サブポルフィラジンの合成と物性)

梁　旭

平成 27 年

Doctor Thesis

Synthesis and Properties of Push-Pull Type Dipyrrins and Subporphyrazines

(Push-Pull 置換基を有するジピリンと

サブポルフィラジンの合成と物性)

Xu Liang

2015

Contents

Abbreviations

CD	Circular Dichorism
CT	Charge Transfer
DFT	Density Function Theory
FL	Fluorescence
ESI	Electrospray Ionization
GPC	Gel Permeation Chromatography
HOMO	Highest occupied Molecular Orbitals
HPLC	High Performance Liquid Chromatography
HR	High Resolution
ICT	Internal Charge Transfer
LUMO	Lowest unoccupied Molecular Orbitals
MCD	Magnetic Circular Dichorism
MO	Molecular Orbital
MS	Mass Spectrometry
NMR	Nuclear Magnetic Resonance
ORTEP	Oak Ridge Thermal-Ellipsolid
Pc	Phthalocyanine
Pz	Porphyriazine
SubPc	Subphthalocyanine
SubPz	Subporphyrazine
TOF	Time of Flight

Preview of This Thesis

This doctor thesis entitled "Synthesis and Properties of Push-Pull Type Dipyrrins and Subporphyrazines" was finished in the Department of Chemistry, Graduate School of Science, Tohoku University under the supervision of Prof. Dr. Nagao Kobayashi. This thesis described the design, synthesis, properties and theoretical calculations of a series of push-pull type chromophores, including push-pull type dipyrrins, subporphyrazines and porphyrazines. Some of measurements were finished in the research and analytical center for giant molecules in Tohoku University.

1.1 Background of Phthalocyanine Chemistry

An unidentified blue compound, which is now known to be metal-free phthalocyanine, was first reported in 1907.[1] In 1927, Swiss researchers accidentally synthesized copper phthalocyanine, copper naphthalocyanine, and copper octamethylphthalocyanine in an attempted conversion of *o*-dibromobenzene into phthalonitrile and further reacted with CuCl.[2] All these scientists were focused on the enormous stability of these complexes but did not further characterize these blue complexes. In the same year, copper phthalocyanine was also discovered at Scottish Dyes company and finally used as the commercial dyes or pigments.[3] Although phthalocyanine analogues have been investigated over 100 years, but the research interests covers all fields of phthalocyanine chemistry and application are still growing. It is because of phthalocyanine analogues preformed good properties in various high-tech fields,[4] including solar cells,[5] molecular electronics and photonics,[6] nonlinear optics,[7] photodynamic therapy (PDT),[8] and also electrocatalysis.[9] The compounds are stable and have relatively low reactivity due to their heteroaromatic-systems, and have been reported to have low toxicity.[10] Currently, there is interest in phthalocyanines in various diverse topics ranging from fundamental theory to industrial applications, since the -system can absorb and emit strongly in the red/near-infrared (NIR) due to the relatively high molar extinction of the lowest energy $\pi \rightarrow \pi^*$ band (usually referred to as the Q band), which is considerably more intense than the corresponding bands in the spectra of porphyrins and tetraazaporphyrins.[11]

One of the most interesting in this research filed is the spectroscopic investigations of phthalocyanine analogues. For example, most of free-base or metallo-phthalocyanines is that complexes that have the lowest lying absorption band (referred to as the Q band) in the 650~680 nm region.[12] Complexes with a Q band at the longer wavelength regions are usually preferred, because of chromophores with longer wavelength absorptions have great potential applications in various high-tech fields. Since the red-shift of the Q band reflects a decrease in the HOMO-LUMO gap,

and hence is often associated with a decrease in the first oxidation potential. There has been a strong focus on the design and synthesis of new highly stable phthalocyanine complexes with different electronic structures.[13] Although the phthalocyanine Q band can be shifted to longer wavelength through fused-ring-expansion with benzene rings to form naphthalocyanine (Nc)[14] and then anthracocyanine (Ac),[15] the marked destabilization of HOMO level makes these compounds unstable and in the absence of peripheral substituents there are also issues with solubility. In addition to design new phthalocyanine analogues with large substituents effect will be attracted.
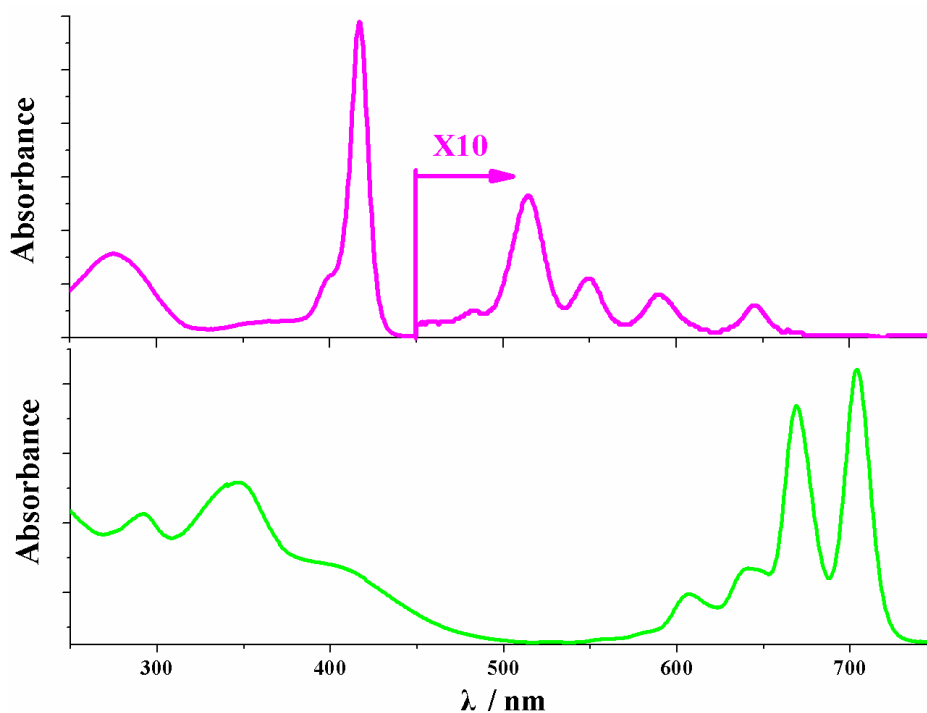
Figure 1-1 UV-vis absorption spectra of free base *meso*-tetraphenylporphyrin (up, pink) and free base beta,beta-diphenylphthalocyanine (bottom, green).

1.2 Brief Introduction of Push-Pull Chromophores

Push-pull chromophores, with strong electron donating substituents connected by conjugated molecules to strong electron withdrawing substituents, have been investigated for decades.[16] Nevertheless, interest in such systems is still growing, in view of their promising optoelectronic properties, such as large second[17] and third-

order nonlinear optical (NLO) effects,[18] and their potential for application as advanced functional materials in molecular devices.[19]   The guidelines for evaluating and tuning the HOMO-LUMO gap in strong push-pull chromophores will be provided. Whereas chromophore design, synthesis, and UV/vis measurements took place at different groups, especially the researches in ETH by dirich, the research of push-pull chromophores are mainly focused on the spectroscopic properties, electrochemical properties and the determination of nonlinear optical properties were performed in the various references.[20]

Chromophores with push- and pull-substituents generally exhibit the main absorption bands at the longer wavelength region relative to the chromophores without push- and pull-substituents.   It is because of introduction of electron donating (push-) substituents will destabilized both the HOMO orbitals and the LUMO orbitals, especially the HOMO orbitals will be destabilized.   In addition to introduce electron withdrawing (pull-) substituents to the porphyrinic chromophores, both the HOMO orbitals and the LUMO orbitals will be stabilized, especially the LUMO orbitals will be stabilized.   The decrease of the gap between the HOMOs and the LUMOs can be attributed to the introduction both electron donating (push-) substituents and electron withdrawing (pull-) substituents.
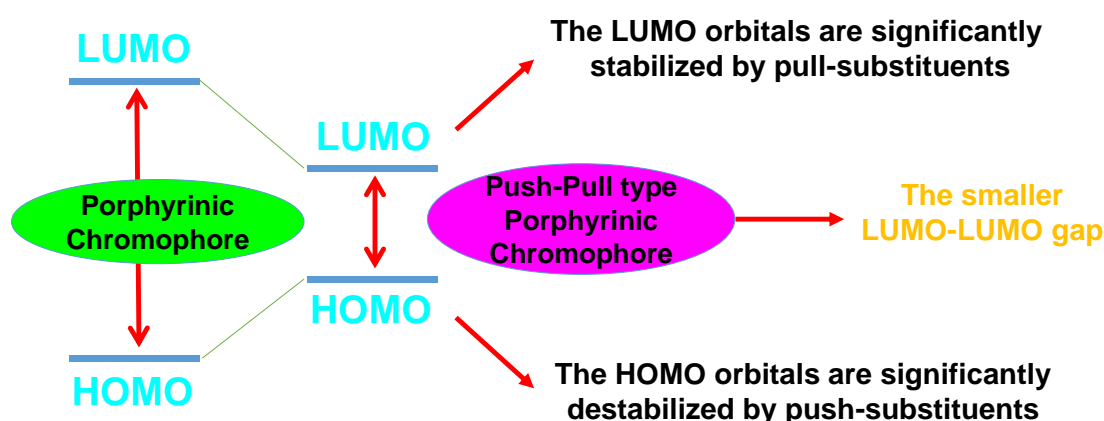
Figure 1-2 Concept of push-pull effect.

In 2014, F. Diederich reported a series of push-pull chromophores with various substituents.   Considering cyano units have strong electron withdrawing abilities, and the red-shift of main absorption bands can be explained as the increase of the electron donating (push-) abilities of aryl-substituents.[21]   Similar research have been well done by the same group and these push-pull chomorphores illustrated that control the main absorption bands can be achieved by introducing substituents which have a large perturbation on the electronic structures in a simple manner.[22]
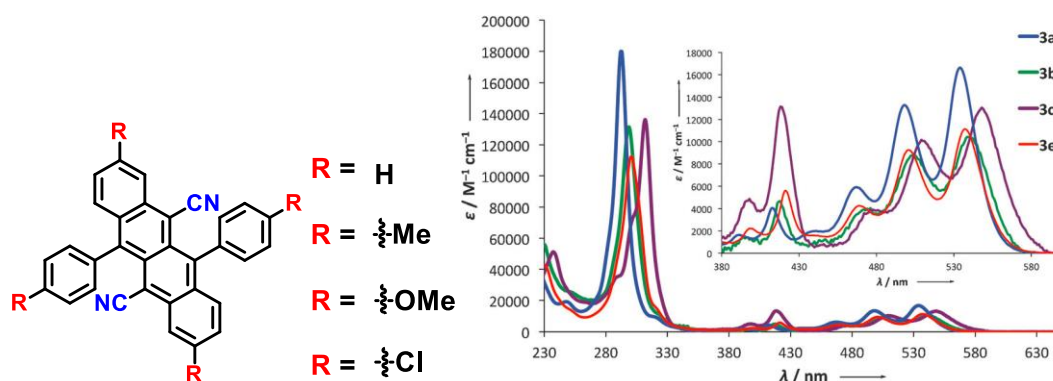
Figure 1-3 Molecular structures and absorption spectra of push-pull chromophores.

In the case of porphyrinic chromophores, the push-pull strategies are still effective in order to control the main absorptions.   Considering the substituents which directly connected to the chromophores have a large effect on the electronic structures, introduction of push-pull substituents to the beta-positions of porphyrinic chromophores have a large effect on the control of the electronic sturctures of porphyrinic chromophores.   It is well-known that nitro-substituent has strong electron-withdrawing effect, from the previous literatures, control the main absorption of push-pull type porphyrinic chromophores can be achieved not only the increase of the electron donating abilities of push-substituents (**Figure 1-4**, up), but also increase the number of the electron donating substituents (**Figure 1-5**, bottom).[23]
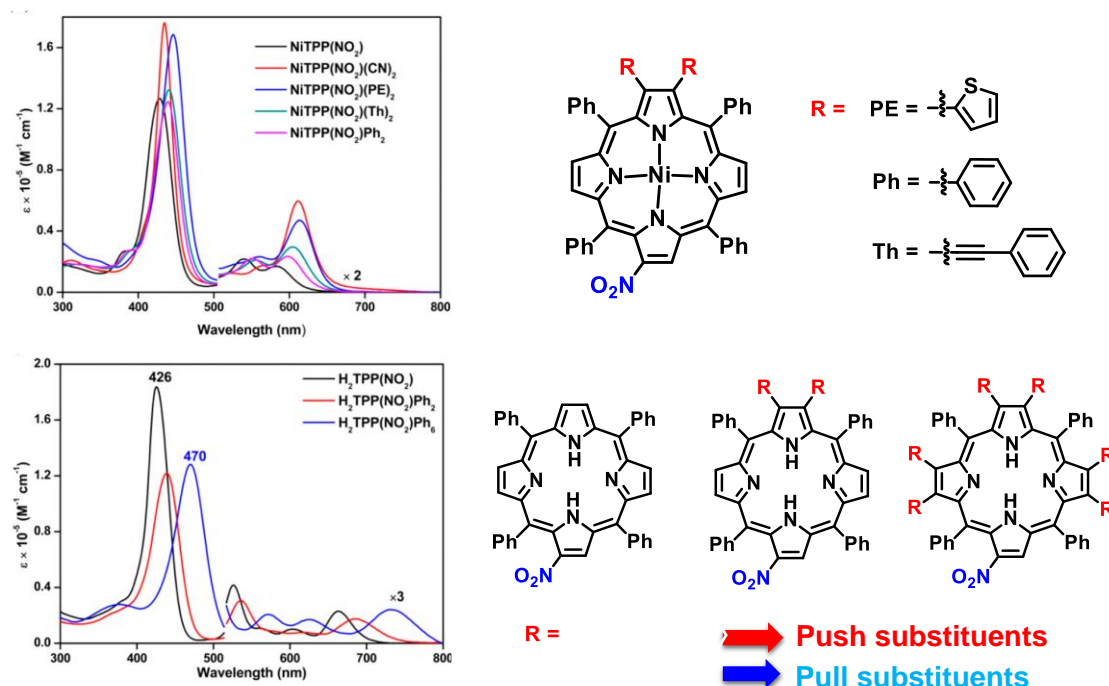
Figure 1-4 absorption spectra (left) and molecular structures (right) of push-pull chromophores.

The first example of the control of porphyrinoid chromophore symmetry based on the positional isomerism of peripheral push-pull substituents has been achieved by preparing tetraazaporphyrins (TAPs) with C_{4h}, D_{2h}, C_{2v}, and C_s symmetry due to the asymmetric arrangement of peripheral push-pull substituents, tert-butylamino and cyano groups, respectively. In addition to consider the large perturbation from push-pull substituents to the porphyrinic chromophores, the different spectroscopic properties were observed for all geometric isomers based on the asymmetric arrangement of push- and pull-substituents.[24]
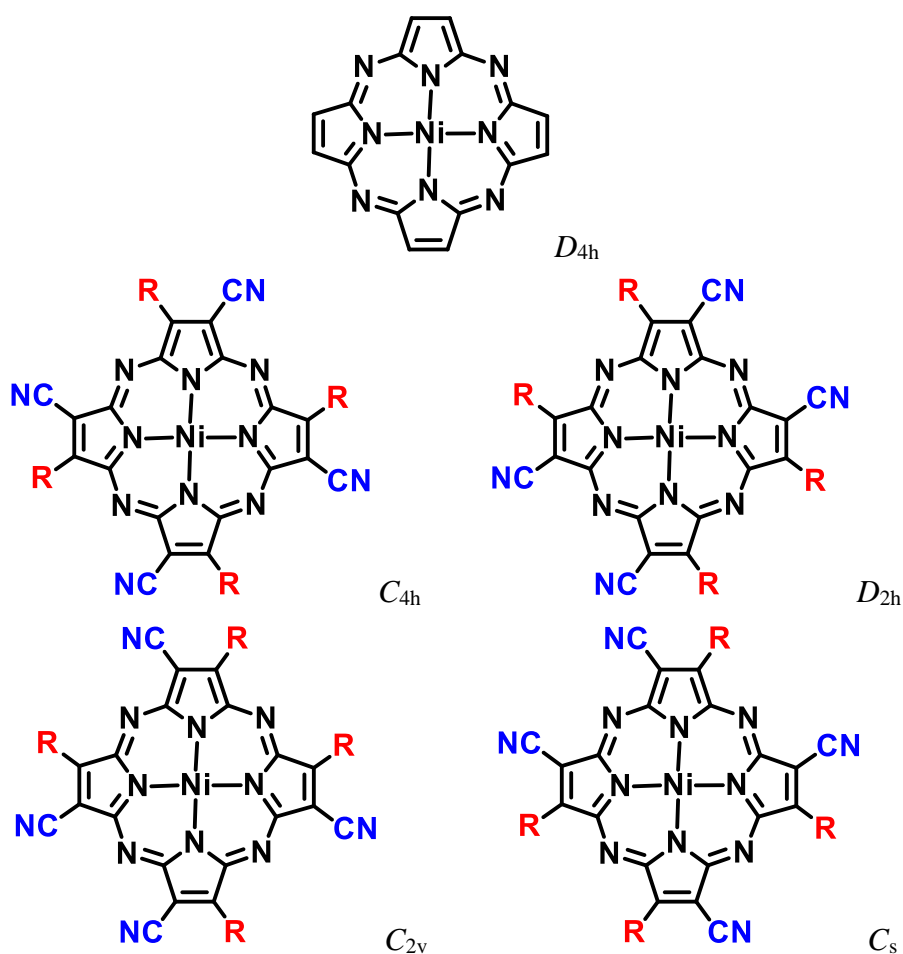
Figure 1-5 Molecular structure and chromophore symmetry of regular porphyrazine and push-pull type porphyrazines.

Thus, control the main absorption bands of chromophore can be successfully achieved by introduction of push-pull substituents in a simple manner. Design, synthesis, spectroscopic investigations of new push-pull chromophores may interesting for us, and this doctor thesis will be focused on the design, synthesis, spectroscopic properties investigations, theoretical calculations of new push-pull chromophores.

1.3 Basic theory of this study

1.3.1 UV-vis absorption

Absorption spectroscopy [25] refers to spectroscopic techniques that measure the absorption of radiation, as a function of frequency or wavelength, due to its interaction

with a sample. The Beer–Lambert law relates the attenuation of light to the properties of the material through which the light is traveling. The law is commonly applied to chemical analysis measurements and used in understanding attenuation in physical optics, for photons, neutrons or rarefied gases. In mathematical physics, this law arises as a solution of the BGK equation. The transmissivity (ability to transmit) is expressed in terms of an absorbance which is defined as:

$$A = -\ln\left(\frac{I}{I_0}\right). \quad \text{or} \quad A' = -10\log_{10}\left(\frac{I}{I_0}\right)(dB)$$

Considering push-pull substituents have large perturbation on the electronic structures, the UV-vis spectra will give direct evidence of the change of the electronic structures before and after introduction of push-pull substituents. Generally, the red-shift of the main absorption band on the UV-vis spectra is an evidence to consider the influence of push-pull effect.

1.3.2 MCD Theory

Magnetic Cicular Dichlorism (MCD) technique is based on the wavelength dependent absorption of circularly polarized light to form excited electronic states. The UV−vis absorption and MCD spectra of a molecular complex contain the same set of spectral bands, but the band morphologies are different due to the effect of the applied magnetic field and the use of a differential absorbance intensity scale from the CD spectrometer used for the measurements.[26]

1.3.2.1 Faraday A term

A derivative-shaped band, the so-called Faraday A term of either positive sign (positive lobe to higher energy of the crossover point) or negative sign (positive lobe to lower energy of the crossover point) appears when the excited states are degenerate, associated with absorption peaks. Thus, Faraday A terms are generally predicted only when the molecule possesses at least a three-fold axis of symmetry
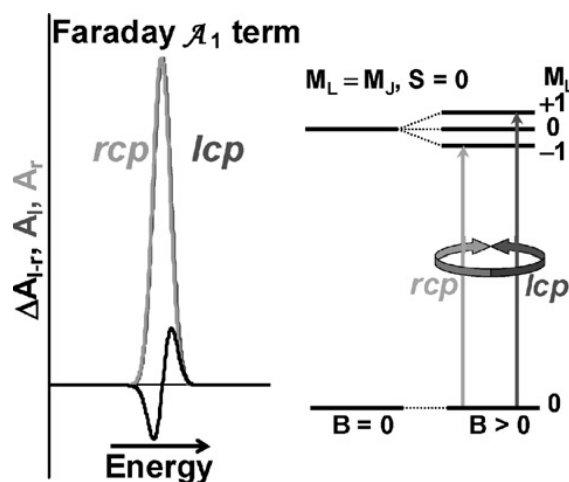
Figure 1-5 The spectral sharp of Faraday A_1 term on the MCD spectra.

1.3.2.2 Faraday B term and persudo Faraday A term

Faraday B terms, i.e. Gaussian-shaped bands of either positive or negative sign, are observed when an excited state is mixed with nearby transitions by the magnetic field, and have integral-type envelopes near the relevant absorption peaks. Interacting B terms give spectral envelopes of opposite sign.

Therefore, in the case of D2h or metal-free porphyrinoids, the two B terms lying under the two absorption components indicate that these are the symmetry-split x and y polarized transitions. When the energy splitting of the x and y polarized transitions is small, the observed MCD curve appears like a Faraday A term (this is called a pseudo-A term). However, the difference from the A term is that the negative and positive envelope positions are close to the two absorption peaks.
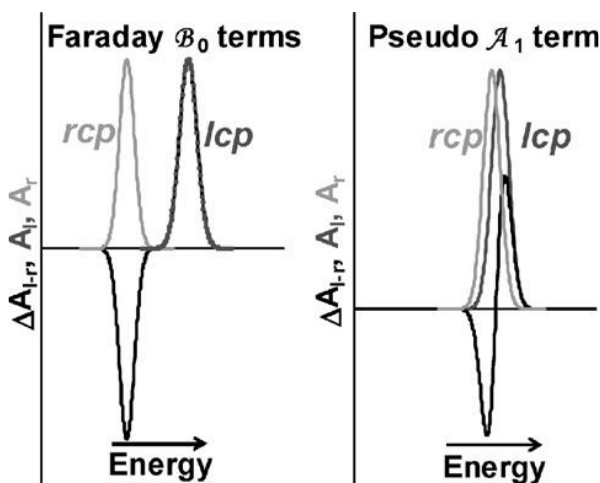
Figure 1-6 The spectral sharp of Faraday B_0 and pseudo A_1 term on the MCD spectra.

1.3.2.3 Faraday *C* term

Faraday *C* terms appear when the ground state is orbitally degenerate. Its shape is close to that of the Faraday B term, but its intensity is inversely proportional to the absolute temperature. Thus *C* terms have often been observed in organic radicals and metal complexes. Temperature dependence of the spectral intensities arises from the change in Boltzmann distribution across the split orbital components of the degenerate ground state.
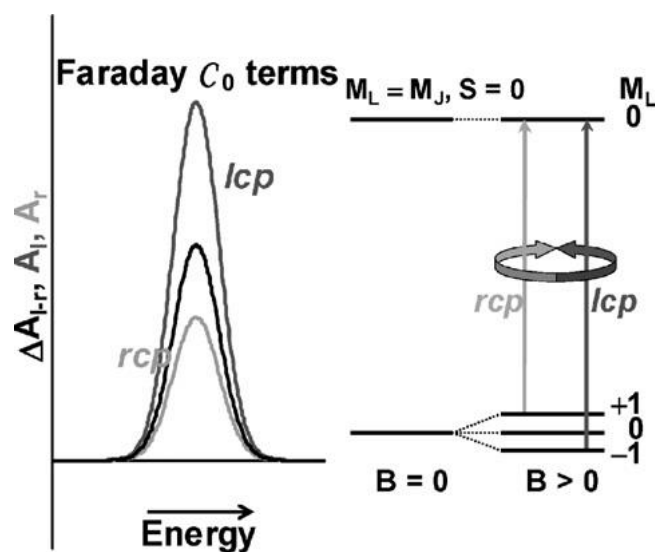
Figure 1-6 The spectral sharp of Faraday C_0 term on the MCD spectra.

1.4 Overview of This Thesis

From the previous reported literatures, push-pull effect can be more significant for small conjugated molecules. When push-pull effect is significant, even chromophore symmetry can be controlled. Porphyrinic chromophores with novel electronic structure may have potential applications in various high-tech fields. All of these advantages promote us design, synthesis new push-pull chromophores, and investigations on their electronic structures by spectroscopy and theoretical calculations.

In the chapter II, the synthesis, properties and theoretical calculations of push-pull type dipyrins will be described. Dipyrrins with push- and pull-substituents can be easily synthesized from pyrrole and related aryl-aldehyde. Control of the spectroscopic properties of push-pull type dipyrrins can be achieved by modification of push-substituents, and the push-pull dipyrrins with expanded molecular structure exhibit red-shift of the main absorption band.
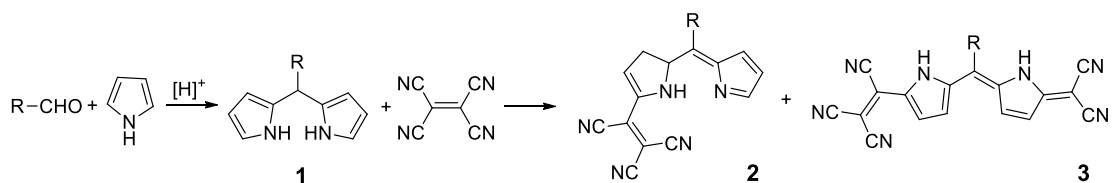
In the chapter III, the synthesis, properties and theoretical calculations of push-pull type subporphyrazine will be described. Push-pull type subporphyrazine can be easily synthesized from aryl-tricyanoethylene and boron(III)trichloride, and the spectroscopic properties can be controlled by push-pull effect. The significant red-shift of the main absorption bands arising from both destabilization of the HOMO orbitals and stabilizations of the LUMO orbitals by push-pull substituents. Based on the asymmetry arrangement of push- and pull-substituents and bowl shaped molecular structures of subporphyrazine, both diastereomers and enantiomers were observed and successfully separated.
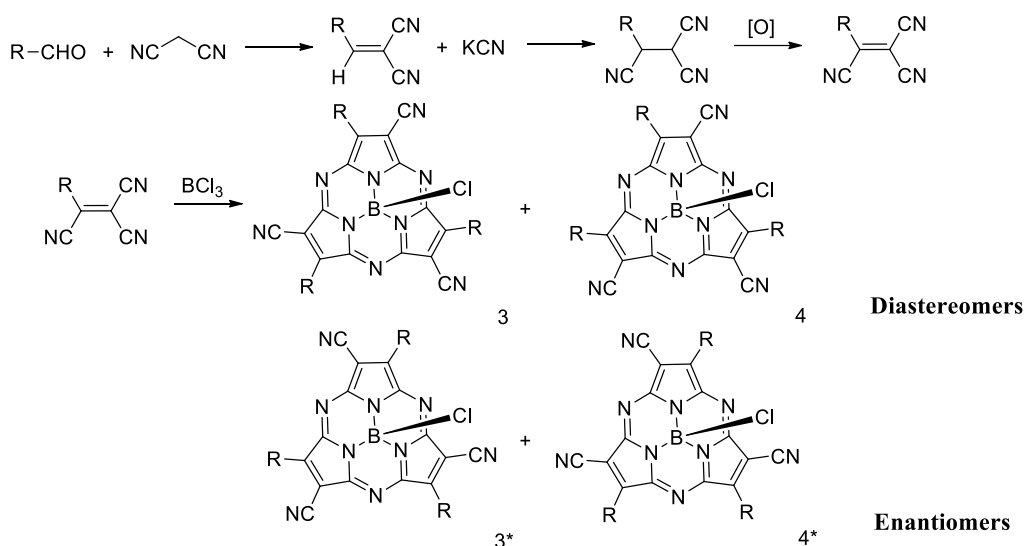
In the chapter IV, the synthesis of properties of push-pull type porphyrazine will be described. Push-pull type porphyrazine can be synthesized from tricyanoethylene in 1-butanol and the electronic structure was studied by spectroscopic analysis. Introduction of push-pull substituents to the porphyrazine causes the significant red-shift of the main absorption bands of porphyrazines, and the broad range of the absorptions covered all visible region.
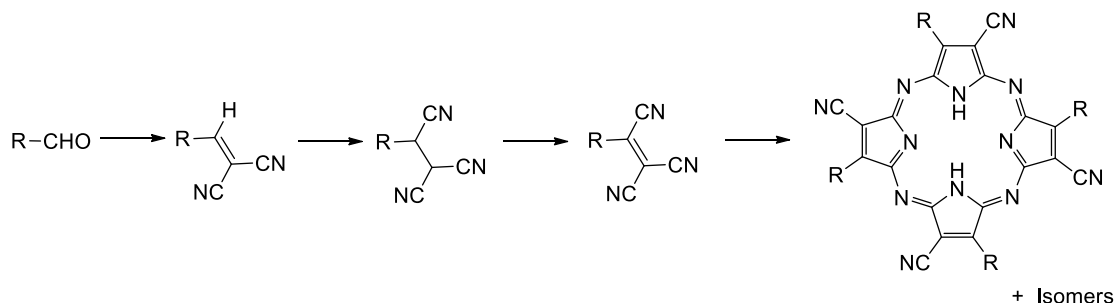
In the chapter V, the conclusion of design, synthesis, properties and theoretical calculations of push-pull type porphyrinic chromophores will be described. Considering small chromophores with red-shift and broad range of the main absorption bands are being required in the field of the photo-energy conversion, such as solar cell , the simple modifications of optical properties of dipyrrins, subporphyrazines and porphyrazines reveralled in this doctor thesis is useful for the design of fuctional molecules based on conjugated system of porphyrinic chromophores.

18

1.5 Reference

[1] Braun, A.; Tcherniac, J. *Berichte der deutschen chemischen Gesellschaft.* **1907**, *40*, 2709-2714.

[2] Diesbach, H. D.; Weid, E. V. D. *Helvetica Chimica Acta.* **1927**, *10*, 886-888.

[3] a) H_2-Phthalocyanine, CAS: 574-93-6; b) Cu(II)-phthalocyanine, CAS:147-14-8; c) Co(II)-phthalocyanine, CAS:3317-67-7.

[4] a) Mack, J.; Kobayashi, N. *Chem. Rev.* **2011**, *111*, 281-321. b) Claessens, C. G.; Hahn, U.; Torres, T. *Chem. Rec.* **2008**, *8*, 75-97.

[5] a) Wohrle, D.; Meissner, D. *Adv. Mater.* **1991**, *3*, 129. b) Rostalki, J.; Meissner, D. *Sol. Energy Mater. Sol. Cells* **2000**, *63*, 37. c) Koeppe, R.; Sariciftci, N. S.; Troshin, P. A.; Lyubovskaya, R. N. *Appl. Phys. Lett.* **2005**, *87*, 244102.

[6] a) Turek, P.; Petit, P.; Andre, J. J.; Simon, J.; Even, R.; Boudjema, B.; Guillaud, G.; Maitrot, M. *J. Am. Chem. Soc.* **1987**, *109*, 5119-5122. b) Jiang, J.; Kasuga, K.; Arnold, D. P. In *Supramolecular Photosensitive and Electroactive Materials* Nalwa, H. S., Ed.; Academic Press: New York, 2001; p 113. c) Ng, D. K. P.; Jiang, J. *Chem. Soc. Rev.* **1997**, *26*, 433-442. d) Jiang, J.; Liu, W.; Arnold, D. P. *J. Porphyrins Phthalocyanines* **2003**, *7*, 459-473. e) Chen, Y.; Su, W.; Bai, M.; Jiang, J.; Li, X.; Liu, Y.; Wang, L.; Wang, S. *J. Am. Chem. Soc.* **2005**, *127*, 15700-15701.

[7] a) de la Torre, G.; Vazquez, P.; Agullo-Lopez, F.; Torres, T. *Chem. Rev.* **2004**, *104*, 3723-3750. b) Flom, S. R. In *The Porphyrin Handbook*; Kadish, K. M., Smith, K. M., Guilard, R., Eds.; Academic Press: New York, 2003; Vol. 19, pp 179-190.

[8] Ben Hur, E.; Chan, W. S. In *The Porphyrin Handbook*; Kadish, K. M., Smith, K. M., Guilard, R., Eds.; Academic Press: New York, 2003; Vol. 19, pp 1-35.

[9] Nicholson, M. M. In *Phthalocyanine. Properties and Applications*; Lever, A. B. P., Leznoff, C. C., Eds.; VCH: New York, 1993; Vol. 3, pp 71-118.

[10] Rio, Y.; Rodriguez-Morgade, M. S.; Torres, T. *Org. Biomol. Chem.* **2008**, *6*, 1877-1894.

[11] a) Linstead, R. P.; Whalley, M. J. *J. Chem. Soc*. **1952**, 4839-4846. b) Shimizu, S.;

Haseba, Y.; Yamazaki, M.; Kumazawa, G.; Kobayashi, N. *Chem. Eur. J.* **2014**, *20*, 4822-4828. c) S. Shimizu, S.; Ito, Y.; Oniwa, K.; Hirokawa, S.; Miura, Y.; Matsushita, O.; Kobayashi, N. *Chem. Comm.* **2012**, *48*, 3851-3853.

[12] a) Fukuda, T.; Kobayashi, N. *In Handbook of Porphyrin Science;* Kadish, K.M., Smith, K. M., Guilard, R., Eds.; World Scientific: Singapore, 2010; Vol. 9, pp1-650. b) Nyokong, T. Struct. Bonding **2010**, *135*, 45. c) Muranaka, A.; Yonehara, M.; Uchiyama, M. *J. Am. Chem. Soc.* **2010**, *132*, 7844-7845. d) Rio, Y.; Rodriguez-Morgade, M. S.; Torres, T. *Org. Biomol. Chem.* **2008**, *6*, 1877-1894. e) Khene, S.; Geraldo, D. A.; Togo, C. A.; Limson, J.; Nyokong, T. *Electrochim. Acta* **2008**, *54*, 183-191. f) Fox, J. P.; Goldberg, D. P. *Inorg. Chem.* **2003**, *42*, 8181-8191.

[13] Kobayashi, N.; Furuyama, T.; Satoh, K. *J. Am. Chem. Soc.* **2011**, *133*, 19642-19645.

[14] Bradbrook, E. F.; Linstead, R. P. *J. Chem. Soc.* **1936**, 1739-1744. b) Mikhalenko, S. A.; Lukuyanets, E. A. *J. Gen. Chem. USSR* (Engl. Transl.) **1969**, *39*, 2495-2503. *Zh. Obshch. Khim.* **1969**, *39*, 2554-2558.

[15] Freyer, W.; Minh, L. Q. *Monatsh. Chem.* **1986**, *117*, 475-489.

[16] Gompper, R.; Wagner, H.-U. *Angew. Chem., Int. Ed.* **1988**, *27*, 1437–1455.

[17] Barlow, S.; Marder, S. R. Muller, T. J. J., Bunz, U. H. F., Eds.; Wiley-VCH: Weinheim, Germany, 2007; pp 393-437. Szablewski, M.; Thomas, P. R.; Thornton, A.; Bloor, D.; Cross, G. H.; Cole, J. M.; Howard, J. A. K.; Malagoli, M.; Meyers, F.; Bre´das, J.-L.; Wenseleers, W.; Goovaerts, E. *J. Am. Chem. Soc.* **1997**, *119*, 3144–3154.

[18] Tykwinski, R. R.; Gubler, U.; Martin, R. E.; Diederich, F.; Bosshard, C.; Gunter, P. *J. Phys. Chem. B* **1998**, *102*, 4451–4465.

[19] Forrest, S. R., Thompson, M. E., Guest Eds. *Chem. Rev.* **2007**, *107*, 923-1386.

[20] a) Tykwinski, R. R.; Diederich, F. *Liebigs Ann./Rec.* **1997**, 649–661. b) Tykwinski, R. R.; Schreiber, M.; Carlon, R. P.; Diederich, F.; Gramlich, V. *Helv. Chim. Acta* **1996**, *79*, 2249–2281. c) Nielsen, M. B.; Schreiber, M.; Baek, Y. G.; Seiler, P.; Lecomte, S.; Boudon, C.; Tykwinski, R. R.; Gisselbrecht, J.-P.; Gramlich, V.;

Skinner, P. J.; Bosshard, C.; Gunter, P.; Gross, M.; Diederich, F. *Chem. Eur. J.* **2001**, *7*, 3263–3280. d) Moonen, N. N. P.; Boudon, C.; Gisselbrecht, J.-P.; Seiler, P.; Gross, M.; Diederich, F. *Angew. Chem., Int. Ed.* **2002**, *41*, 3044–3047. e) Bures, F.; Schweizer, W. B.; May, J. C.; Boudon, C.; Gisselbrecht, J.-P.; Gross, M.; Biaggio, I.; Diederich, F. *Chem. Eur. J.* **2007**, *13*, 5378–5387.

[21] Gawel, P.; Dengiz, C.; Finke, A. D.; Trapp, N.; Boudon, C.; Gisselbrecht, J. P.; Diederich, F. *Angew. Chem. Int. Ed*. **2014**, *53*, 4341-4345.

[22] a) Kivala, M.; Diederich, D. *Acc. Chem. Res*. **2009**. *42*, 235-248. b) Finke, A. D.; Dumele, O.; Zalibera, M.; Confortin, D.; Cias, P.; Jayamurugan, G.; Gisselbrecht, J. P.; Boudon, C.; Schweizer, W. B.; Gescheidt, G.; Diederich F. *J. Am. Chem. Soc.* **2012**, *134*, 18139-18146. c) Jarowski, P. D.; Wu, Y. L.; Schweizer W. B.; Diederich, F. *Org. Lett.* **2008**, *10*, 3347-3350.

[23] a) Medforth, C. J.; Senge, M. O.; Smith, K. M.; Sparks, L. D.; Shelnutt, J. A. *J. Am. Chem. Soc*. **1992**, *114*, 9859-9869; b) Kumar, R.; Sankar, M. *Inorg. Chem.* **2014**, *53*, 12706-12719.

[24] a) Shimizu, S.; Haseba, Y.; Yamazaki, M.; Kumazawa, G.; Kobayashi, N. *Chem. Eur. J.* **2014**, *20*, 4822-4828**.** b) Kopranenkov, V. N.; Goncharova, L. S.; Luk'yanets, E. A. *Zh. Obshch. Khim.* **1979**, *49*, 1408 –1412.

[25] a) Schatz, P. N.; McCaffery, A. J. ; Suetaka, W.; Henning, G. N.; Ritchie, A. B.; Stephens, P. J.; *J. Chem. Phys.*, **1966**, *45*, 722-734; b) Henning, G. N.; McCaffery, A. J.; Schatz, P. N.; Stephens, P. J. *J. Chem. Phys.*, **1968**, *48*, 5656-5661.

[26] a) Mack, J.; Stillman, M. J.; Kobayashi, N. *Coord. Chem. Rev.* **2007**, *251*, 429–453. b) P. J. Stephens, *Adv. Chem. Phys.* **1976**, *35*, 197-264. c) Piepho, S. B.; Schatz, P. N. *Group Theory in Spectroscopy with Applications to Magnetic Circular Dichroism*, Wiley, New York, 1983. d) Kobayashi, N.; Muranaka, A.; Mack, J. *Circular Dichroism and Magnetic Circular Dichroism Spectroscopy for Organic Chemists*, RSC Publishing, 2012. e) Kobayashi, N.; Nakai K. *Chem. Commun.*, **2007**, 4077–4092.

Chapter II

Synthesis, Properties and Theoretical Calculations of Push-Pull Type Dipyrrins

2.1 Introduction

2.1.1 Chemistry of dipyrrins

Dipyrromethane is a key intermediate in the porphyrin synthesis and is easily synthesized from an acid-catalyzed reaction of pyrrole and aryl-aldehydes, and also possibly synthesized from Grignard reagent or InCl$_3$ catalyzed reactions.[1]
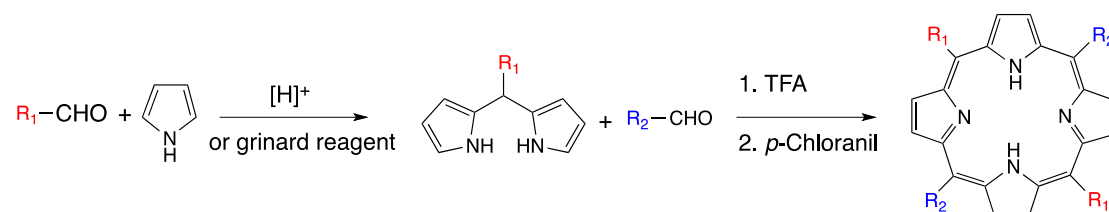
Scheme 2.1 Synthesis of *meso*-aryl-dipyrromethanes and porphyrins.

Development of reliable methods for the preparation of dipyrrins by oxidation of dipyrromethanes has became one of the most important advances in dipyrrin chemistry recently.[2]   But the dipyrrin is frequently utilized as a mono-valence bi-coordinated ligand having less academic attractions of itself as a functional chromophore molecule. *meso*-Aryl dipyrrin generally exhibits broad and featureless absorption in the higher-energy visible region at around 400 nm, which can be, however, tunable by introduction of substituents at appropriate positions to perturb its electronic structure.
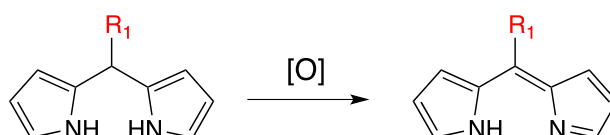
Scheme 2.2. Synthesis of aryl-dipyrrin.

2.1.2 Chemistry of boron(III)-dipyrrins (BODIPYs).

Research on the dipyrrin chemistry is mainly focus on the boron-[3] or metallo-coordinated[4] dipyrrins (BODIPYs), a structural analogue of the boron-porphyrins, have been the focus of considerable research interest over the last three decades and the synthesis of BODIPY dyes was firstly described by Treibs and Kreuzer in 1968.[5] Studies on this boron coordinated BODIPYs subsequently started to be used

extensively as laser dyes, fluorescent stains and labels in fluorescence imaging, and as indicator dyes in sensor applications.[6]   A simple BODIPY derivative, 1,3,5,7-tetramethyl-*meso*-phenyl-BODIPY (**Figure 2-1**) exhibits the narrow spectral bands and the mirror imaged emission band.   In addition to investigate the spectroscopic changes based on the structural modification of BODIPY derivatives, introduction of various functional substituents which containing different electron-donating abilities may cause the different shift of the main absorption bands (**Figure 2-2**).[7]
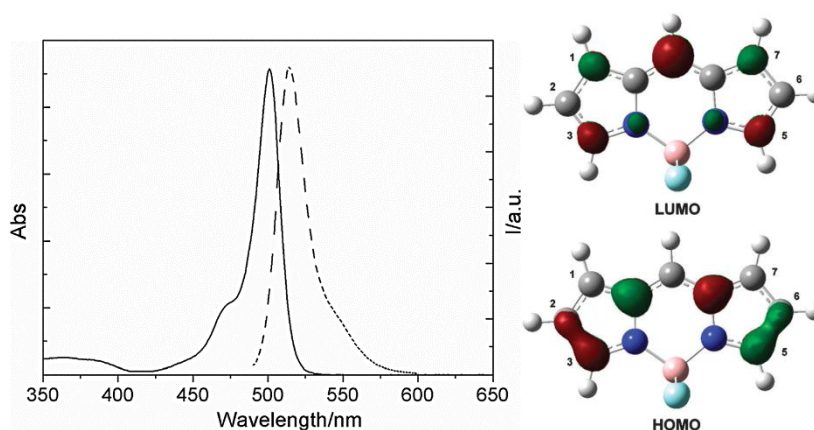
Figure 2-1 Absorption (solid line), fluorescence (dashed line) spectra and

TDDFT calculation of BODIPY.
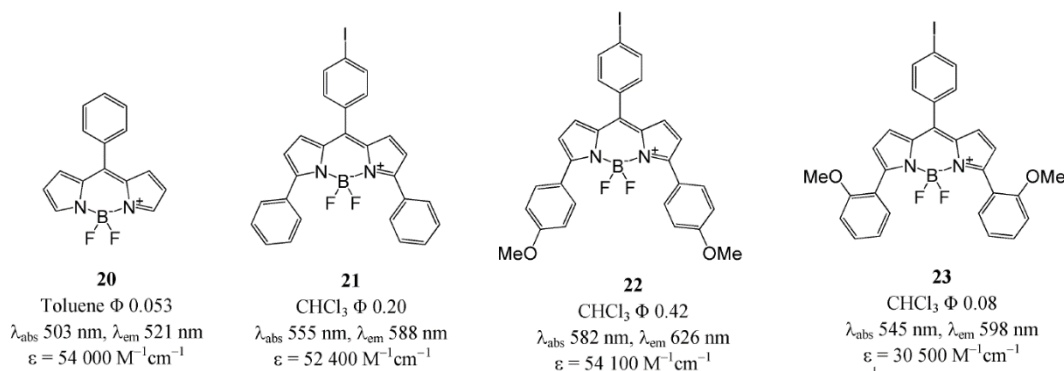
Figure 2-2 Structural modification and spectroscopic data of α-substituted BODIPYs.

2.1.3 Chemistry of Metallo-Dipyrrins

On the other hand, dipyrromethenes or dipyrrins can also be applied as useful ligands, Surprisingly, whereas many dpm based metal complexes have been reported for the construction of heterometallic architectures[8] as well as for their catalytic activity,[9] luminescent species have been much less investigated, in spite of the early

report by Falk and Neufingerl in 1979 on the photophysical properties of a Zn-dipyrrin complexes, and the fine determination of the molecular sturcure of Ni(II)-dipyrrin complexes.[10]
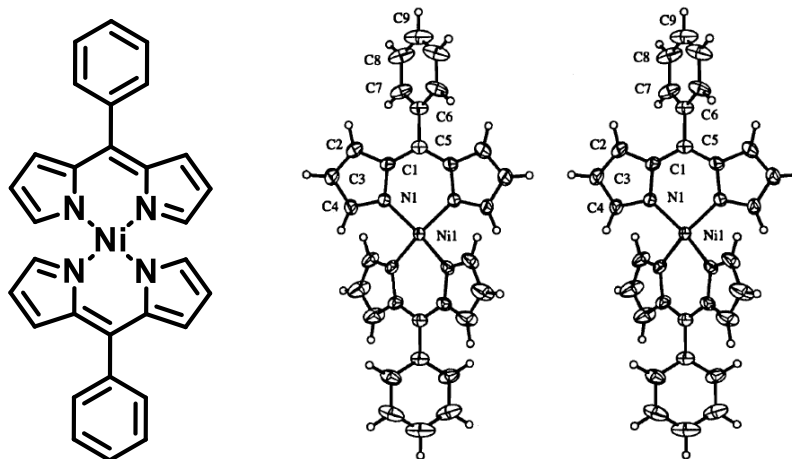
Figure 2-3 *meso*-phenyl Ni(II)-dipyrrin X-ray crystal structure.

Both boron(III)dipyrrin and metallo-dipyrrins have wide range of potential applications in various fields. This result lead chemists produced new dipyrrrin analogues with different electronic structures.   My research will focused on the design, synthesis, structural characterizations, spectroscopic properties studies, theoretical calculations of new dipyrrin derivatives have different electronic sturctures.

2.2 Propose of This Research

The boron-dipyrrin (BODIPY) and metallo-dipyrrin chemistry have been well progressed in the past decades, but studies on the chemistry of dipyrrins as chromophores have not been investigated in detailed. Considering introduction of electron donating (push-) and electron withdrawing (pull-) substituents have large contribution on the decrease of the gap between the HOMOs and the LUMOs, we would like to introduce electron donating (push-) and electron withdrawing (pull-) substituents to the dipyrrin core which can be easily synthesized from pyrrole and aryl-aldehyde. The studies on the electronic structure of these new push-pull dipyrrin derivatives by spectroscopic investigations and theoretical calculation will give useful information to in-depth understand the relationship between the observed spectroscopic properties and effect of push-pull substituents.

Push-Pull Dipyrrin

➡ **Push substituents**

➡ **Pull substituents**
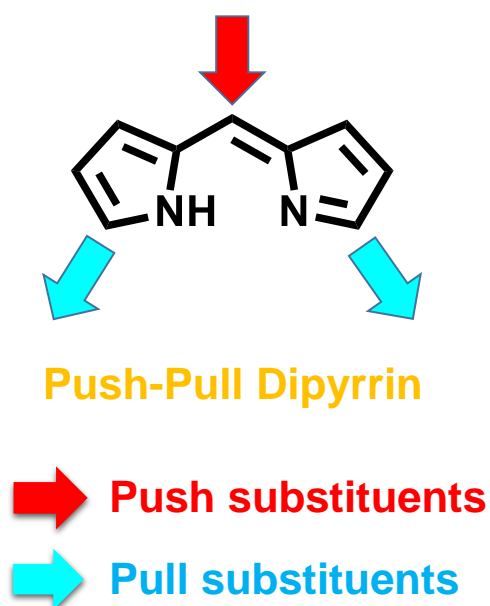
2.3 Experimental Section

2.3.1 Chemicals and Instruments

Electronic absorption spectra were recorded on a JASCO V-570 spectrophotometer. ^{1}H NMR and ^{1}H-^{1}H COSY spectra were recorded on a Bruker AVANCE III 500 spectrometer (operating at 500.13 MHz) or JEOL ECA-600 spectrometer (operating at 594.17 MHz) using residual solvents as an internal references for 1H (δ = 2.05 ppm for acetone-d_6, 5.32 ppm for CD_2Cl_2, and 7.26 ppm for $CDCl_3$). High-resolution mass spectra were recorded on a Bruker Daltonics Apex-III spectrometer or a Bruker Daltonics solariX 9.4T spectrometer. Preparative separations were performed by silica gel column chromatography (Merck Kieselegel 60H) and a recycling preparative GPC-HPLC (JAI LC-9210) with preparative JAIGEL-2H and 2.5H columns. All reagents and solvents were of commercial reagent grade and were used without further purification except where noted.

2.3.2 Crystallographic Data Collection and Structure Refinement

Crystallographic data collection and structure refinement: Suitable crystals for X-ray analysis were obtained from slow diffusion of hexane into an ethylacetate solution of 3e. Data collection was carried out at −173(2) ℃ on a Bruker APEXII CCD diffractometer with MoKa radiation (λ = 0.71073 Å). The structure was solved by a direct method (SHLEXS-971) and refined using a full-matrix least squares technique (SHELXL-97).[11] Yadokari-XG[12] software was used as a GUI for SHELXL-97. Solvent molecules were severely disordered and as we were unable to model them satisfactorily, the structure of 3e was refined without the effect of the solvent molecules by using the PLATON SQUEEZE technique.[13]

2.3.3 Computational Methods

Computational methods: The Gaussian 09[14] software package4 was used to carry out DFT and TDDFT calculations using the B3LYP functional and 6-31G(d) basis sets. Structural optimization was performed on model compounds of **2a**, **2d**, **3a**, **3d** and *meso*-phenyl dipyrrin **4**.

2.3.4 Synthesis of Push-Pull Type Dipyrrins
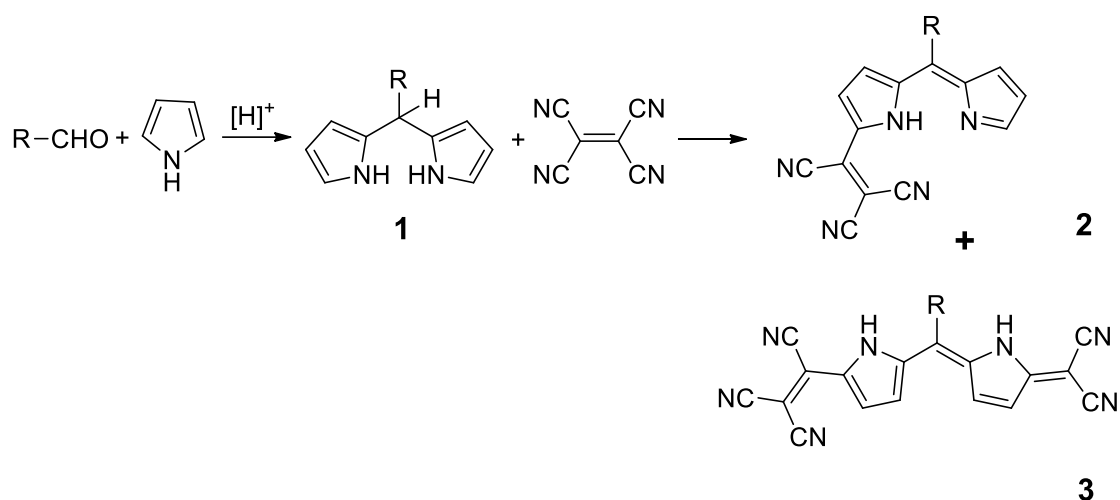
Scheme 2.3 Synthesis of push-pull type diyprrins.

General synthetic procedure was shown in **Scheme 2-1**. To a mixture of arylaldehyde (1 mmol) and freshly distilled pyrrole (0.5 mL) was added trifluoroacetic acid (50   L), the resultant mixture was stirred at room temperature for 30 min under N_2.   After removing the unreacted pyrrole, the residue was purified on silica-gel column using chloroform as an eluent to provide meso-aryl-substituted dipyrromethane 1 in about 20–25% yields.   Then **1** was dissolved in pyridine (2 mL), and tetracyanoethylene (64 mg, 0.5 mmol, 2.0 eq) was added.   The resultant mixture was heated at 60 ℃ for 15 min under air to provide **3** and in the case of **1c** and **1d**, **2c** and **2d** were also successfully isolated.   **2** and **3** were purified by silica gel column chromatography and recycling GPC-HPLC.   **3** was finally obtained in a pure form by recrystallization from ethylacetate and hexane.

Synthesis of 1a. To a mixture of benzaldehyde (1 mmol) and freshly distilled pyrrole (0.5 mL) was added trifluoroacetic acid (TFA, 50 μL). The resultant mixture was stirred at room temperature for 30 min under N_2. After removing the unreacted pyrrole, the residue was purified by silica gel column using chloroform as an eluent to provide *meso*-aryl-substituted dipyrromethane **1** in about 20–25% yields.

Synthesis of **2** and **3**. Then **1** was dissolved in pyridine (2 mL), and tetracyanoethylene (64 mg, 0.5 mmol, 2.0 eq) was added. The resultant mixture was heated at 60 ℃ for 30 min under air to provide **3**, and in the case of **2a** and **2d**, **3a** and **3d** were also obtained. **2** and **3** were purified by silica gel column chromatography and recycling GPC-HPLC. **3** was finally obtained in a pure compound by recrystallization from ethyl acetate and hexane.

Synthesis of 2c: **2c** was obtained from the reaction mixture in the synthesis of **3c**. Purification by silica gel column chromatography using $CHCl_3$ as an eluent provided **2c**, which was further purified by recycling GPC-HPLC ($CHCl_3$, detection at 540 nm). **2c** was obtained in 14% yield (7.7 mg). HR-ESI-FT-ICR-MS (*m/z*): 365.3303 (calcd for $C_{20}H_9N_6O_2 = 365.3305$ [M –H]); ^{1}H NMR (CD_2Cl_2, 500 MHz, 298 K): $\delta = 9.92$ (br s, 1H; NH), 8.02 (d, 1H; $J = 7.1$ Hz; phenyl), 7.64 (dd, 1H, $J_1 = 7.1$ Hz, $J_2 = 8.1$ Hz; phenyl), 7.54 (d, 1H, $J = 8.1$ Hz; phenyl), 7.32-7.30 (m, 2H; phenyl and pyrrole β-CH), 7.23 (br s, 1H; pyrrole α-CH), 6.94 (br s, 1H; pyrrole β-CH), 6.39 (d, 1H, $J = 3.5$ Hz; pyrrole β-CH), 6.36 ppm (d, 1H, $J = 3.5$ Hz; pyrrole β-CH); UV/vis (CH_3Cl): λ_{max} [nm] ($\varepsilon\,M^{-1}cm^{-1}$) = 531 (25000).

Synthesis of 2d: 2d was obtained from the reaction mixture in the synthesis of **3d**. Purification by silica gel column chromatography using $CHCl_3$ as an eluent provided **2d**, which was further purified by recycling GPC-HPLC ($CHCl_3$, detection at 655 nm). **2d** was obtained in 15% yield (5.1 mg). HR-ESI-FT-ICR-MS (*m/z*): 363.1362 (calcd

for $C_{22}H_{15}N_6 = 363.1363$ [M^--H]); ^{1}H NMR (CDCl$_3$, 600 MHz, 298 K): $\delta = 7.73$ (br s, 1H; pyrrole α-CH), 7.56 (d, 2H; $J = 7.2$ Hz, phenyl), 7.11 (d, 1H, $J = 4.2$ Hz; pyrrole β-CH), 7.06 (d, 1H, $J = 4.2$ Hz; pyrrole β-CH), 6.96 (d, 1H, $J = 4.2$ Hz; pyrrole β-CH), 6.81 (d, 2H, $J = 7.2$ Hz; phenyl), 6.59 (d, 1H; $J = 4.2$ Hz, pyrrole β-CH), 3.16 ppm (s, 6H; -NMe$_2$).   UV/vis (CHCl$_3$): λ_{max} [nm] (ε) = 339 (16400), 398 (5880), 655 (39700).

Synthesis of 3a: Column chromatography was preformed by silica gel column (ethyl acetate/CHCl$_3$ = 1:1).   **3a** was obtained as a blue solid in 10% yield (5.8 mg).   HR-ESI-FT-ICR-MS (*m/z*): 384.1001 (calcd for $C_{23}H_{10}N_7 = 384.1003$ [M^--H]$^-$); ^{1}H NMR (acetone-d_6, 500 MHz, 298 K): $\delta = 12.50$ (br s, 1H; NH), 12.10 (br s, 1H; NH), 7.52-7.48 (m, 5H; phenyl), 6.99 (br s, 1H; pyrrole β-CH), 6.87 (d, 1H, $J = 4.5$ Hz; pyrrole β-CH), 6.77 (br s, 1H; pyrrole β-CH), 6.33 ppm (d, 1H, $J = 4.5$ Hz; pyrrole β-CH); UV/vis (MeOH): λ_{max} [nm] (ε / M^{-1}cm^{-1}) = 405 (31800), 644 (16600).

Synthesis of 3b: Column chromatography was preformed by silica gel column (ethyl acetate/CHCl$_3$ = 1:1).   **3b** was obtained as a blue solid in 8.7% yield (5.4 mg).   HR-ESI-FT-ICR-MS (*m/z*): 414.1106 (calcd for $C_{24}H_{12}N_7O = 414.1108$ [M^--H]); ^{1}H NMR (acetone-d_6, 500 MHz, 298 K): $\delta = 12.49$ (br s, 1H; NH), 12.09 (br s, 1H; NH), 7.39 (d, 2H, $J = 8.5$ Hz; phenyl), 7.06 (d, 2H, $J = 8.5$ Hz; phenyl), 6.99 (br s, 1H; pyrrole β-CH), 6.92 (br s, 1H; pyrrole β-CH), 6.76 (br s, 1H; pyrrole β-CH), 6.37 (br s, 1H; pyrrole β-CH), 3.89 ppm (s, 3H; -OMe); UV/vis (MeOH): λ_{max} [nm] (ε) = 415 (36500), 647 (17800).

Synthesis of 3c: Column chromatography was preformed by silica gel column (ethyl acetate/CHCl$_3$ = 1:1).   **3c** was obtained as a blue solid in 15% yield (9.9 mg).   HR-ESI-FT-ICR-MS (*m/z*): 429.0851 (calcd for $C_{23}H_9NO_2 = 429.0854$ [M^--H]); ^{1}H NMR (acetone-d_6, 500 MHz, 298 K): $\delta = 12.38$ (br s, 1H; NH), 11.93 (br s, 1H; N-H), 8.17 (d, 1H, $J = 7.5$ Hz; phenyl), 7.88 (dd, $J_1 = J_2 = 7.5$ Hz, 1H; phenyl), 7.80 (dd, $J_1 = J_2 = 7.5$

Hz, 1H; phenyl), 7.64 (d, 1H, J = 7.5 Hz; phenyl), 6.95 (br s, 1H; pyrrole β-CH), 6.77 (br s, 2H; pyrrole β-CH), 6.13 ppm (d, 1H, J = 4.0 Hz; pyrrole β-CH); UV/vis (MeOH): λ_{max} [nm] (ε) = 403 (28900), 641 (18400).

Synthesis of 3d: Column chromatography was preformed by silica gel column (ethyl acetate/CHCl$_3$ = 1:1).   **3d** was obtained as a blue-violet solid in 2.7% yield (1.7 mg). HR-ESI-FT-ICR-MS (m/z): 427.1422 (calcd for C$_{25}$H$_{15}$N$_8$ = 427.1425 [M^-–H]); ^{1}H NMR (acetone-d_6, 500 MHz, 298 K): δ = 12.52 (br s, 1H; NH), 12.11 (br s, 1H; NH), 7.30 (d, 2H, J = 8.5 Hz; phenyl), 6.99 (br s, 2H; pyrrole β-CH), 6.84 (d, 2H, J = 8.5 Hz; phenyl), 6.73 (br s, 1H; pyrrole β-CH), 6.45 (br s, 1H; pyrrole β-CH), 3.05 ppm (s, 6H; -NMe$_2$); UV/vis (MeOH): λ_{max} [nm] (ε) = 403 (29600), 477 (19600), 655 (18900).

Synthesis of 3e: Column chromatography was preformed by silica gel column (ethyl acetate/CHCl$_3$ = 1:1).   **3e** was obtained as a green solid in 7.3% yield (4.8 mg).   HR-ESI-FT-ICR-MS (m/z): 434.1157 (calcd for C$_{27}$H$_{12}$N$_7$ = 434.1159 [M^-–H]); ^{1}H NMR (acetone-d_6, 500 MHz, 298 K): δ = 12.50 (br s, 1H; NH), 12.04 (br s, 1H; N-H), 8.05 (d, 1H, J = 8.0 Hz; naphthyl), 8.00 (d, 1H, J = 8.0 Hz; naphthyl), 7.73 (d, 1H, J = 8.0 Hz; naphthyl), 7.63 (dd, 1H, J_1 = J_2 = 8.0 Hz; naphthyl), 7.56-7.51 (m, 2H; naphthyl), 7.44 (dd, 1H, J_1 = J_2 = 8.0 Hz; naphthyl), 6.88 (br s, 1H; pyrrole β-CH), 6.72 ppm (br s, 1H; pyrrole β-CH), 6.58 (d, 1H, J = 4.5 Hz; pyrrole β-CH), 5.93 ppm (d, 1H, J = 4.5 Hz; pyrrole β-CH); UV/vis (MeOH): λ_{max} [nm] (ε) = 405 (30000), 641 (19700).

Synthesis of 3f: Column chromatography was preformed by silica gel column (ethyl acetate/CHCl$_3$ = 1:1).   **3f** was obtained as a green solid in 6.0% yield (4.4 mg).   HR-ESI-FT-ICR-MS (m/z): 484.1314 (calcd for C$_{31}$H$_{14}$N$_7$ = 484.1316 [M^-–H]); ^{1}H NMR (acetone-d_6, 500 MHz, 298 K): δ = 12.59 (br s, 1H; N-H), 12.10 (br s, 1H; N-H), 8.73 (s, 1H, anthryl), 8.16 (d, 2H, J = 8.5 Hz; anthryl), 7.85 (d, 2H, J = 7.5 Hz; anthryl), 7.52 (d, 2H, J = 7.5 Hz; anthryl), 7.45 (d, 2H, J = 7.5 Hz; anthryl), 6.82 (br s, 1H; pyrrole β-

CH), 6.67 (br s, 1H; pyrrole β-CH), 6.23 (d, 1H, J = 5.0 Hz; pyrrole β-CH), 5.65 ppm (d, 1H, J = 5.0 Hz; pyrrole β-CH); UV/vis (MeOH): λ_{max} [nm] (ε) = 405 (29600), 642 (15500).

2.4 Results and Discussions

2.4.1 ^{1}H NMR

^{1}H NMR spectra of **3e** in acetone-d_6 reveals four protons at δ = 6.88, 6.72, 6.58, 5.93 ppm from β-positions of pyrrole rings, and seven protons from napthyl-rings indicate the two electron-withdrawing substituents were introduced at a-positions of pyrrole rings with a low molecular symmetry. In the case of ^{1}H NMR spectra of **2d** in CDCl₃, four protons from phenyl rings, and five protons from pyrrole rings indicate the mono-substituted molecular structure.   In addition to confirm the proton signal at δ = 7.73 ppm of **2d** by H-H COSY measurement and it can be assigned as the alfa-proton of pyrrole which was not appeared in the case of **3e**.
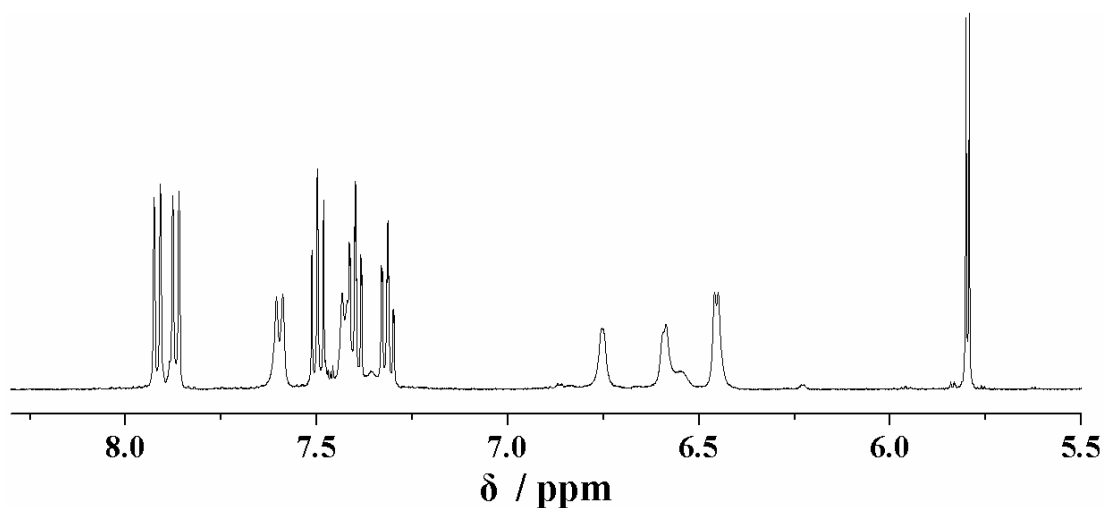

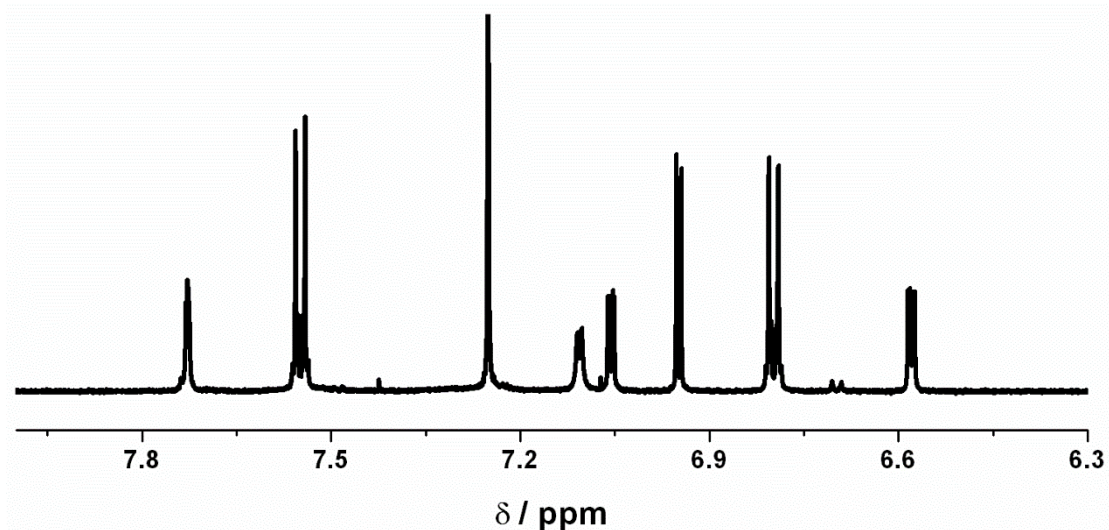**Figure 2-5** ^{1}H NMR spectra of **3e** in acetone-d_6

Figure 2-6 ^{1}H NMR spectra of **2d** in CDCl$_3$

2.4.2 Crystal structure for 3e

The suitable crystal was obtained by slow difssion a **3e** ethylacetate solution into hexane at toom temperature and structure of **3e** was finally explicitly elucidated by X-ray analysis on single crystals, the view of the crystal structure was shown in **Figure 2-7** and the crystal data was summarized in the **Table 2-1**. Both of the pyrrole rings in **3e** possess N-H hydrogen atoms, which cause an inverted arrangement of the pyrrole rings with respect to those of dipyrrins due to the repulsion between the NH atoms. The pyrrole rings are slightly tilted to each other with a dihedral angle of 25 °, whereas the tricyanovinyl unit and the dicyanomethylene unit are almost co-planar with the neighboring pyrrole rings. A double bond nature of dicyanomethylene unit was observed from the bonding distances of 1.380(7)Å, and the expanded π-conjugated system through the tricyanovinyl unit was also inferred from the rather short C-C bonding distance of 1.410(6) Å between the α-carbon atom of the pyrrole ring and the tricyanovinyl carbon atom.

Table 2-1: Crystallographic data for **3e**:

Empirical formula $\qquad$ $C_{27}H_{13}N_7$

Formula Weight $\qquad$ 385.12

Crystal system $\qquad$ monoclinic

Lattice parameter $\qquad$ $a = 39.777(12)$ Å, $b = 11.229(3)$ Å, $c = 14.209(4)$ Å;

$\qquad\qquad\qquad\qquad$ $\beta = 108.523(4)\,°$, $V = 6017.76(300)$ Å^3,

Space group $\qquad$ $C2/c$

Z value $\qquad$ $Z = 8$;

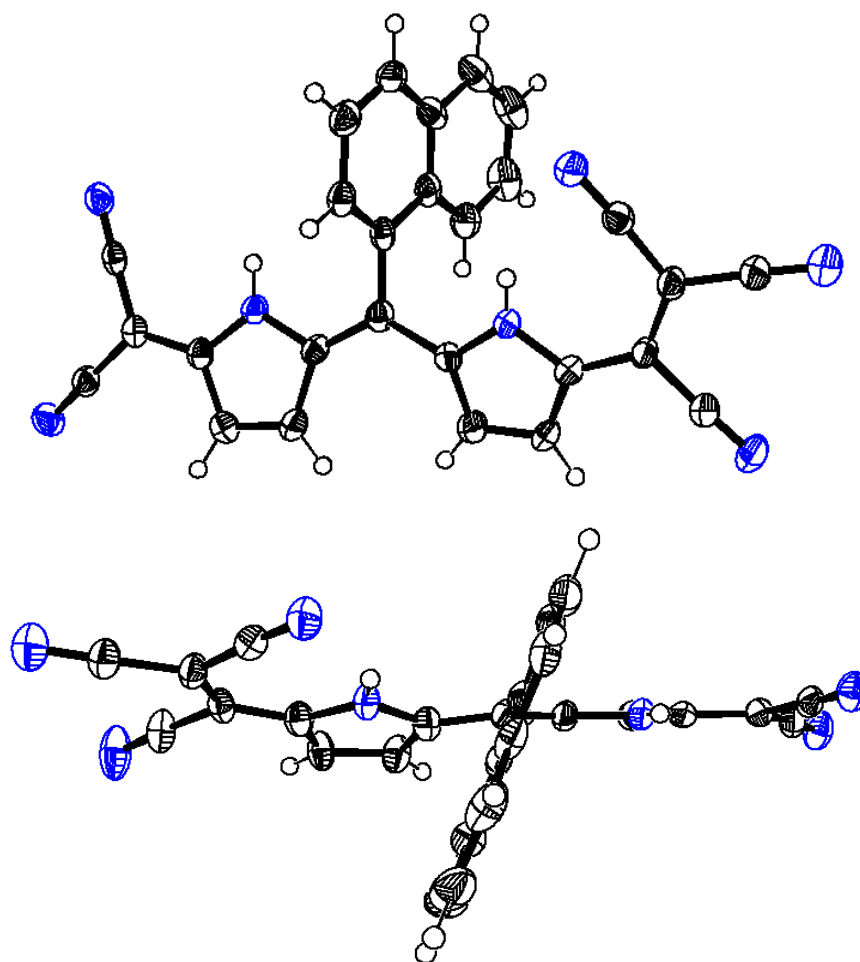Residuals: R; R$_w$ $\qquad$ $R = 0.0980$; $R_w = 0.334$

Figure 2-7. Crystal structure of **3e**, top view (top) and side view (bottom). The thermal elipsolids are scaled to the 50% probability level. Solvent molecules were omitted for clarity.

2.4.3 Spectroscopic Properties

The UV-vis absorption spectra of a-tricyanovinyl substituted **2c** and **2d** exhibited rather intense and sharp absorption in the lower-energy region at 531 for **2c**, and 655 nm for **2d**. Compared with the regular *meso*-phenyl-substituted dipyrrin **4** as a reference compound (**Figure 2-8**), the significant red-shift from **4** to **2c** (about 99 nm) and **2d** (about 223 nm) was observed. Considering *meso-o*-nitrophenyl substituent has the minor perturbation on the electronic structure of **2c**, the strong pull-substituent tricyanovinyl unit at the α-position has a large effect on the red-shift of the main absorption band.   In addition to consider the further red-shift in the case of **2d**, the *meso-N,N*-dimethylaminophenyl substituent has a strong electron donating ability which significantly destabilized the HOMO orbitals.

The expanded dipyrrin **3** exhibited significantly different absorption spectra compared with that of **2** and regular dipyrrin **4**, two intense bands at around 400 and 640 nm (**Figure 2-9**). Similar absorption spectra of a series of **3** indicate a small effect of the *meso*-substituent on the electronic structures of **3** due to the moderately tilted arrangement of the *meso*-substituents from the dipyrrin moiety (ca. 64 °for **3e** in the crystal structure).   In the case of **3d**, strong electron donating substituent *meso-N,N*-dimethylaminophenyl was introduced, an extra absorption at 477 nm was exceptionally observed and the absorption spectra covered all visible region.
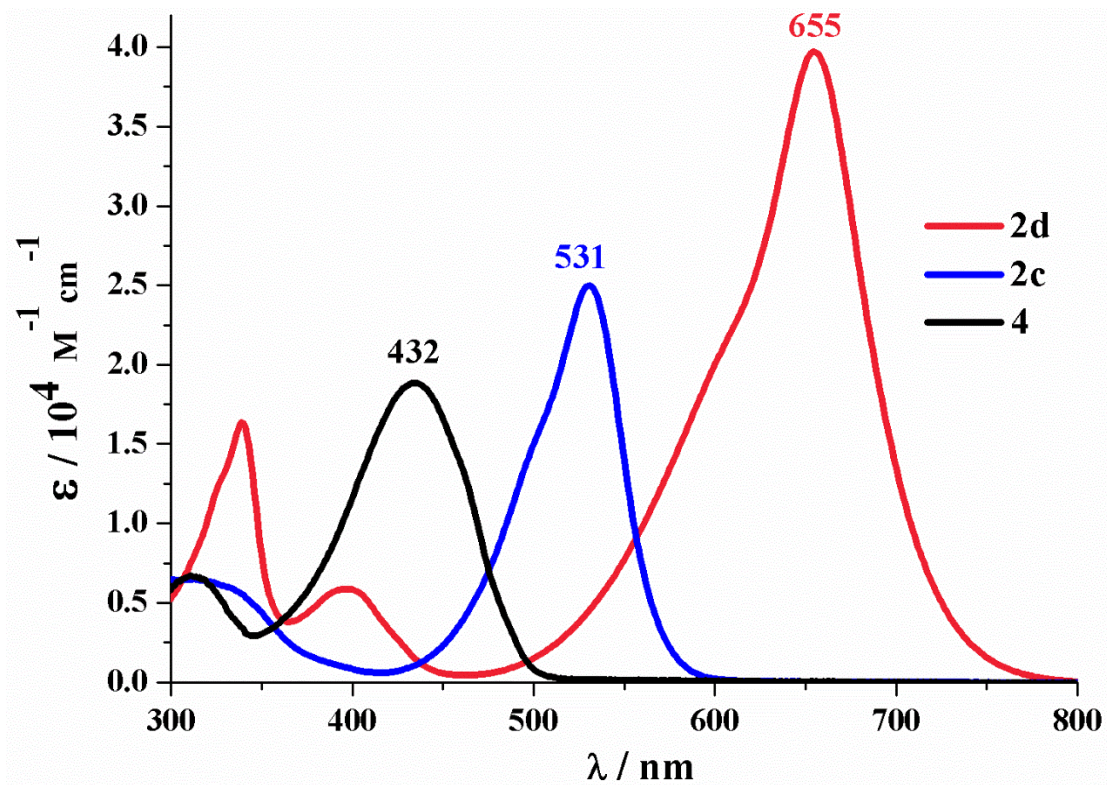
Figure 2-8 UV-vis absorption spectra of **2c** (blue), **2d** (red) and **4** (black) in CHCl$_3$
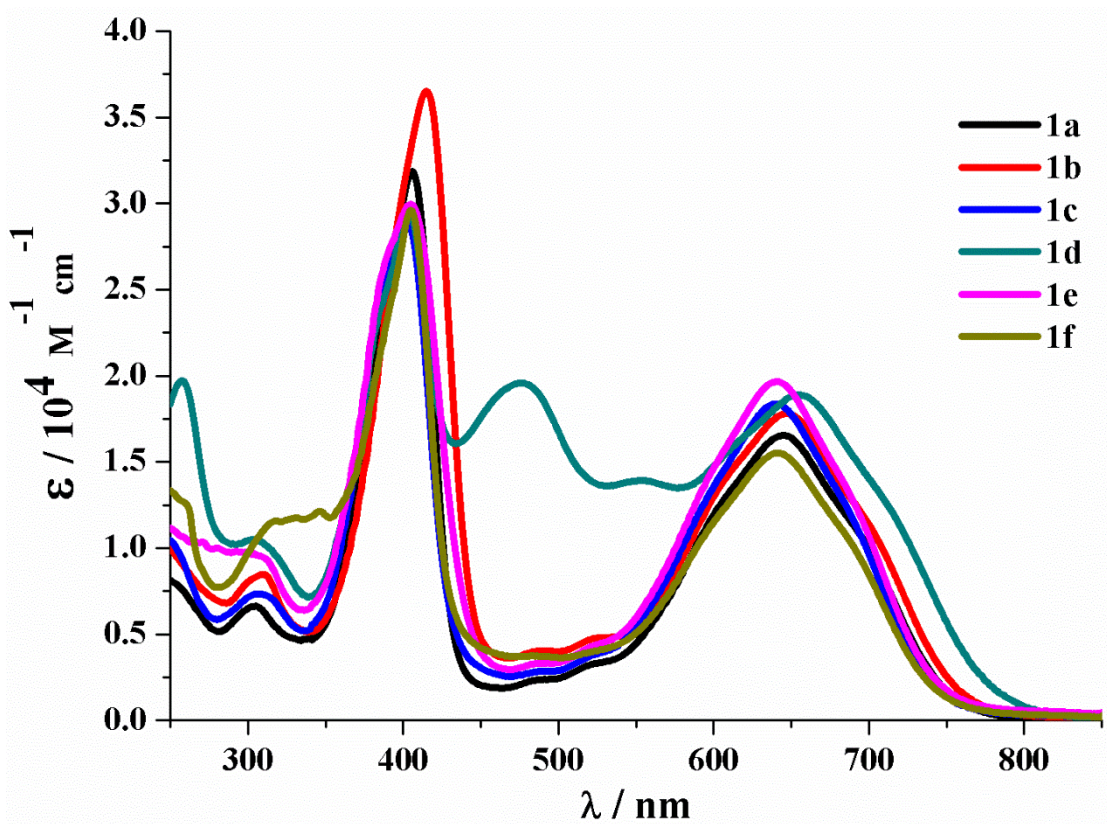
Figure 2-9 UV-vis absorption spectra of **3** in MeOH

2.4.4 Absorption Spectra in Various Solvents

To investigate the solvent effect on the photophysical behavior of these push-pull type dipyrrin analogues, we also measured their absorption spectra in various solvents from THF, ethylacetate and MeOH (**Figure 2-11~14**).   In contrast with these small conjugated molecules with push-pull substituents, the solvent effect is not very dramatic indicating that CT effects for these molecules are small.

Figure 2-10. UV-Vis spectra of **3a** in various solvents.

Figure 2-11. UV-Vis spectra of **3b** in various solvents.
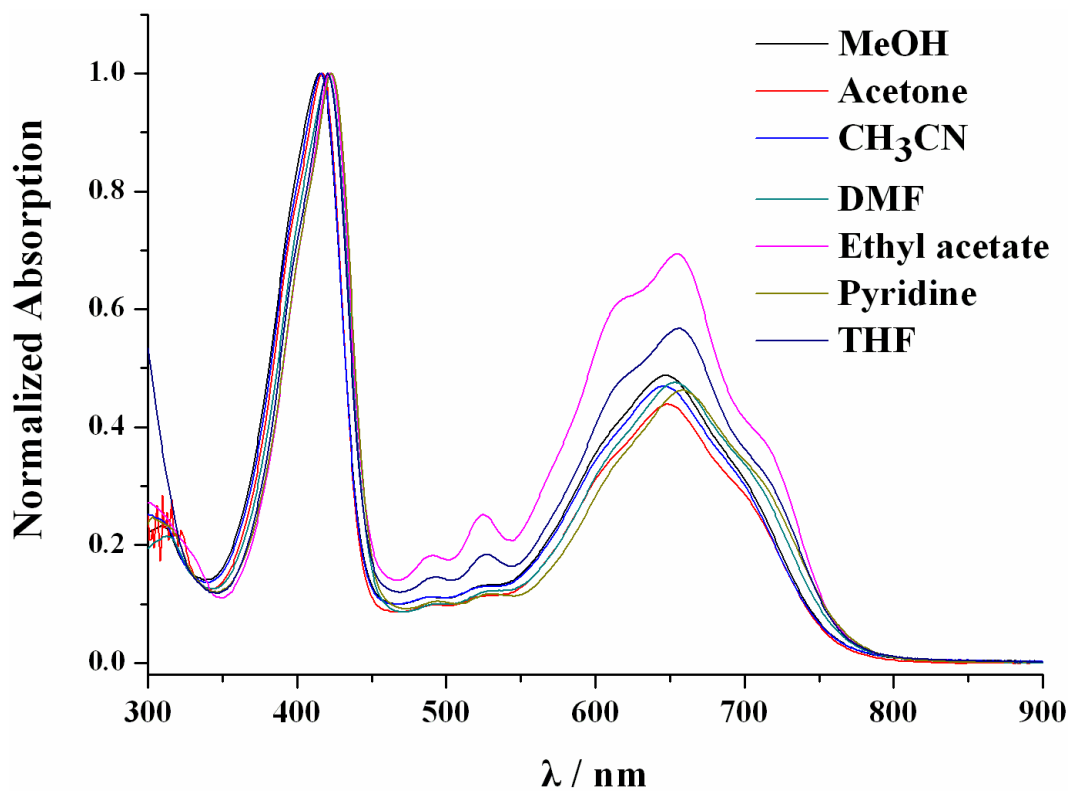
Figure 2-12. UV-Vis spectra of **3e** in various solvents.
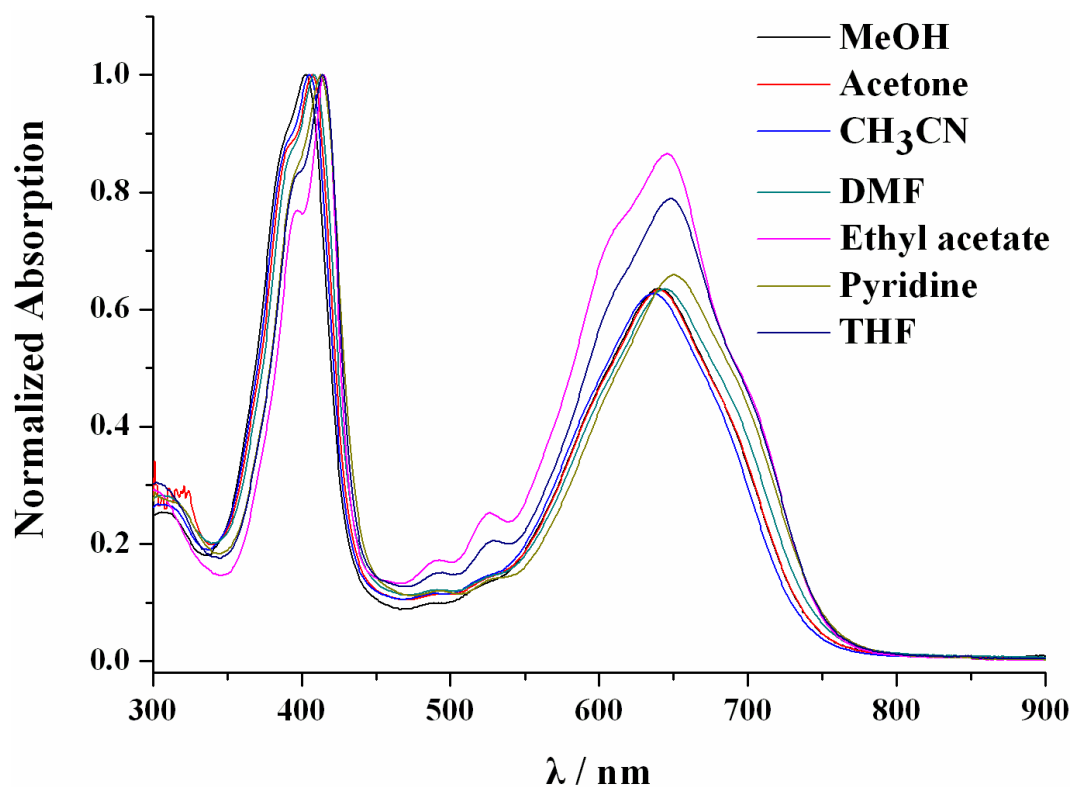
Figure 2-13. UV-Vis spectra of **3f** in various solvents.

2.5 Theoretical Calculations

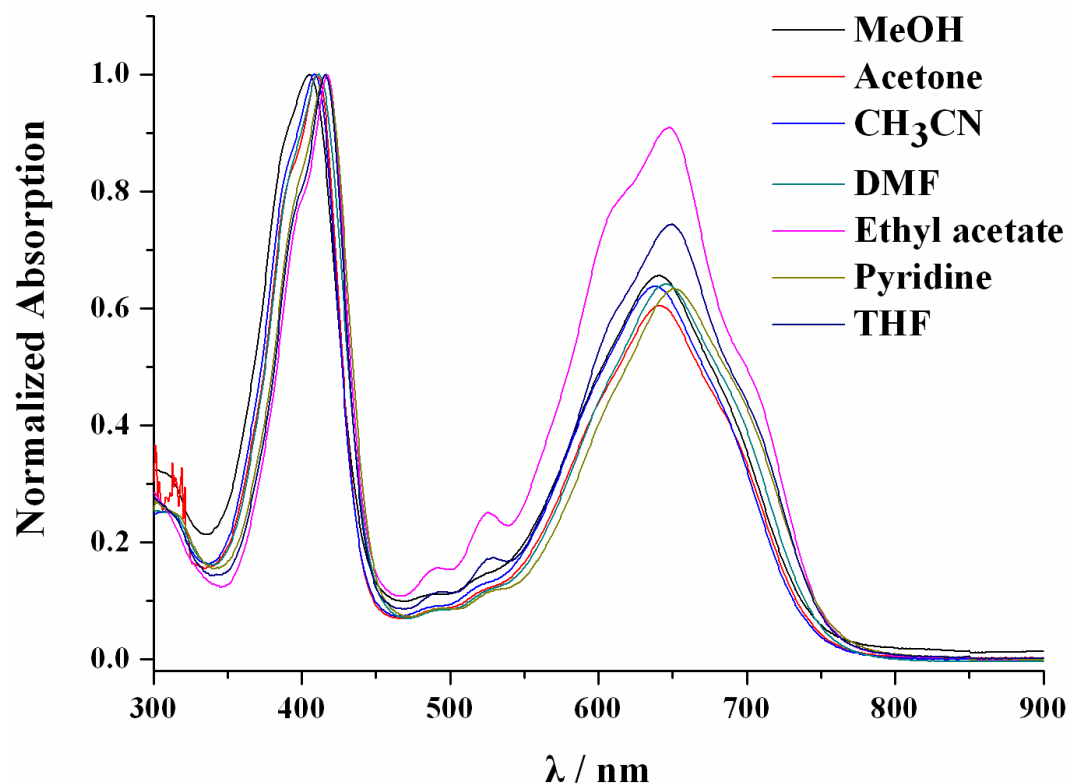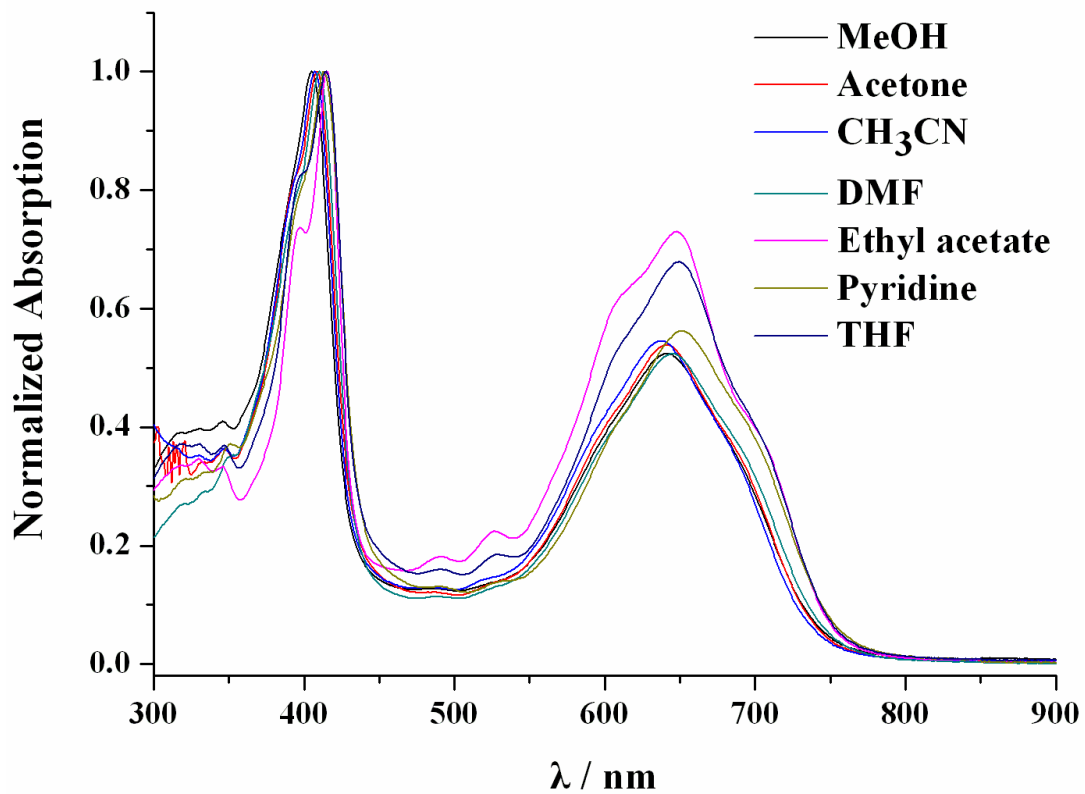Structural optimization using **2a** (the *o*-nitrophenyl ring was replace by phenyl ring for simplicity due to the *meso-o*-nitrophenyl has a mirror effect on the electronic structures of **2a**, **2d, 3a**, **3d,** and regular *meso*-phenyl-dipyrrin **4** as theoretical models was performed based on the DFT method at the B3LYP/6-31G(d) level, while time-dependent (TD) DFT calculations were also carried out at the same level.

The TDDFT calculation on **2a** revealed major contribution of the HOMO-to-LUMO transition to the lowest energy band. In addition to the similar distribution patterns of MO coefficients of the HOMO and LUMO of **2a** on the dipyrrin moiety with respect to those of **4**, these MOs are also delocalized onto the tricyanovinyl unit (**Figure 2-14**). The energy levels of both orbitals of **2a** are stabilized relative to those of **4**, the extent of which is more significant for the LUMO. The observed red-shift of the main absorption of **2c** from **4** can, therefore, be attributed to the smaller HOMO-

39

LUMO gap (2.61 eV for **2a** and 3.27 eV for **4**) due to the pull-effect of the tricyanovinyl substituent. In contrast to the essentially similar MO distribution patterns of **2a** to those of **4**, the frontier orbitals of **2d** are significantly perturbed by the electron-rich *meso*-substituent; the HOMO of **2d** with large MO coefficients on the *meso-N,N*-dimethylaminophenyl substituent lies at 5.70 eV, which is significantly destabilized relative to that of **2a**, whereas the energy levels and distribution patterns of the HOMO–1 and LUMO are very similar to those of the HOMO and LUMO of **2a**, respectively. TDDFT calculations on **2d** disclosed major contribution of intramolecular charge transfer transition from the HOMO to the LUMO. The observed red-shift of **2d** from **2c** can, therefore, be ascribed to synergetic effects of the push (*N,N*-dimethylaminophenyl) and pull (tricyanovinyl) substituents.
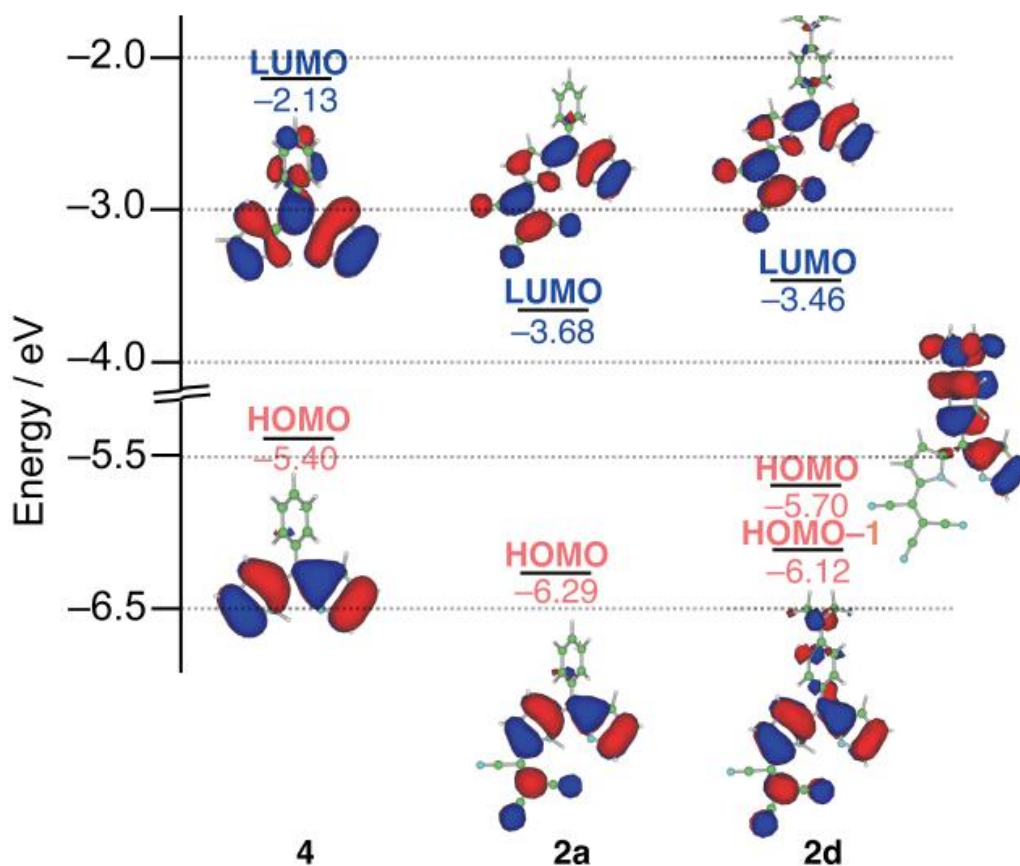

Figure 2-14. MO diagrams of regular *meso*-phenyl dipyrrin **4**, push-pull dipyrrin **2a** (middle) and **2d** (right).

Based on the TDDFT calculations, the absorption spectra of **3** (**Figure 2-15**) are mainly composed of transitions between the frontier orbitals including the HOMO–1, HOMO, LUMO, and LUMO+1; the observed two characteristic bands of **3** at 640 and 400 nm mainly comprise a transition from the HOMO to the LUMO and transitions from the HOMO to the LUMO+1 and the HOMO–1 to the LUMO, respectively (Table 1). These frontier orbitals are delocalized on the entire molecules (**Figure 2-15**), which is in agreement with the expanded conjugation as inferred from the crystal structure of **3e**. Due to the expanded conjugation, the density distribution patterns of the frontier orbitals of **3** appear to be different from those of regular meso-aryl substituted dipyrromethene as exemplified by **4** in **Figure 2-14**. In the case of **3d** bearing an strong electron-donating N,N-dimethylphenyl group at the meso-position, the HOMO is largely perturbed, and the HOMO and HOMO–1 of **3d** originate from a linear combination of the MOs of **3** and the N,N-dimethylphenyl substituent. The allowed transitions from these orbitals to the LUMO result in two split bands at 748 and 536 nm based on the TDDFT calculations (**Table 2-3**). This result reproduces the observed two absorption bands of 3f at 656 and 476 nm.
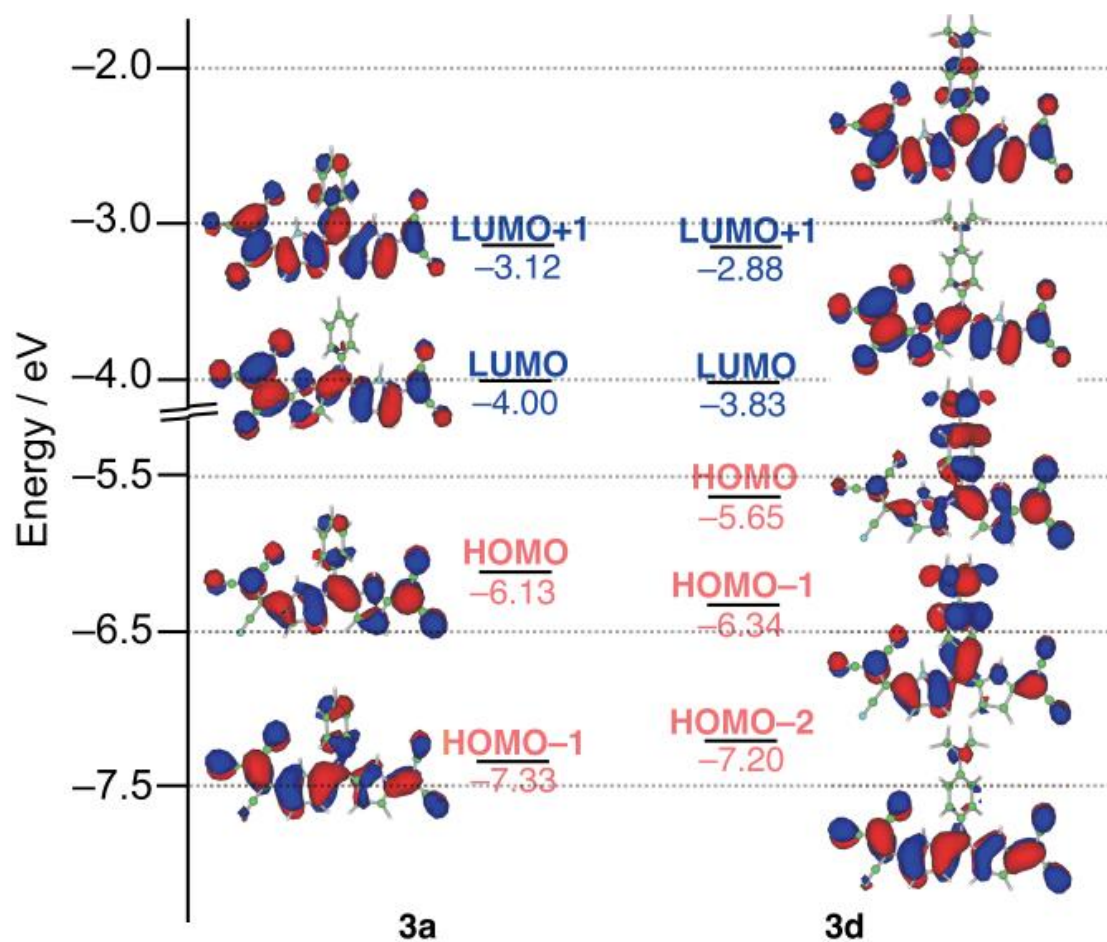
Figure 2-15 MO diagrams of push-pull dipyrrin **3a** (left) and **3d** (right).

Table 2-3: Selected transition energies and wave functions of **3a**, **3d**, **2a** and **2d** calculated based on the TDDFT (B3LYP/6-31G(d)) method.

| No.	Energy (nm)	f	Wavefunction[b]
3a	563.55	0.9261	$0.695 \mid L \leftarrow H > -0.145 \mid L+1 \leftarrow H > +...$
	458.18	0.3378	$0.584 \mid L+1 \leftarrow H > -0.358 \mid L \leftarrow H-1 > +0.176 \mid L \leftarrow H > +...$
	316.91	0.1025	$0.494 \mid L+1 \leftarrow H-1 > -0.429 \mid L \leftarrow H-4 > -0.214 \mid L \leftarrow H-6 > +...$
3d	747.97	0.1898	$0.657 \mid L \leftarrow H > -0.243 \mid L \leftarrow H-1 > + 0.176 \mid L+1 \leftarrow H > +...$
	535.70	0.5181	$0.632 \mid L \leftarrow H-1 > -0.243 \mid L+1 \leftarrow H > + 0.195 \mid L \leftarrow H > +...$
	484.09	0.6896	$0.636 \mid L+1 \leftarrow H > +0.210 \mid L \leftarrow H > +0.207 \mid L \leftarrow H-1 > -0.114 \mid L \leftarrow H-2 > +...$
2a	477.48	0.4627	$0.706 \mid L \leftarrow H > -0.118 \mid H \leftarrow L > +...$
	398.54	0.1108	$0.650 \mid L \leftarrow H-2 > -0.255 \mid L+2 \leftarrow H > +...$
2d	477.81	0.5831	$0.676 \mid L \leftarrow H-1 > +0.154 \mid L \leftarrow H-1 > +0.101 \mid L+1 \leftarrow H > -0.105 \mid L \leftarrow H > -0.103 \mid H-1 \leftarrow L > +...$
	402.01	0.1315	$0.687 \mid L+1 \leftarrow H > -0.119 \mid L \leftarrow H-1 > +...$
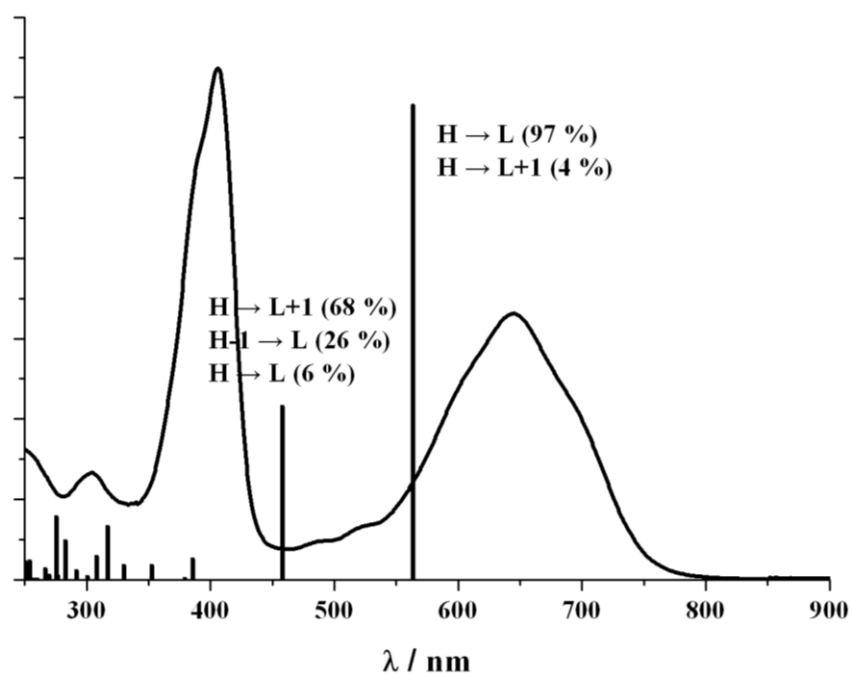
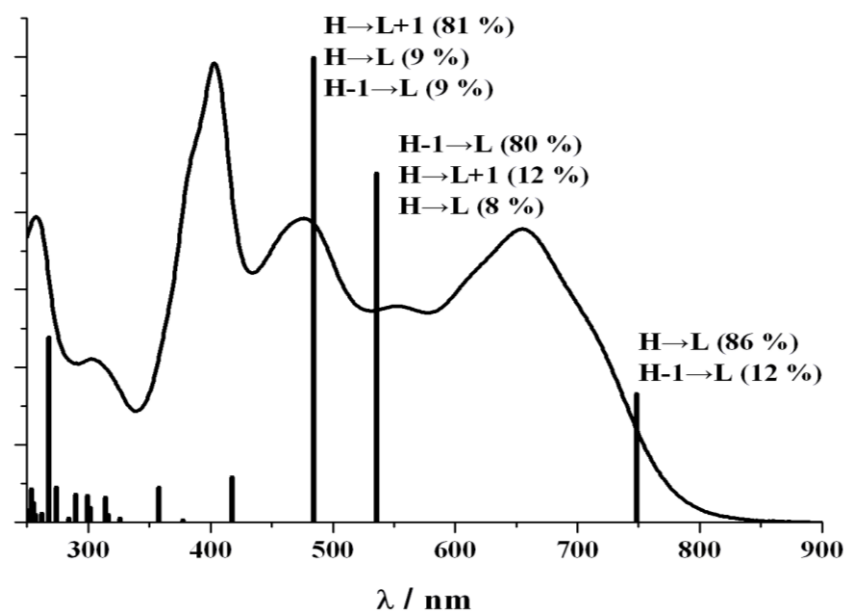**Figure 2-16** Selected transitions and UV-vis spetra of **3a**.

Figure 2-17 Selected transitions and UV-vis spetra of **3d**.
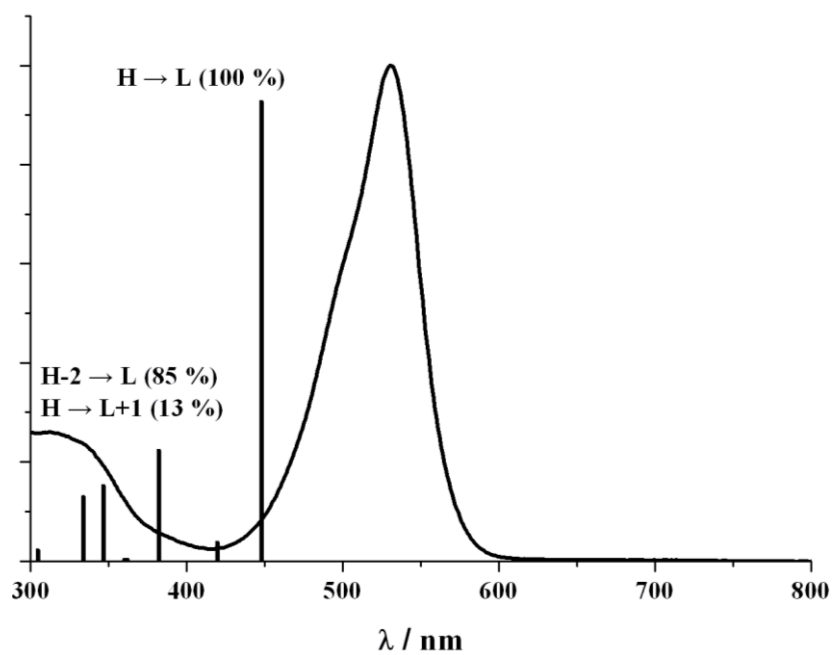
Figure 2-18 Selected transitions and UV-vis spetra of **2a**.
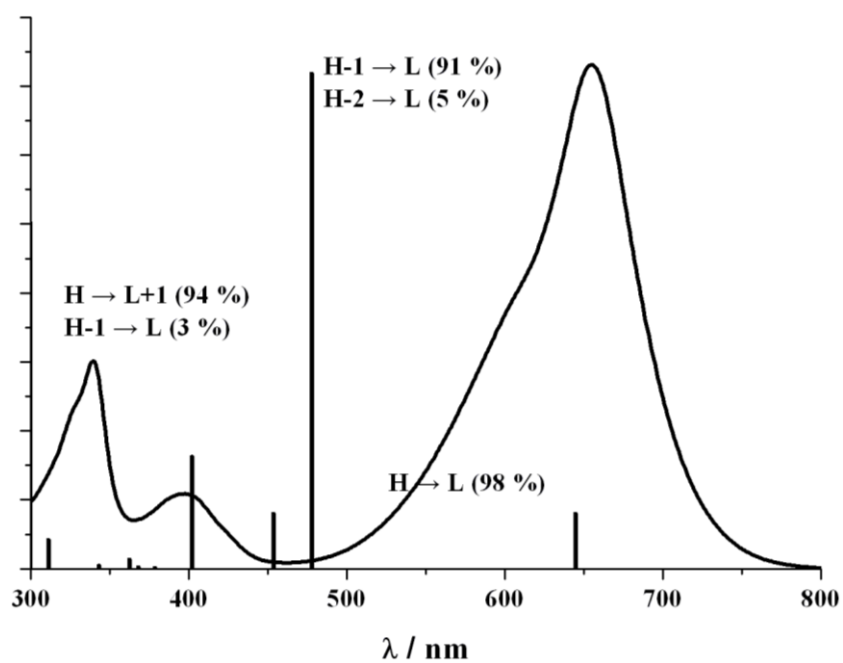
Figure 2-19 Selected transitions and UV-vis spetra of **2d**.

2.6 Protonation Behavior Studies.

1a-**1e** showed similar spectral changes upon addition of TFA to a MeOH solution (**Figure 2-23~Figure 2-26**). The amount amount of acid, at which was necessary to reach the equilibrium was found to increase with increasing the electron donating abilities of *meso*-substituents (20 eq., 40 eq., 40 eq., 60 eq., 8 eq. for **1a**-**1e**, respectively). As a result of adding the acid, the peak around 640 nm was decreased and a new absorption band appeared around 580 nm. **Figure 2-21**, **2-22** and **2-23** show the spectral changes of **1b**, **1c** and **1e** upon addition of TFA in MeOH.
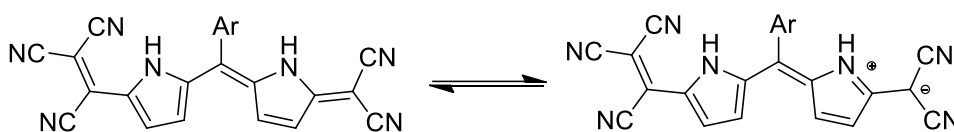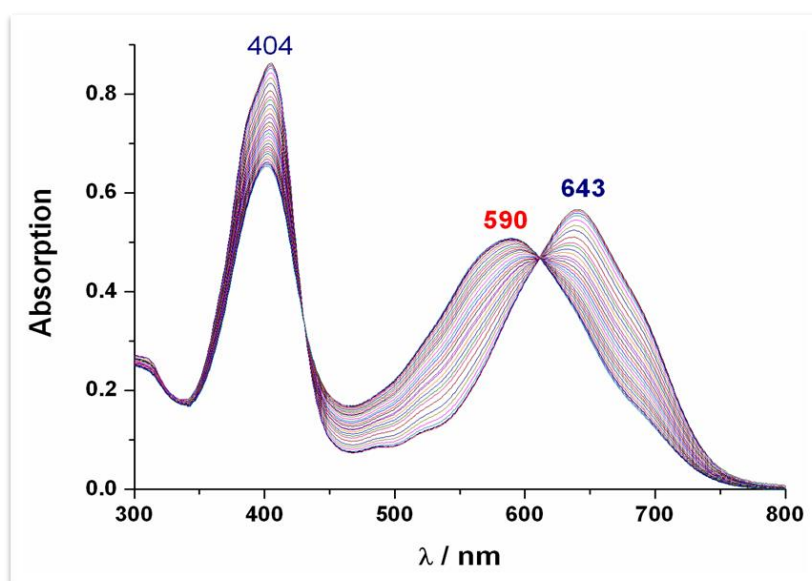
Scheme 2.3 A plausible of mechanism of protonation behavior of push-pull dipyrrins.
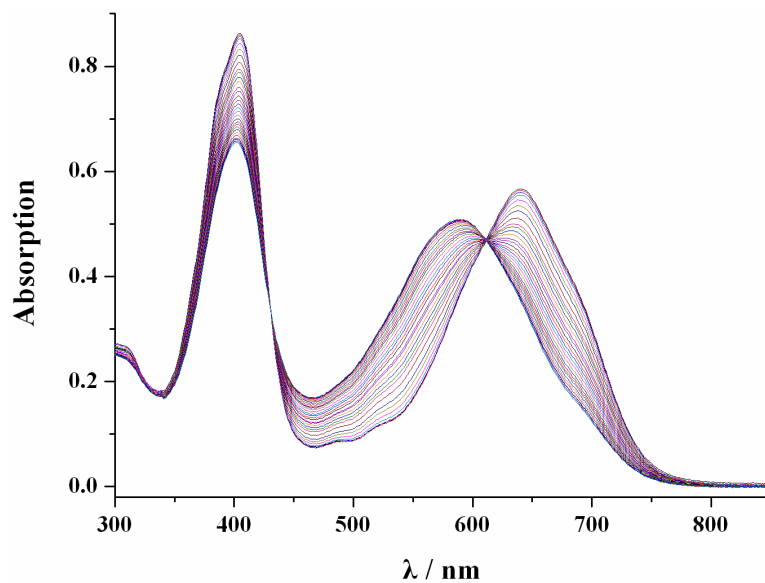
Figure 2-21. Spectral changes of **1b** upon addition of TFA in MeOH.
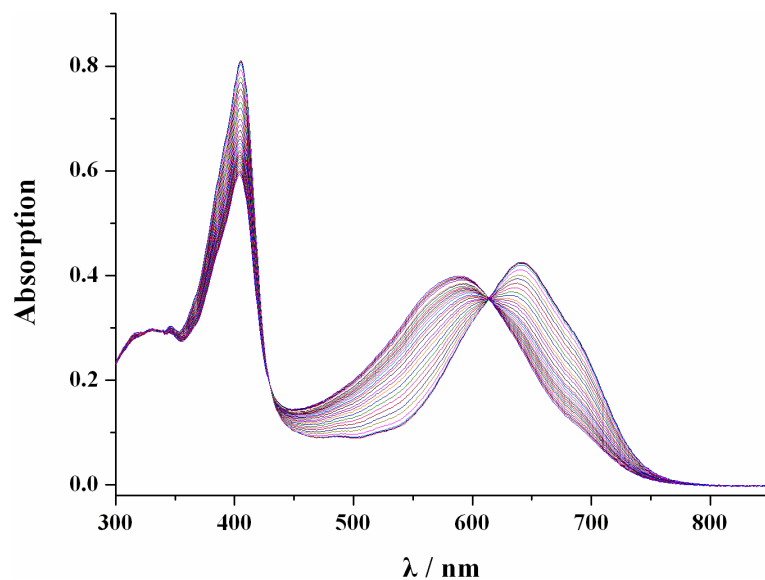
Figure 2-22. Spectral changes of **1d** upon addition of TFA in MeOH.
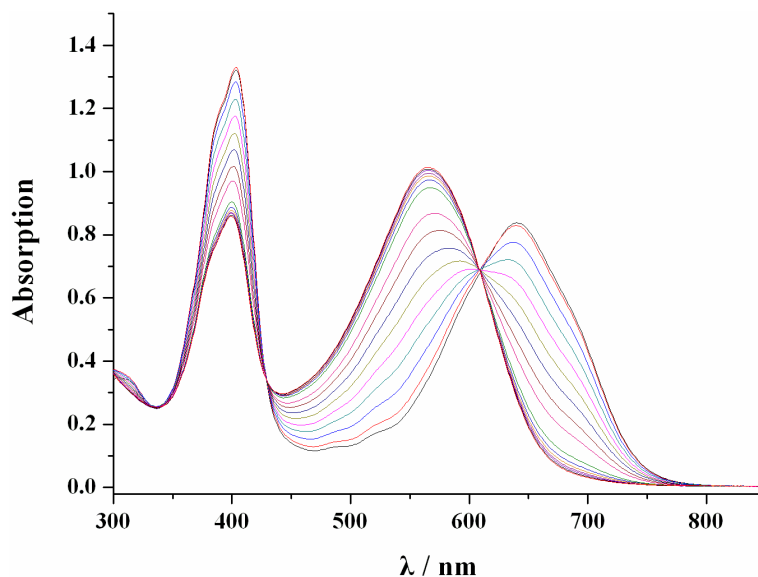
Figure 2-23. Spectral changes of **1e** upon addition of TFA in MeOH.

Further investigation was made in order to understand the mechanism of the protonation process.　The protonated species of **Pro-1b** can also be generated from **1b** by addition of acid.　**1b** was dissolved in the MeOH and TFA (40 eq.) was added, and the mixture was stirred at room temperature for about 30 min.　After removing the solvent under vacuum, the protonated **1b** (**1b-Pro**) is also stable, can be purified by silica gel column chromatography.

^{1}H NMR spectra of **1b-Pro** (**Figure 2-24**) were recorded in acetone-d_6, at room temperature.　Comparing the ^{1}H NMR spectrum of **1b-Pro** with **1b**, the signals appeared at lower field and N-H proton appeared at the higher field. The integration values of the **1b** N-H proton are 0.35 and 0.65, which was increased to 1.00 and 1.05 in **1b-pro**.　It was indicated that the protonation probably took place at the pyrrole nitrogen atom.　The crystal structure of **1b** exhibits an almost planar structure and when the pyrrole nitrogen atom is completely protonated, the distortion probably appears at the *meso*-position.　In addition to changing the conjugation of the compound, the main absorption band shifted to the shorter wavelength.　The ^{1}H NMR spectra of **1b-Pro** can also be successfully recorded in CDCl_3 (**Figure 2-25**).　The

peaks of pyrrole and naphthalene exhibit a large change.　The N-H proton shows the signals at δ = 10.6 and 11.1 ppm in acetone-d_6, and at δ = 9.30 and 7.80 ppm in CDCl$_3$ confirmed by addition of D$_2$O.
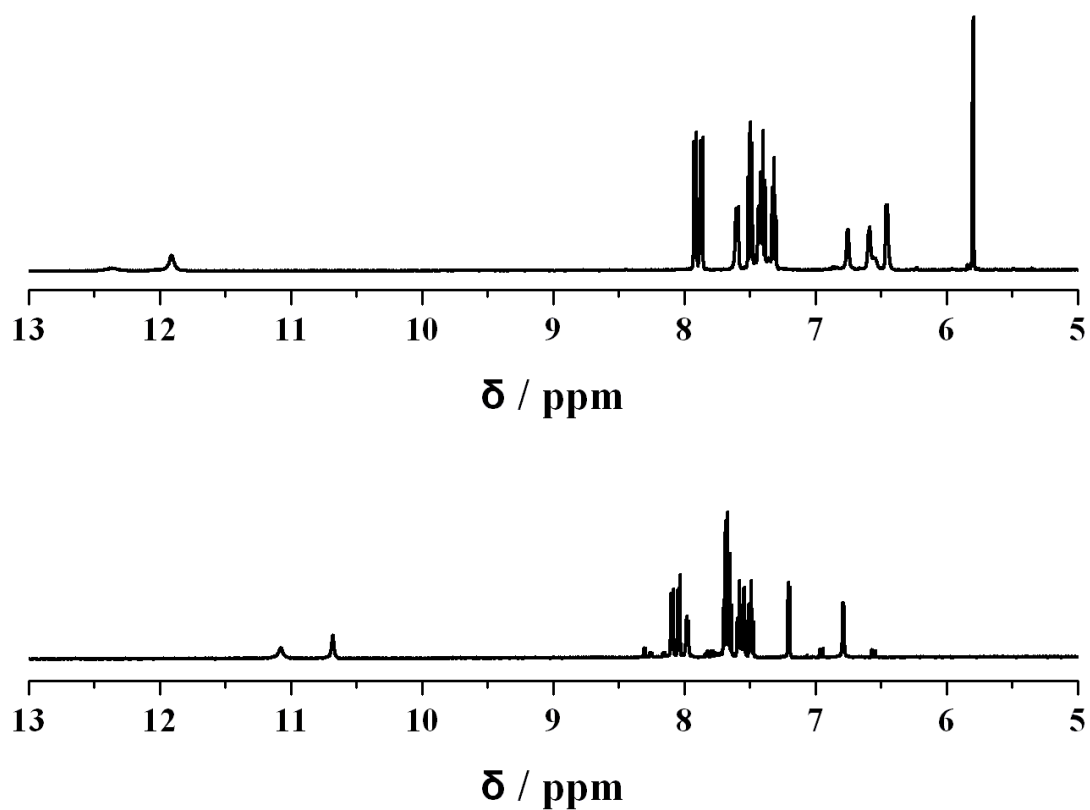
Figure 2-24. ^{1}H NMR spectra of **1b** (top) and **1b-Pro** (bottom) in acetone-d_6.
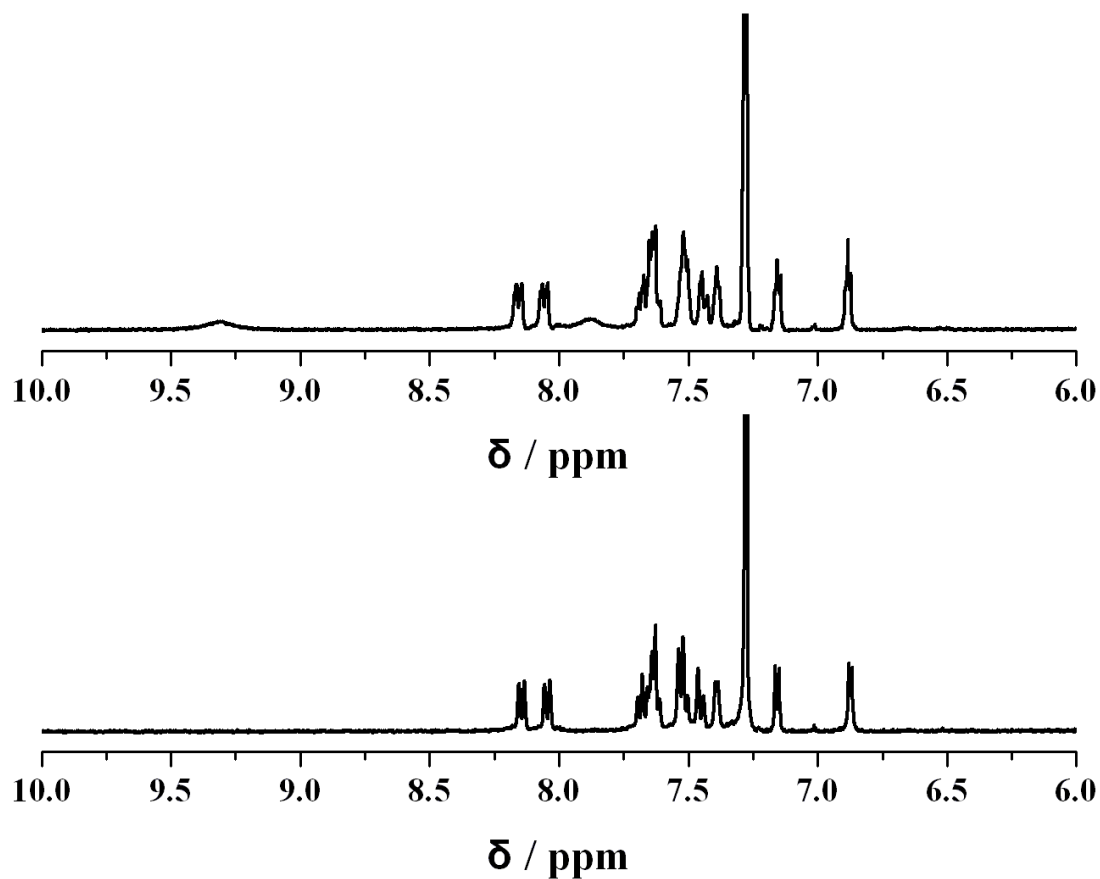
Figure 2-25. ^{1}H NMR spectra of **1b-Pro** (top) and D$_2$O exchanged (bottom) in CDCl$_3$.

2.7 A Plausible mechanism of dipyrrin synthesis
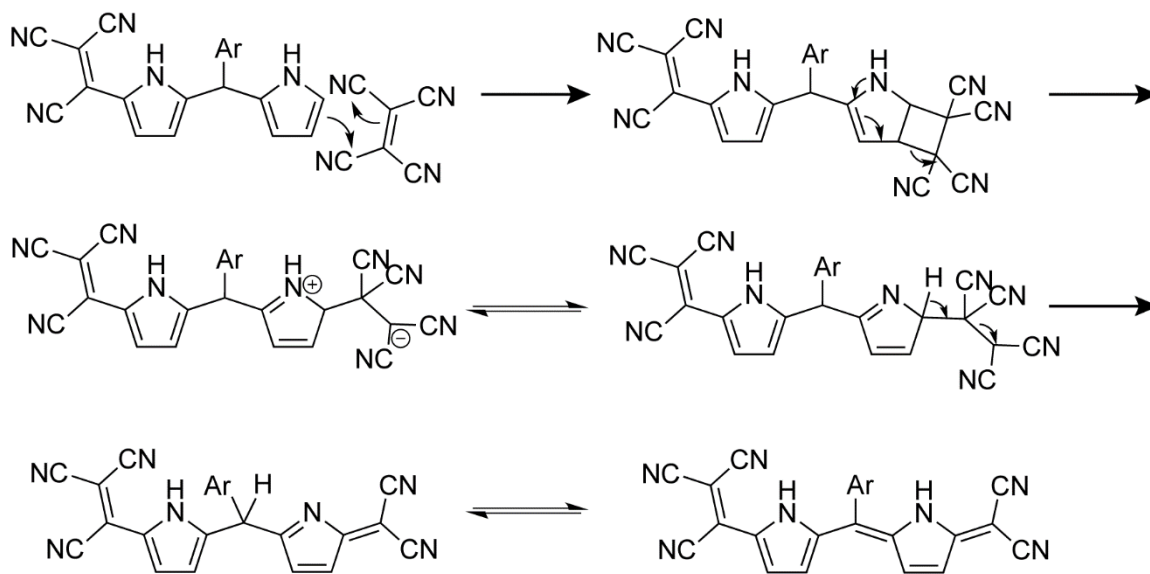
Scheme 2-4 A plausible of mechanism of push-pull dipyrrin synthesis.

2.8 Summary

In this chapter, push-pull type dipyrrins were successfully obtained via facile synthesis for the first time. α-Tricyanovinyl-α-dicyanovinyl-dipyrrins **3** with expanded dipyrrin molecular structure, exhibits the marked red-shift and broad range of absorption, which tails beyond 640 nm.   **3d** also exhibits an additional band at 476 nm, resulting in absorption in the whole visible region. α-Tricyanovinyl- dipyrrins **2** exhibit the red-shift of main absorption band, which was further enhanced by the push-substituent at the *meso*-position.

2.9 References

[1] Lindsey, J. S. *In The Porphyrin Handbook*; Kadish, K. M., Smith, K. M., Guilard, R., Eds.; Academic Press: San Diego, 2000; Vol. 1, p 45.

[2] Fischer, H.; Orth, H. *Die Chemie des Pyrroles*; Akademische Verlagsgesellschaft M. B. H.: Liepzig, 1934.

[3] Lu, H.;, Mack, J.; Yang, Y. C.; Shen Z. *Chem. Soc. Rev.* **2014**, *43*, 4778-4823. b) Amiot, C. L.; Xu, S.; Liang, S.; Pan, L.; Xiao J.; Zhao, J.; *Sensors*, **2008**, *8*, 3082-3105. c) Zhou, J.; Liu, Z.; Li, F.; *Chem. Soc. Rev.* **2012**, *41*, 1323–1349. d) Wu, W.; Yao, L.; Yang, T.; Yin, R.; Li, F.; Yu, Y. *J. Am. Chem. Soc.* **2011**, *133*, 15810–15813. e) Escobedo, J. O.; Rusin, O.; Lim, S.; Strongin, R. M. *Curr. Opin. Chem. Biol.* **2010**, *14*, 64–70. f) Fu, M.; Xiao, Y.; Qian, X.; Zhao, D.; Xu, Y. *Chem. Commun.* **2008**, 1780–1782. g) Koide, Y.; Urano, Y.; Hanaoka, K.; Terai, T.; Nagano, T. *J. Am. Chem. Soc.* **2011**, *133*, 5680–5682. h) Koide, Y.; Urano, Y.; Hanaoka, K.; Terai, T.; Nagano, T. *ACS Chem. Biol.* **2011**, *6*, 600–608. i) Ceroni, P. *Chem. Eur. J.* **2011**, *17*, 9560–9564. j) Qian, G.; Wang, Z. Y. *Chem. Asian J.* **2010**, *5*, 1006–1029. k) Fan, J.; Hu, M.; Zhan, P.; Peng, X. *Chem. Soc. Rev.* **2013**, *42*, 29–43.

[4] a) Wood, T. E.; Thompson, A.; *Chem. Rev.* **2007**, *107*, 1831-1861. b) Baudron, S. A.; *Dalton Trans.*, **2013**, *42*, 7498–7509; c) Yu, L.; Muthukumaran, K.; Sazanovich, I. V.; Kirmaier, C.; Hindin, E.; Diers, J. R.; Boyle, P. D.; Bocian, D. F.; Holten, D.; Lindsey, J. S. *Inorg. Chem.* **2003**, *42*, 6629-6647. d) Bruckner, C.; Zhang, Y.; Rettig, S. J.; Dolphin, D. *Inorg. Chim. Acta* **1997**, *263*, 279-286. e) Al-Sheikh-Ali, A.; Cameron, K. S.; Cameron, T. S.; Robertson, K. N.; Thompson, A. *Org. Lett.* **2005**, *7*, 4773-4775. f) Cohen, S. M.; Halper, S. R. *Inorg. Chim. Acta* **2002**, *341*, 12-16.

[5] Treibs, A.; Kreuzer, F. H.; *Justus Liebigs Ann. Chem.* **1968**, *718*, 208–223.

[6] a) A. Gomez-Hens and M. P. Aguilar-Caballos, TrAC, *Trends Anal. Chem.* **2004**, *23*, 127–136. b) *Near-Infrared Applications in Biotechnology,* ed. R. Raghavachari, Practical Spectroscopy Series, vol. 25, Marcel Dekker, Inc., 2001. c) E. Terpetschnig and O. S. Wolfbeis, in *Near-Infrared Dyes for High Technology*

Applications, ed. S. DIhne, U. Resch- Genger and O. S. Wolfbeis, Kluwer Academic, Dordrecht, 1998, pp. 161–182. d) Yuan, L.; Lin, W.; Zheng, K.; He L.; Huang, W. *Chem. Soc. Rev.* **2013**, *42*, 622–661. e) T. Vo-Dinh, *Biomedical Photonics Handbook*, Taylor & Francis, Inc., 2002, ISBN 0-8493-1116-0. f) Hilderbrand, S. A.; Weissleder, R. *Curr. Opin. Chem. Biol.* **2010**, *14*, 71–78.

[7] a) R. W. Wagner and J. S. Lindsey, *Pure Appl. Chem.* **1996**, *68*, 1373–1380. b) L. H. Thoresen, H. Kim, M. B. Welch, A. Burghart and K. Burgess, *Synlett* **1998**, 1276–1278. c) Burghurt, A.; Kim, H.; Welch, M. B.; Thoresen, L. H.; Reibenspies, J.; Burgess, K.; Bergstrem, F.; Johansson, L. *J. Org. Chem.* **1999**, *64*, 7813–7819.

[8] a) S. A. Baudron, *CrystEngComm*, **2010**, *12*, 2288-2295. b) Halper, S. R.; Cohen, S. M. *Inorg. Chem.*, **2005**, *44*, 486-488; c) Murphy, D. L.; Malachowski, M. R.; Campana, C. F.; Cohen, S. M. *Chem. Commun.*, **2005**, 5506-5508; d) S. R. Halper, L. Do, J. R. Stork and S. M. Cohen, *J. Am. Chem. Soc.* **2006**, *128*, 15255-15268; e) J. R. Stork, V. S. Thoi and S. M. Cohen, *Inorg. Chem.* **2007**, *46*, 11213-11223; f) Garibay, S.; Stork, J. R.; Wang, Z.; Cohen S. M.; Telfer, S. G. *Chem. Commun.* **2007**, 4881-4883. g) Salazar-Mendoza, D.; Baudron S. A.; Hosseini, M. W. *Chem. Commun.* **2007**, 2252-2254; h) Salazar-Mendoza, D.; Baudron S. A.; Hosseini, M. W. *Inorg. Chem.* **2008**, *47*, 766-768; i) Pogozhev, D.; Baudron S. A.; Hosseini, M. W. *Inorg. Chem.* **2010**, *49*, 331–338; j) Kilduff, B.; Pogozhev, D.; Baudron S. A.; Hosseini, M. W. *Inorg. Chem.* **2010**, *49*, 11231-11239; k) B éziau, A.; Baudron S. A.; Hosseini, M. W. *Dalton Trans.* **2012**, *41*, 7227-7234.

[9] a) Yadav, M.; Singh, A. K.; Pandey, D. S. *Organometallics* **2009**, *28*, 4713-4723. b) King, E. R. Betley, T. A. *Inorg. Chem.* **2009**, *48*, 2361-2363; c) King, E. R.; Hennessy, E. T.; Betley, T. A. *J. Am. Chem. Soc.* **2011**, *133*, 4917-4923; d) Scharf A. B.; Betley, T. A. *Inorg. Chem.* **2011**, *50*, 6837-6845; d) Chisholm, M. H.; Choojun, K.; Gallucci J. C.; Wambua, P. M. *Chem. Sci.* **2012**, *3*, 3445-3447; e) King, E. R.; Sazama, G. T.; Betley, T. A. *J. Am. Chem. Soc.* **2012**, *134*, 17858-17861. f) Rausaria, S.; Kamadulski, A.; Rath, N. P.; Bryant, L.; Chen, Z.; Salvemini,

D.; Neumann, W. L. *J. Am. Chem. Soc.* **2011**, *133*, 4200-4203; g) El Ghachtouli, S.; Wójcik, K.; Copey, L.; Szydlo, F.; Framery, E.; Goux-Henry, C.; Billon, L.; Charlot, M.-F.; Guillot, R.; Andrioletti B.; Aukauloo, A. *Dalton Trans.* **2011**, *40*, 9090-9093; h) Nakano, K.; Kobayashi, K.; Nozaki, K. *J. Am. Chem. Soc.* **2011**, *133*, 10720-10723.

[10] a) Wood, T. E.; Thompson, A.; *Chem. Rev.*, **2007**, *107*, 1831-1861. b) Brückner, C.; Karunaratne, V.; Rettig, S. J.; Dolphin, D. *Can. J. Chem.* **1996**, *74*, 2182-2193.

[11] Sheldrick, G. M. SHELXL-97, Program for the Solution and Refinement of Crystal Structures, University of Göttingen, Göttingen, Germany, 1997.

[12] Yadokari-XG, Software for Crystal Structure Analyses, K. Wakita, (2001); Release of Software (Yadokari-XG 2009) for Crystal Structure Analyses, Kabuto, C.; Akine, S.; Nemoto, T.; Kwon, E. *J. Cryst. Soc. Jpn.*, 2009, **51**, 218.

[13] a) Sluis, P. V.; Spek, A. L. *Acta Crystallogr. Sect. A: Found. Crystallogr.* **1990**, *46*, 194; b) Spek, A. L. *Acta Crystallogr. Sect. A: Found. Crystallogr.* **1990**, *46*, C34.

[14] Gaussian 09, Revision A.02, Frisch, M. J.; Trucks, G. W.; Schlegel, H. B.; Scuseria, G. E.; Robb, M. A.; Cheeseman, J. R.; Scalmani, G.; Barone, V.; Mennucci, B.; Petersson, G. A.; Nakatsuji, H.; Caricato, M.; Li, X.; Hratchian, H. P.; Izmaylov, A. F.; Bloino, J.; Zheng, G.; Sonnenberg, J. L.; Hada, M.; Ehara, M.; Toyota, K.; Fukuda, R.; Hasegawa, J.; Ishida, M.; Nakajima, T.; Honda, Y.; Kitao, O.; Nakai, H.; Vreven, T.; Montgomery, Jr., J. A.; Peralta, J. E.; Ogliaro, F.; Bearpark, M.; Heyd, J. J.; Brothers, E.; Kudin, K. N.; Staroverov, V. N.; Kobayashi, R.; Normand, J.; Raghavachari, K.; Rendell, A.; C. Burant, J.; Iyengar, S. S.; Tomasi, J.; Cossi, M.; Rega, N.; Millam, J. M.; Klene, M.; Knox, J. E.; Cross, J. B.; Bakken, V.; Adamo, C.; Jaramillo, J.; Gomperts, R.; Stratmann, R. E.; Yazyev, O.; Austin, A. J.; Cammi, R.; Pomelli, C.; Ochterski, J. W.; Martin, R. L.; Morokuma, K.; Zakrzewski, V. G.; Voth, G. A.; Salvador, P.; Dannenberg, J. J.; Dapprich, S.; Daniels, A. D.; Farkas, O.; Foresman, J. B.; Ortiz, J. V.; Cioslowski, J.; Fox, D. J. Gaussian, Inc., Wallingford CT, 2009.

Chapter III

Synthesis, Properties and Theoretical Calculations of Push-Pull Type Subporphyrazines

3.1 Introduction

3.1.1 Chemistry of Subphyrazines

Subporphyrazines (SubPzs), a contracted congener of porphyrazines (Pzs) and removal of three benzene rings from subpthalocyanines (SubPcs) which comprising three isoindole units bridged by imino-nitrogen atoms, show great potential as functional chromophores due to their strong fluorescence and strong yellow-green absorptions.[1]   As far as we concerned, peripheral substituents which directly attached to the macrocyclic core has a greater effect on the electronic structures, and various β-aryl substituted subporphyrazines have been reported to study the effect of substituents on the electronic structures.[2]   The small 14π conjugated molecular structures of SubPzs limit their main absorption bands are all at yellow-green light region only with an exceptional $β,β'$-sp3 hybrid subchlorin analogue as the only one example which has thermal main absorption band at longer wavelength region.[3]   Although the synthesis and properties of subporphyrazine analogues have been reported by Hanack, Torres and Kobayashi the chemistry of SubPzs was lack due the difficulties in the synthesis and the poor stabilities.[4]
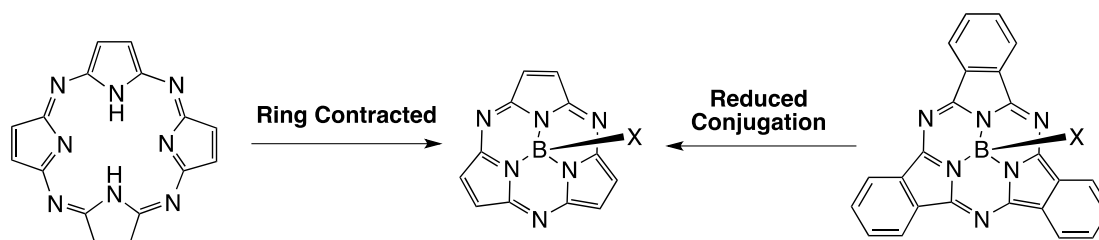
Figure 3-1. Molecular structure of porphyrazine (Pz, left), subporphyrazine (SubPz, middle) and subphthalocyanine (SubPc, right).

Dicyanoethylene was used as the key-precursor for subporphyrazine synthesis, after reacted with BCl_3, the 14π conjugated subporphyrazine can be isolated as the chloro axial chloro-substituted aromatic compound.   Kobayashi and co-workers published the research results combined the synthesis, spectroscopic properties and theoretical calculation of subporphyrazine in 2006.[4]   This new derivative exhibits the

main absorption band (Q-band) at around 500 nm and nearly degenerated excited states. Due to the limit of the synthetic method, the difficulities in the isolation and poor stability, the chemistry of subporphyrazine was still lack compared with subphthalocyanines and porphyrazines.
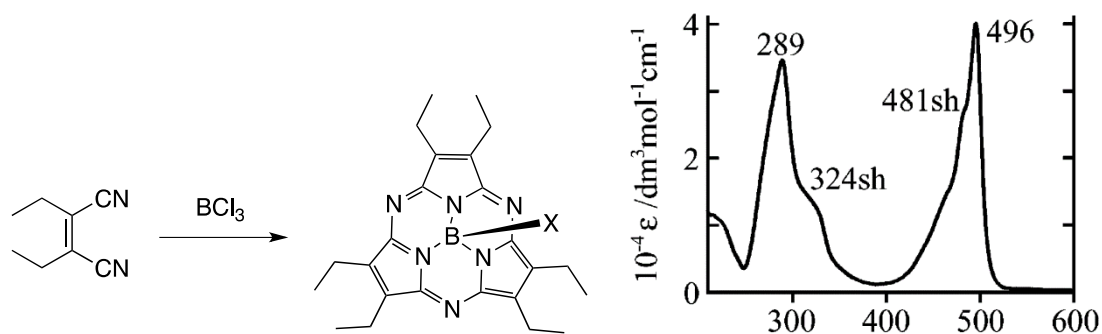
Figure 3-2. Synthetic procedure (left) and absorption spectra of β,β'-hexethyl subporphyrazine

In order to obtain the new subporphyrazines derivatives, which exhibit novel spectroscopic properties, in 2005, Torres reported the synthesis and characterizations of a new series of subporphyrazine derivatives bearing thioalkyl chains. Spectroscopic investigation reveals the changes of the optical properties of these macrocycles which was induced by the formal replacement of all isoindole rings in the SubPc framework by pyrrole moieties and the main absorption band was shifted to the longer wavelength region, at 559 nm. Considering the macrocycle was strongly coupled to their peripheral substitutents, which is of great interest for further applications of these types of systems to areas like, for example, nonlinear optics.

Figure 3-3 Synthetic procedure of SubPzs (left), and the UV/Vis spectra of SubPc (right, dashed line), SubPz **4a** (thick line), and SubPz **4d** (thin line)

Recently, A. Osuka and T. Torres succeeded in the post-modification of the peripheral substituents with aryl groups using Pd-catalyzed copper(I) thiophene-2-carboxylate (CuTC)-mediated coupling of boronic acids with heteroaromatic thioethers. The introduced aryl substituents exert notable perturbations on the optical and electronic properties of the SubPz core, making these modifications a promising tool to tune SubPzs. With the increasing of the post-coupled aryl-substituents, the 1st reduction potential was decreased with great linear correlation on the Hammett plot of first reduction potentials of SubPzs.
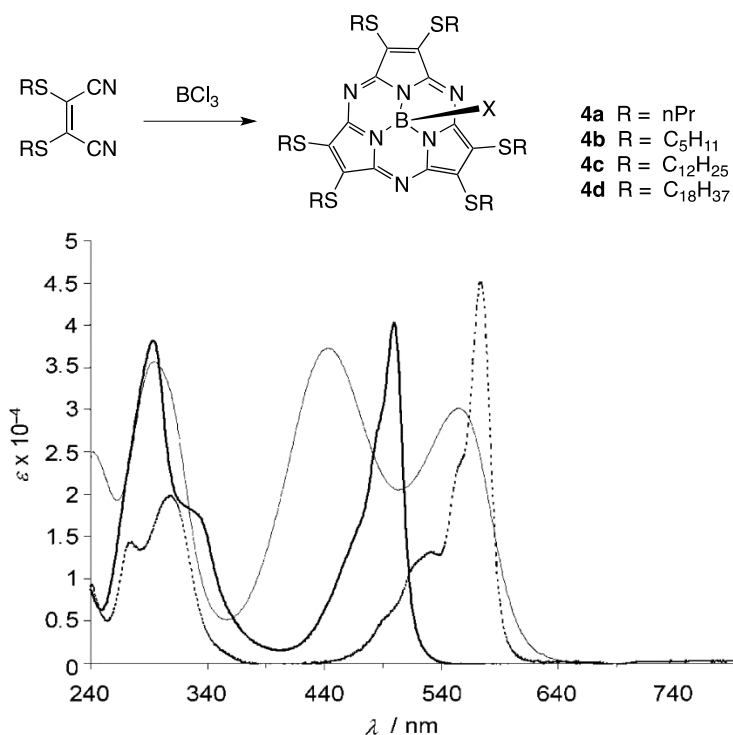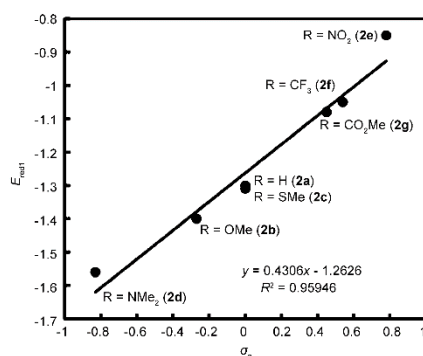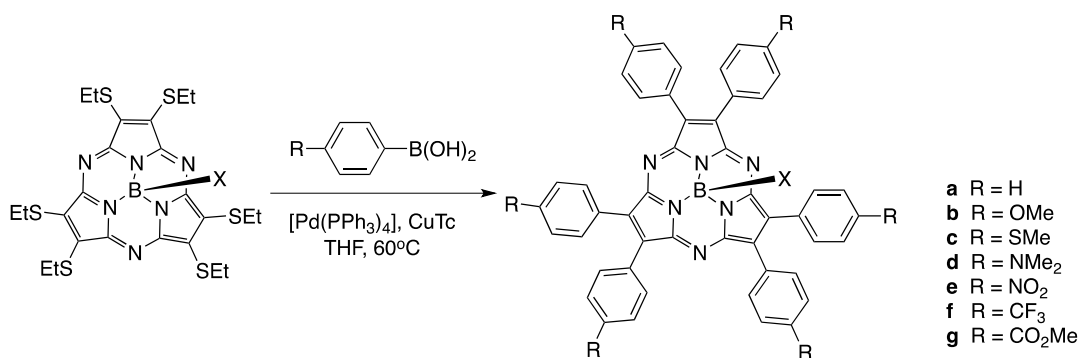
Figure 3-4 Synthetic procedure of SubPzs (left), and the UV/Vis spectra of SubPc (right, dashed line), SubPz **4a** (thick line), and SubPz **4d** (thin line)

3.1.2 Disateromers and Enantiomers of Subphthalocyanine

Following the first suggestion of inherent molecular chirality in asymmetrically substituted subphthalocyanines by Torres and co-workers in 2000, which the constitutional isomers of chloro-(2,9,16(17)triodosubphthalocianato)-boron(III) have been separated by column chromatography on silica gel. Furthermore, the enantiomers of each of these C_1- and C_3-regioisomers have been resolved by HPLC on a chiral analytical column.   The diatromers of subphthalocyanines can be easily characterized by ^{1}HNMR spectra and C_1 symmetry isomer exhibits splitted HNMR signals at the aromatic region.[5]
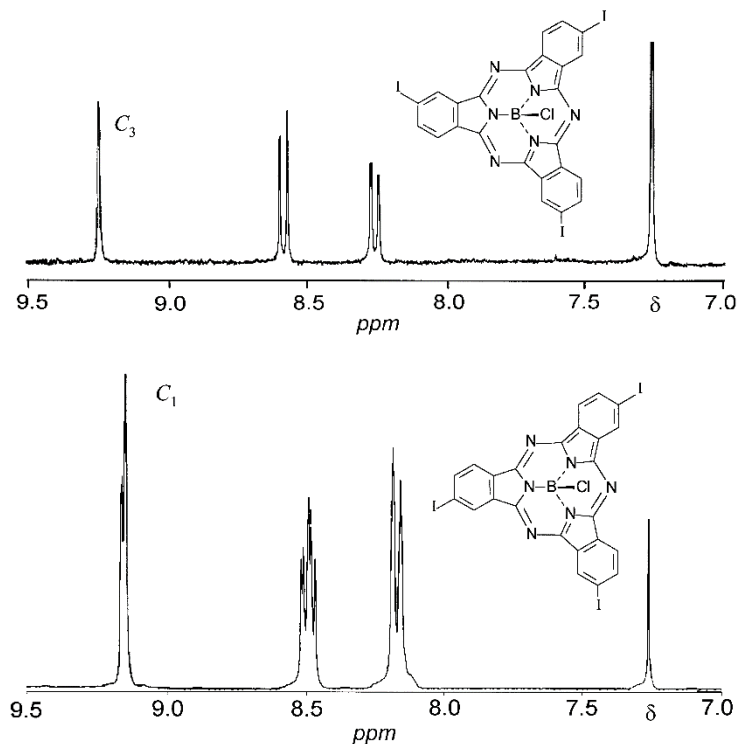
Figure 2-5 ^{1}HNMR spectra of C_3 (up) and C_1 (bottom) symmetry isomers of β-iodine substituted subphthalocyanine

The research interests about chiral subpthalocyanine chemistry is still growing after Torres's first paper, but it has not been possible to link the CD signs and intensities to their absolute structures due to its poor solubility. In 2011, the separation and characterization of all of the diastereomers and enantiomers of 1,2-subnaphthalocyanine was succeeded as the first example in the chemistry of inherently chiral subphthalocyanine by S. Shimizu and N. Kobayashi. After characterized by ^{1}H NMR and X-ray crystallized analysis, negative CD signs in the Q-band region are indicative of a molecular structure where the naphthalene moieties are arranged clockwise, while the positive CD signs in that region indicate an anticlockwise arrangement.[6]
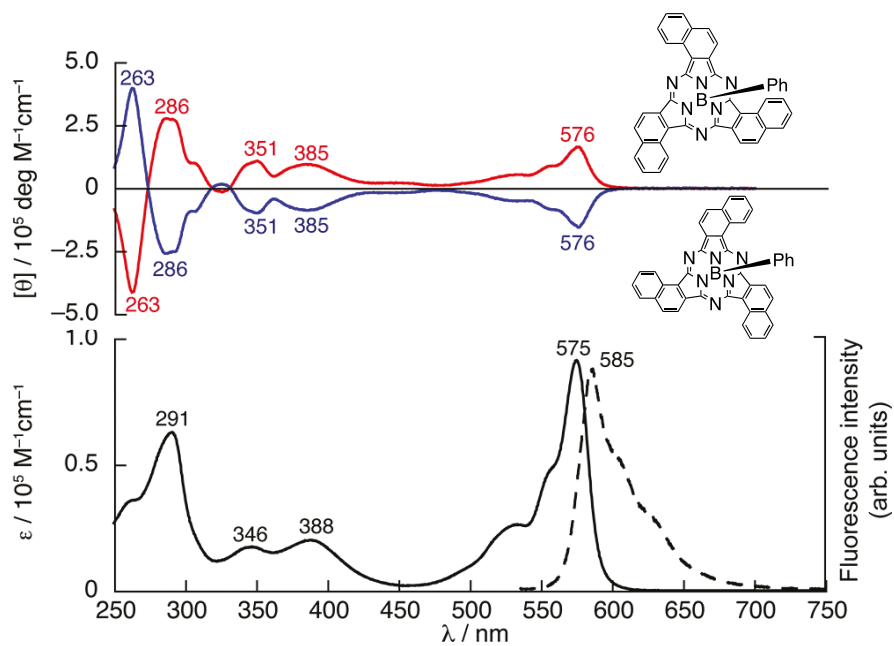
Figure 2-6 Absorption and circular dichlorism (CD) spectra of chiral
subphthalocyanines.

3.2 Propose of This Research

Subporphyrazine (SubPz), a contracted analogue of tetraazaporphyrin (TAP) or in other words the meso-nitrogen-substituted congener of subporphyrin, has become an attractive class of chromophore molecules because of its intense Q band absorption and fluorescence in the visible region. Considering introduction of electron donating (push-) and electron withdrawing (pull-) substituents have large contribution on the decrease of the gap between the HOMOs and the LUMOs, and push-pull type dipyrrins have been succeeded. Introduction of push-pull substituents to the subporphyrazines will test the push-pull effect based on the subporphyrazine chromophores. Based on the asymmetric arrangement of push-pull substituents and the bowl shaped molecular structure, both diasteromers and enantiomers will also be observed. The studies on the electronic structure of these new push-pull subporphyrazine derivatives by spectroscopic investigations and theoretical calculation will give useful information to in-depth understand the relationship between the observed spectroscopic properties and effect of push-pull substituents.

Push-Pull Subporphyrazine

Push substituents

Pull substituents
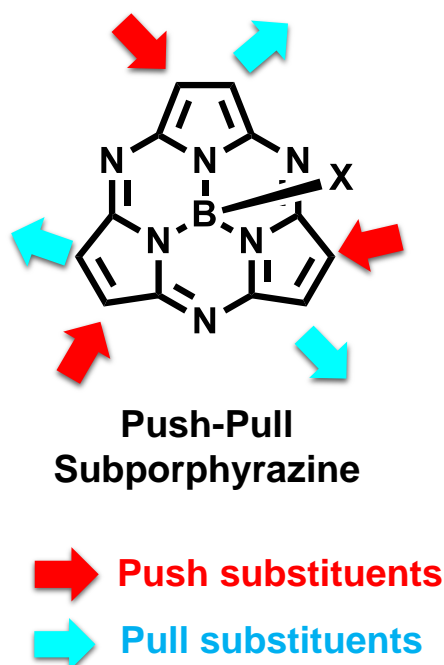
3.3 Synthesis

3.3.1 Chemicals and instruments

Electronic absorption spectra were recorded on a JASCO V-570 spectrophotometer. Circular dichroism (CD) and magnetic circular dichroism (MCD) spectra were recorded on a JASCO J-725 spectrodichrometer equipped with a JASCO electromagnet, which produces magnetic fields of up to 1.03 T (1 T = 1 tesla) with both parallel and antiparallel fields. The magnitudes were expressed in terms of molar ellipticity ($[\theta]$/deg dm^3 mol^{-1}cm^{-1}) and molar ellipticity per tesla ($[\theta]_M$/deg dm^3 mol^{-1}cm^{-1}T^{-1}), respectively. Fluorescence spectra were measured on a Hitachi F-4500 spectrofluorimeter. Absolute fluorescence quantum yields were measured on a Hamamatsu Photonics C9920-03G calibrated integrating sphere system.

^{1}H NMR spectra were recorded on a Bruker AVANCE 500 spectrometer (operating at 500.13 MHz) using the residual solvent as an internal reference for ^{1}H (δ = 7.26 ppm for CDCl$_3$, δ = 5.32 ppm for CD$_2$Cl$_2$ and δ = 2.09 ppm for toluene-d_8). High resolution mass spectra were recorded on a Bruker Daltonics solariX 9.4T spectrometer. Preparative separations were performed by silica gel column chromatography (Merck Kieselegel 60H) and recycling preparative GPC-HPLC (JAI LC-9201 with preparative JAIGEL-2H, 2.5H, and 3.0H columns). Separation of all the enantiomers was carried out by high-performance liquid chromatography (HPLC) with a preparative CHIRALPAK IA column by monitoring the absorbance at 580 nm. CV measurements were recorded with a Hokuto Denko HZ5000 potentiostat under nitrogen atmosphere in o-dichlorobenzene (o-DCB) solutions with 0.1 M of tetrabutylammonium perchlorate (TBAP) as a supporting electrolyte. Measurements were made with a glassy carbon electrode (area = 0.07 cm^2), an Ag/AgCl reference electrode, and a Pt wire counter electrode. The concentration of the solution was fixed at 1.0 mM and the sweep rates were set to 100 mV/s. The ferrocenium/ferrocene (Fc$^+$/Fc) couple was used as an internal standard. All chemical reagents and solvents were of commercial reagent grade and were used without further purification except where noted.

3.3.2 Crystallographic Data Collection and Structure Refinement

Data collection was carried out at −173(2) ℃ on a Bruker APEXII CCD diffractometer with Mo Kα radiation (λ = 0.71073 Å) for **2c**. The structure was solved by a direct method (SHELXS-97)[7] and refined using a full-matrix least squares technique (SHELXL-97). CCDC-1015544 contain the supplementary crystallographic data for **2c** and the data can be obtained free of charge from the Cambridge Crystallographic Data Centre via www.ccdc.cam.ac.uk/data_request/cif.

3.3.3 Computational methods

The Gaussian 09 software package[8] was used to carry out DFT and TDDFT calculations using the B3LYP functional and 6-31G(d) basis sets. Structural optimization was performed on model compounds of **2a**, **2b**, **2c**, **3c**, and unsubstituted subporphyrazine **4** as a reference compound.

3.3.4 Synthesis of 1,1,2-tricyano-2'-arylethylene
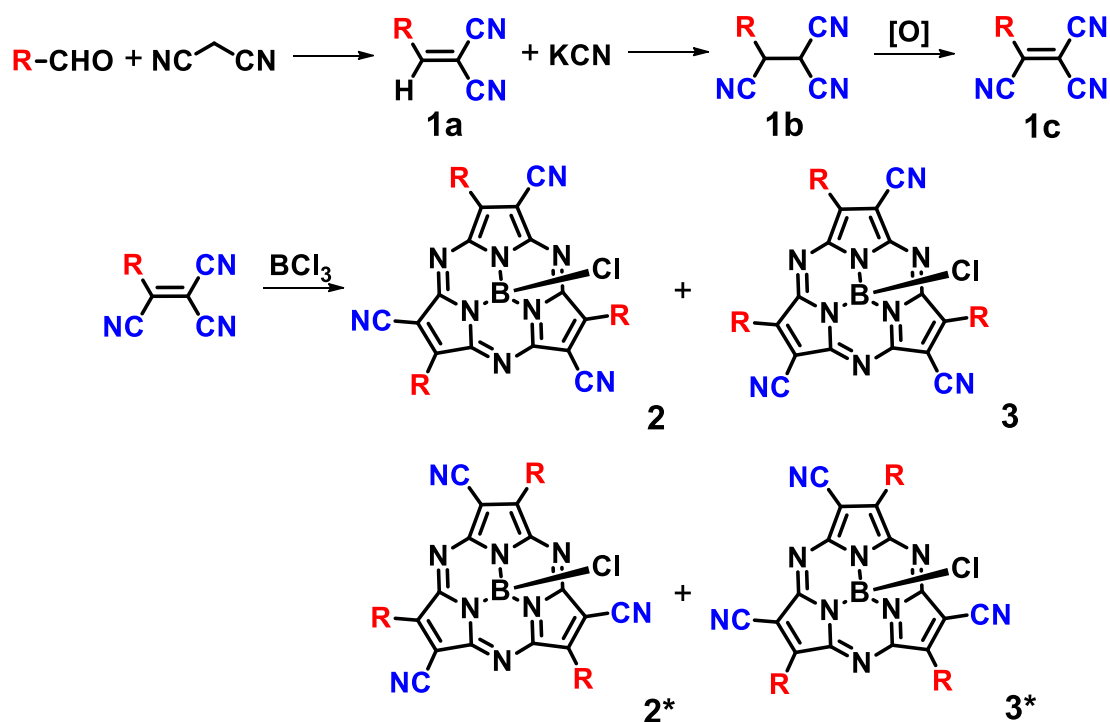
Scheme 3-1. Synthesis of aryl-tricyanoethylene and push-pull subporphyrazines.

R–CHO + NC–CH₂–CN → (1-2) + KCN → (1-3) →[O]→ (1)

$$R\text{-CHO} + NC\frown CN \longrightarrow 1\text{-}2 + KCN \longrightarrow 1\text{-}3 \xrightarrow{[O]} 1$$

1-1	1-2	1-3	1
1a-1 (R = -OMe)	1a-2 (R = -OMe)	1a-3 (R = -OMe)	1a (R = -OMe)
1b-1 (R = -CH₃)	1b-2 (R = -CH₃)	1b-3 (R = -CH₃)	1b (R = -CH₃)
1c-1 (R = -CF₃)	1c-2 (R = -CF₃)	1c-3 (R = -CF₃)	1c (R = -CF₃)
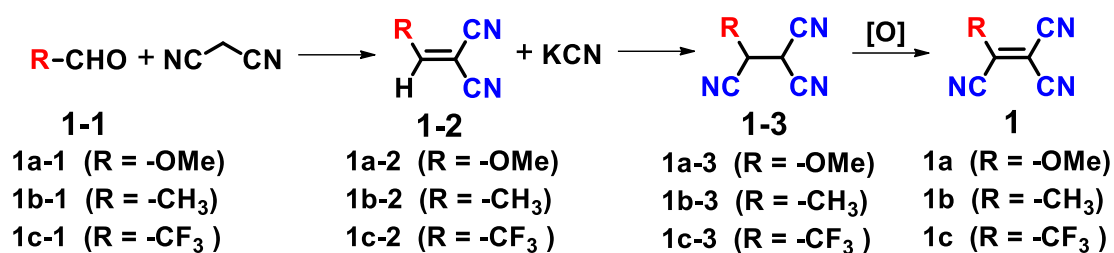
Scheme 3-2. Synthesis of aryl-tricyanoethylene **1a**, **1b** and **1c**.

Synthesis of 1a-2:   A 5 mL water solution of NaOH (16 mg, 0.4 mmol, 0.04 equiv.) was added to a 30 mL methanol solution of *p*-anisaldehyde **1a-1** (13.6 g, 0.1 mol) and malononitrile (7.92 g, 0.12 mol, 1.2 equiv.).   The resulting mixture was stirred at RT for 0.5 h and the solid compounds were collected after filtration.   Further purification was by silica gel column chromatography (CHCl₃) afford the compound 1,1'-dicyano-2'-methoxylethylene **1a-2** in yield 88% (16.2 g). ^{1}H NMR (500 MHz, CDCl₃, 298K): δ = 7.91 (d, 2H, phenyl; *J* = 8.8 Hz), 7.65 (s, 1H, ethylene), 7.01 (d, 2H, phenyl; *J* = 9.0 Hz), 3.92 (s, 3H, -OMe).

Synthesis of 1a-3:   KCN (1.02 g, 15.5 mmol, 1.03 equiv.) was dissolved in 20 mL water, stirred and heated at 60°C. After the KCN was completely dissolved in the water, a 20 mL EtOH solution of 1,1'-dicyano-2-*p*-methoxylphenylethylene **1a-2** (2.76 g, 15.0 mmol) was slowly added and continuously stirred at 60°C for 15 min.   After cooling to room temperature, a solution of acetic acid/water (2 mL in 10 mL water) was added. After removal of solvent, the reaction mixture was dried under vaccum. Further purification was carried out by column chromatography (eluent: CHCl₃:MeOH = 10:1) to afford a white compound.1,1',2-Tricyano-2'-methoxylphenylethane **1a-3** in 65% yield (2.06 g). ^{1}H NMR (500 MHz, CDCl₃, 298K): δ = 7.42 (d, 2H, phenyl; *J* = 8.8 Hz), 7.01 (d, 2H, phenyl; *J* = 8.8 Hz), 4.40 (d, 1H, ethylene; *J* = 6.0 Hz), 4.18 (d, 1H, ethylene; *J* = 6.0 Hz), 3.85 (s, 3H, -OMe).

Synthesis of 1a: 2,3-Dichloro-5,6-dicyano-*p*-benzoquinone (DDQ; 2.3 g 10.0 mmol, 2.0 equiv.) was added to a 50 mL CHCl$_3$ solution of 1,1',2-tricyano-2'-methoxyphenylethane **1a-3** (1.06 g, 5.0 mmol). The resulting mixture was stirred at room temperature for 2h under air. After removal of the solvent, the mixture was firstly purified through alumina gel column chromatrography (eluent: CHCl$_3$) and further purified by silica gel column chromatography (eluent: CHCl$_3$) to give the yellow solid compound 1,1',2-tricyano-2'-methoxyl-phenylethylene **1a** in 95% yield (0.99 g). ^{1}H NMR (500 MHz, CDCl$_3$, 298K): δ = 8.10 (d, 2H, phenyl; *J* = 9.2 Hz), 7.08 (d, 2H, phenyl; *J* = 9.2 Hz), 3.96 (s, 3H, -OMe).

Synthesis of 1b-2: A 5 mL water solution of NaOH (16 mg, 0.4 mmol, 0.04 equiv.) was added to a 30 mL methanol mixture of *p*-tolyaldehyde **1b-1** (12.0 g, 10 mmol) and malononitrile (7.92g, 12 mmol, 1.2 equiv.). The resulting mixture was stirred at RT for 0.5 h and the solid compounds were collected after filtration. Further purification was by silica gel column chromatography (CHCl$_3$) afford the light yellow compound 1,1'-dicyano-2-tolyethylene **1b-2** in 86% yield (14.4 g). ^{1}H NMR (500 MHz, CDCl$_3$, 298K): δ = 7.81 (d, 2H, phenyl; *J* = 8.3 Hz), 7.72 (s, H, ethylene), 7.34 (d, 2H, phenyl; *J* = 8.2 Hz), 2.45 (s, 1H, -CH$_3$).

Synthesis of 1b-3: KCN (1.02 g, 15.5 mmol) was dissolved in 20 mL water, stirred and heated at 60ºC. After the KCN was completely dissolved in the water, a 20 mL EtOH solution of 1,1'-dicyano-2-tolyethylene **1b-2** in EtOH (2.52 g, 15 mmol) was added, and continuously stirred at 60ºC for 15 min. After cooling to room temperature, a solution of acetic acid/water (2 mL in 10 mL water) was added. The solid-state compound was removed and the organic solution evaporated under vacuum. Further purification was carried out by column chromatography (eluent: CHCl$_3$:MeOH = 10:1) to afford a white solid state compound 1,1',2-tricyano-2'-tolylethane **1b-3** in 62% yield

(1.81 g). ^{1}H NMR (CDCl$_3$, 298K): δ = 7.38 (d, 2H, phenyl; J = 8.2 Hz), 7.32 (d, 2H, phenyl; J = 8.2 Hz), 4.41 (d, 1H, ethylene; J = 6.0 Hz), 4.20 (d, 1H, ethylene; J = 6.0 Hz), 2.41 (s, 3H, -CH$_3$).

Synthesis of 1b: 2,3-Dichloro-5,6-dicyano-p-benzoquinone (DDQ; 2.3 g 10.0 mmol, 2.0 equiv.) was added to a 50 mL CHCl$_3$ solution of 1,1',2-tricyano-2'-tolyethane **1b-3** (0.98 g, 5.0 mmol). The resulting mixture was stirred at room temperature for 2h under air. After removal of the solvent, the mixture was firstly purified through alumina gel column chromatrography (eluent: CHCl$_3$) and further purified by silica gel column chromatography (eluent: CHCl$_3$) to give the yellow solid state compound 1,1',2-tricyano-2'-tolyethylene **1b** in 92% yield (0.89 g) ^{1}H NMR (500 MHz, CDCl$_3$, 298K): δ = 7.95 (d, 2H, phenyl; J = 8.5 Hz), 7.41 (d, 2H, phenyl; J = 8.5 Hz), 2.50 (s, 3H, -CH$_3$).

Synthesis of 1c-2: A 5 mL water solution of NaOH (16 mg, 0.4 mmol, 0.04 equiv.) was added to a 30 mL methanol mixture of p-trifluoromethylbenzaldehyde **1c-1** (17.4 g, 10 mmol) and malononitrile (7.92g, 12 mmol, 1.2 equiv.). The resulting mixture was stirred at RT for 0.5 h and the solid state compounds were collected after filtration. Further purification was by silica gel column chromatography (CHCl$_3$) afford the white solid state compound 1,1'-dicyano-2-p-trifluoromethylphenylethylene **1c-2** in 80% yield (17.7 g). ^{1}H NMR (500 MHz, CDCl$_3$, 298K): δ = 8.01 (d, 2H, phenyl; J = 8.8 Hz), 7.84 (s, 1H, ethylene), 7.81 (d, 2H, phenyl; J = 8.4 Hz).

Synthesis of 1c-3: KCN (1.02 g, 15.5 mmol) was dissolved in 20 mL water, stirred and heated at 60°C. After the KCN was completely dissolved in the water, a 20 mL EtOH solution of 1,1'-dicyano-2-p-trifluoromethylphenyethylene **1c-2** (3.4 g, 15 mmol) was added, and continuously stirred at 60°C for 15 min. After cooling to room temperature, a solution of acetic acid/water (2 mL in 10 mL water) was added. The solid-state

compound was removed and the organic solution evaporated under vacuum. Further purification was carried out by column chromatography (eluent: $CHCl_3$:MeOH = 10:1) to afford a white compound 1,1',2-tricyano-2'-*p*-trifluoromethyl- phenylethane **1c-3** in yield 42% (1.57 g). ^{1}H NMR (CDCl$_3$, 298K): δ = 7.82 (d, 2H, phenyl; *J* = 8.2 Hz), 7.68 (d, 2H, phenyl; *J* = 8.2 Hz), 4.53 (d, 1H, ethylene; *J* = 5.7 Hz), 4.31 (d, 1H, ethylene; *J* = 5.7 Hz).

Synthesis of 1c: 2,3-Dichloro-5,6-dicyano-*p*-benzoquinone (DDQ; 2.3 g 10.0 mmol, 2.0 equiv.) was added to a 50 mL CHCl$_3$ solution of 1,1',2-tricyano-2'-*p*-trifluoromethylphenylethane **1b-3** (1.25 g, 5.0 mmol).   The resulting mixture was stirred at room temperature for 2h under air.   After removal of the solvent, the mixture was firstly purified through alumina gel column chromatrography (eluent: CHCl$_3$) and further purified by silica gel column chromatography (eluent: CHCl$_3$) to give the white solid state compound 1,1',2-tricyano-2'-*p*-trifluorophenylethylene **1c** in 75% yield (0.93 g). ^{1}H NMR (CDCl$_3$, 298K): δ = 8.10 (d, 2H, phenyl; *J* = 8.5 Hz), 7.90 (d, 2H, phenyl; *J* = 8.5 Hz).

3.3.5 Synthesis and isolation of *β*-aryl-*β'*-cyano subporphyrazine
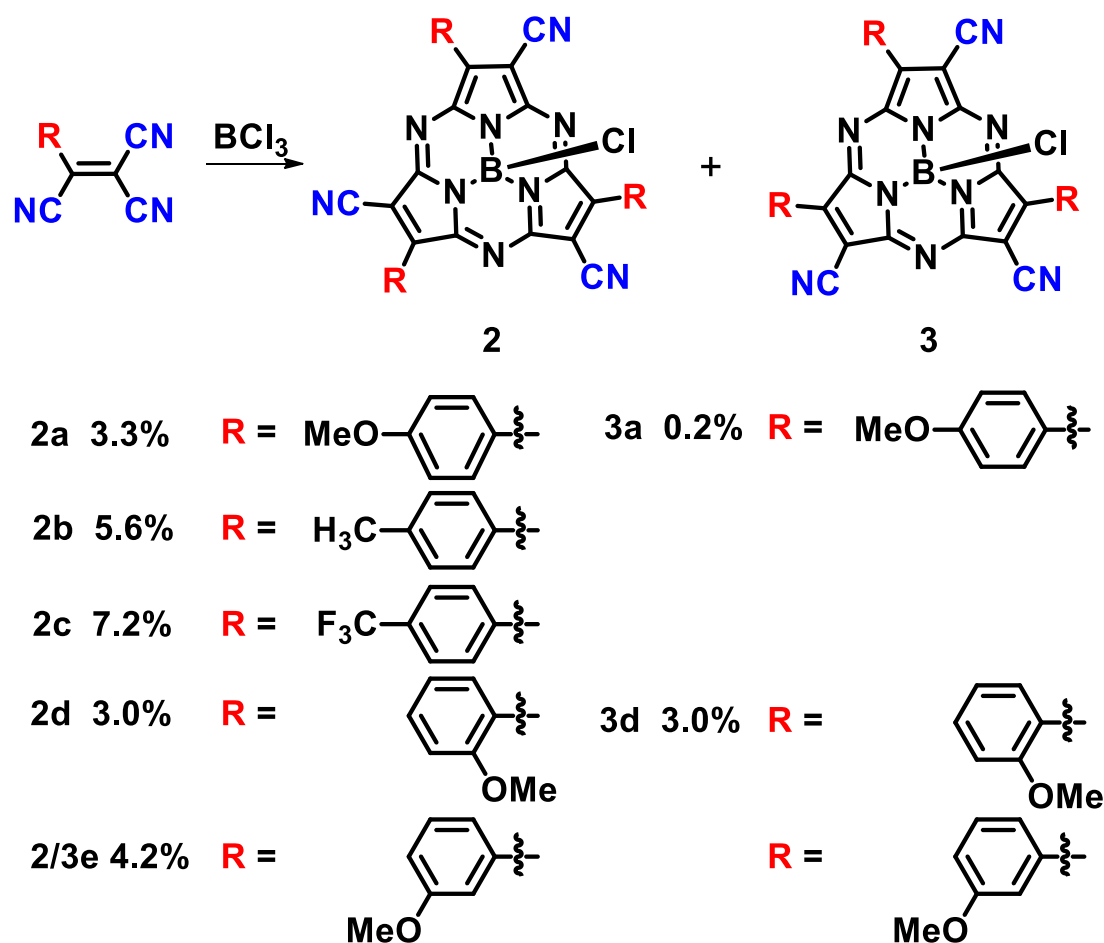
Scheme 3-3 Synthesis of push-pull subporphyrazines

Synthesis of 2a: Boron trichloride (1.0 M *p*-xylene solution, 0.35 mL, 0.35 equiv.) was added to 1,1,2-tricyano-2-*p*-methoxyphenylethylene **1a** (209 mg, 1.0 mmol) at room temperature. The resulting mixture was gradually heated at 140 ℃, and the temperature maintained for 45 min. After removal of the solvent, the reaction mixture was purified by silica gel column chromatography (eluent: toluene:ethylacetate = 10:1) and bio-beads (Sx-1) column (eluent: $CHCl_3$). Recrystallization from toluene and hexane provided compound **2a** in 3.3% yield (7.40 mg). ^{1}H NMR (500 MHz, $CDCl_3$): $\delta = 8.88$ (d, $J = 9.1$ Hz, 6H), 7.24 (d, $J = 9.1$ Hz, 6H), 4.00 ppm (s, 9H; -OMe); UV/vis (toluene): λ_{max} [nm] (ε) = 633 (42300), 435 (17300 M^{-1} cm^{-1}); HR-MALDI-TOF-MS: $m/z = 673.1547$ (Calcd. for $C_{36}H_{21}BClN_9O_3$ [M^+], 673.1544).

Synthesis of 2b: Boron trichloride (1.0 M *p*-xylene solution, 0.35 mL, 0.35 equiv.) was added to 1,1,2-tricyano-2-*p*-tolylethylene **1b** (193 mg, 1.0 mmol) at room temperature. The resulting mixture was gradually heated at 140 ℃, and the temperature maintained for 45 min. After removal of solvents under vacuum, the reaction mixture was purified by silica gel column chromatography (eluent: toluene:ethylacetate = 10:1), GPC-HPLC (eluent: CHCl₃). Recrystallization from toluene and hexane provided compound **2b** in 5.6% yield (11.7 mg). ^{1}H NMR (500 MHz, CDCl₃): δ = 8.71 (d, J = 8.3Hz, 6H), 7.55 (d, J = 8.1 Hz, 6H), 2.63 ppm (s, 9H; -CH₃); UV/vis (toluene): λ_{max} [nm] (ε) = 594 (41200), 419 (15400 M^{-1} cm^{-1}); HR-MALDI-TOF-MS: m/z = 625.1705 (Calcd. for $C_{36}H_{21}BClN_9$ [M^-], 625.1707).

Synthesis of 2c: Boron trichloride (1.0 M *p*-xylene solution, 0.35 mL, 0.35 equiv.) was added to 1,1',2-tricyano-2-*p*-trifloromethylphenyl-ethylene **1c** (193 mg, 1.0 mmol) at room temperature. The resulting mixture was gradually heated at 140 ℃, and the temperature maintained for 45 min. After removal of solvents under vacuum, the crude mixture was purified by silica gel column chromatography (eluent: toluene:ethylacetate = 8:1) and bio-beads (Sx-1) column (eluent: toluene). Recrystallization from toluene and hexane provided compound **2c** in 7.2% yield (18.9 mg). ^{1}H NMR (500 MHz, toluene-d_8): δ = 8.68 (d, J = 8.2Hz, 6H), 7.39 ppm (d, J = 8.3Hz, 6H); UV/vis (toluene): λ_{max} [nm] (ε) = 571 (41200), 390 (14900 M^{-1} cm^{-1}); HR-MALDI-TOF-MS: m/z = 787.0857 (Calcd. for $C_{36}H_{12}BClF_9N_9$ [M^-], 787.0859).

Synthesis of 3a: The subporphyrazine **3a** was isolated from the reaction mixture of the synthesis of **2a**, and the reaction mixture was purified by silica gel column chromatography (eluent: toluene:ethylacetate = 10:1) and bio-beads (Sx-1) column (eluent: CHCl₃). Recrystallization from toluene and hexane provided the target compound in a 0.2% yield (0.45 mg). ^{1}H NMR (500 MHz, CD₂Cl₂): δ = 8.91 (d, J = 9.0 Hz, 2H); 8.78 (d, J =9.0Hz, 2H), 8.71 (d, J = 9.0Hz, 2H), 7.30 (d, J = 9.1Hz, 2H),

7.23 (d, $J = 9.1$ Hz, 2H), 7.20 (d, $J = 9.1$ Hz, 2H), 4.01 (s, 3H; -OMe), 3.98 (s, 3H; -OMe), 3.96 ppm (s, 3H; -OMe); UV/vis (toluene): λ_{max} [nm] (ε) = 629 (41000), 499 (27100), 435 (22700 M^{-1} cm^{-1}); HR-MALDI-TOF-MS: m/z = 673.1553 (Calcd. for $C_{36}H_{21}BClN_9O_3$ [M^-], 673.1555).

Synthesis of 2d: The subporphyrazine **3a** was isolated from the reaction mixture of the synthesis of **2a**, and the reaction mixture was purified by silica gel column chromatography (eluent: toluene:ethylacetate = 10:1) and bio-beads (Sx-1) column (eluent: CHCl$_3$). ^{1}H NMR (500 MHz, CD$_2$Cl$_2$): δ = 8.29 (dd, $J_1 = 1.7$ Hz, $J_1 = 7.7$ Hz 3H); 7.77 (m, 3H), 7.36 (d, $J = 9.0$ Hz, 2H), 7.30 (d, $J = 9.1$ Hz, 2H), 7.23 (d, $J = 9.1$ Hz, 2H), 3.96 ppm (s, 3H; -OMe); UV/vis (toluene): λ_{max} [nm] (ε) = 582 (39000 M^{-1} cm^{-1}); HR-MALDI-TOF-MS: m/z = 673.1548 (Calcd. for $C_{36}H_{21}BClN_9O_3$ [M^-], 673.1545).

Synthesis of 3d: The subporphyrazine **3a** was isolated from the reaction mixture of the synthesis of **2a**, and the reaction mixture was purified by silica gel column chromatography (eluent: toluene:ethylacetate = 10:1) and bio-beads (Sx-1) column (eluent: CHCl$_3$). ^{1}H NMR (500 MHz, CD$_2$Cl$_2$): δ = 8.91 (d, $J = 9.0$ Hz, 2H); 8.78 (d, $J = 9.0$ Hz, 2H), 8.71 (d, $J = 9.0$ Hz, 2H), 7.30 (d, $J = 9.1$ Hz, 2H), 7.23 (d, $J = 9.1$ Hz, 2H), 7.20 (d, $J = 9.1$ Hz, 2H), 4.01 (s, 3H; -OMe), 3.98 (s, 3H; -OMe), 3.96 ppm (s, 3H; -OMe); UV/vis (toluene): λ_{max} [nm] (ε) = 629 (41000), 499 (27100), 435 (22700 M^{-1} cm^{-1}); HR-MALDI-TOF-MS: m/z = 673.1553 (Calcd. for $C_{36}H_{21}BClN_9O_3$ [M^-], 673.1555).

3.4.1 ^{1}HNMR Spectra of Push-Pull Type Subporphyrazines

In the HNMR spectra, C_3 symmetry 2a, 2b and 2c reveal similar proton NMR singals from phenyl substituents. Two doublet peaks appeared at $\delta = 8.88$, 7.24 ppm and only one singlet peak at $\delta = 4.00$ ppm indicate the C_3 symmetry molecular structure of **2c**.
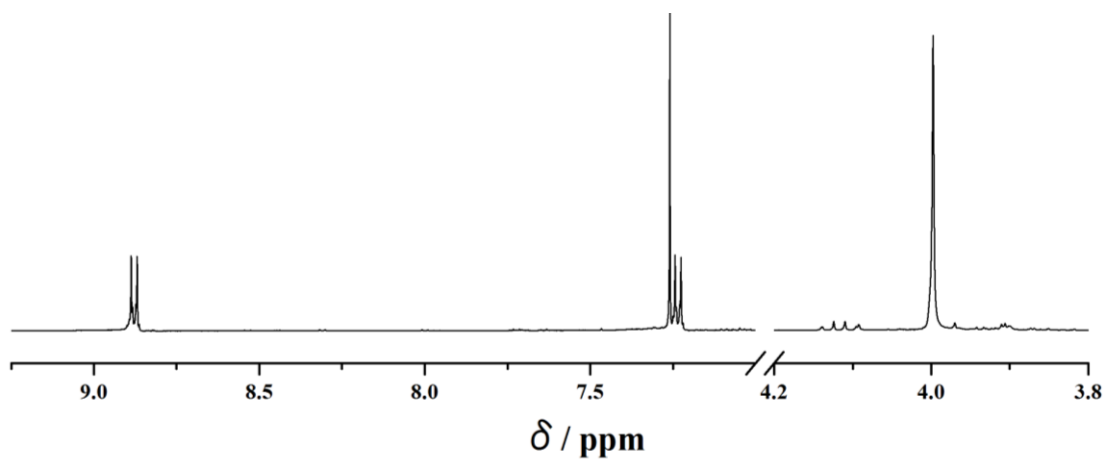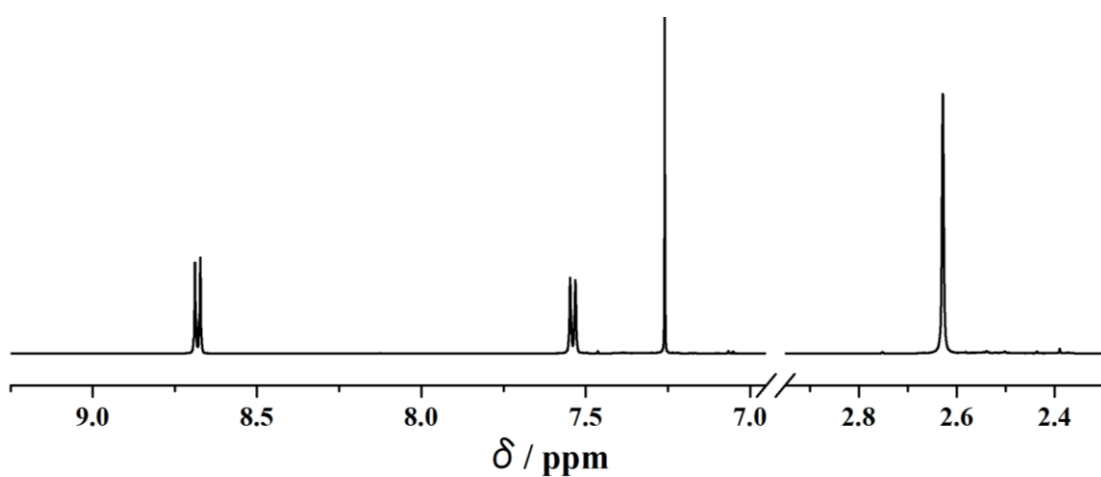
Figure 3-7. ^{1}H NMR spectra of **2a** in CDCl$_3$.

Figure 3-8. ^{1}H NMR spectra of **2b** in CDCl$_3$.
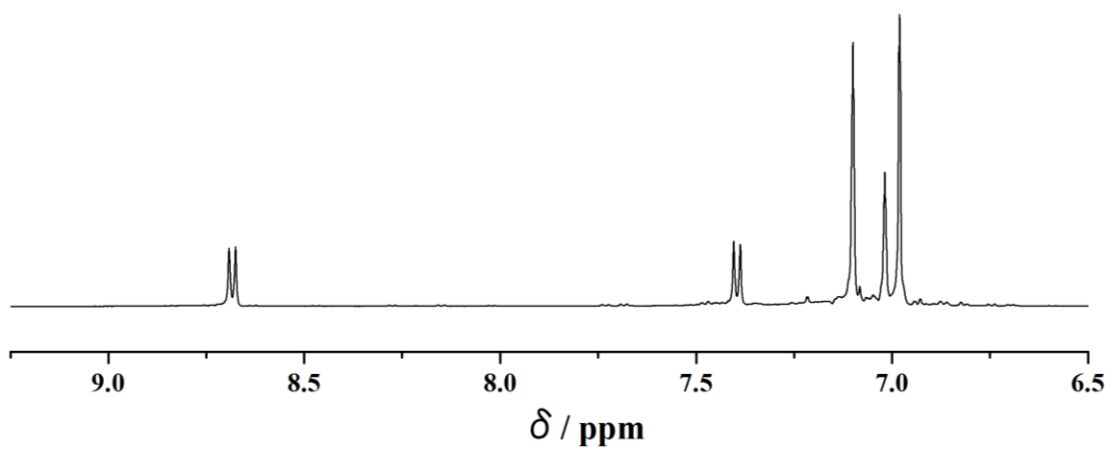

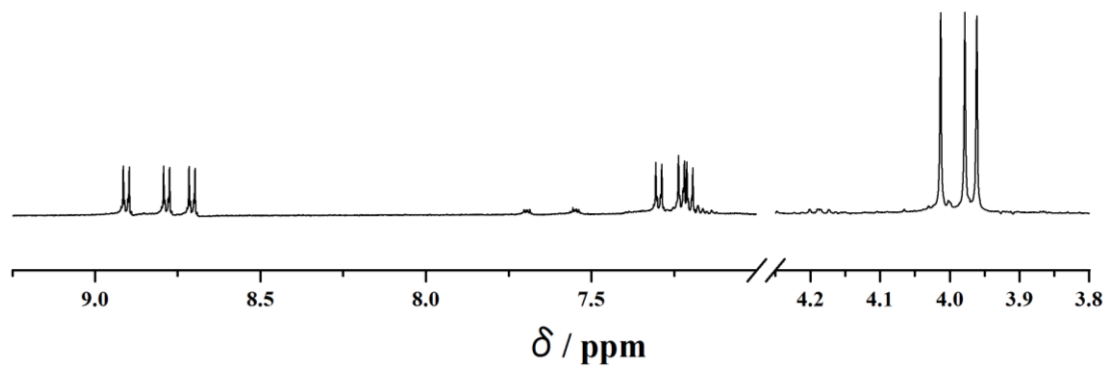**Figure 3-9.** ^{1}H NMR spectra of **2c** in toluene-d_8.

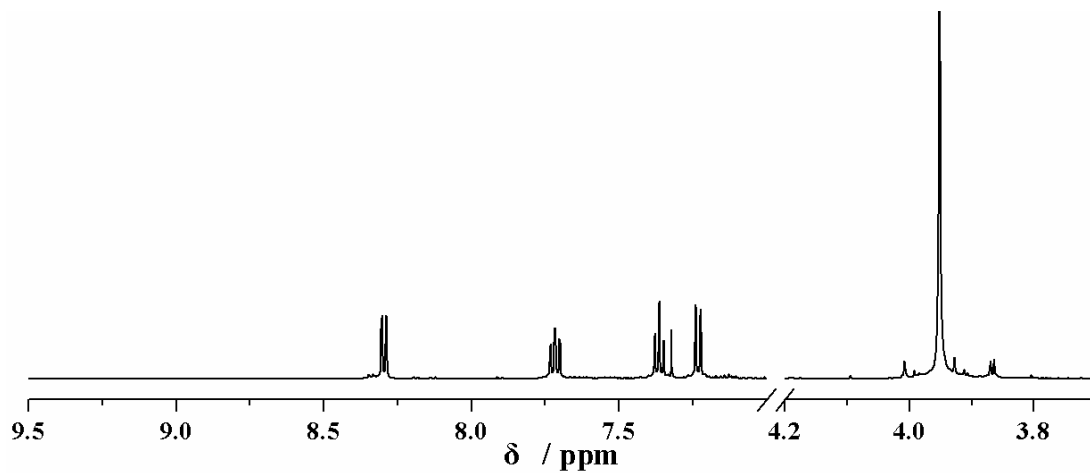**Figure 3-10** ^{1}H NMR spectra of **3a** in CD_2Cl_2.

Figure 3-11 ^{1}H NMR spectra of **2d** in CD_2Cl_2.
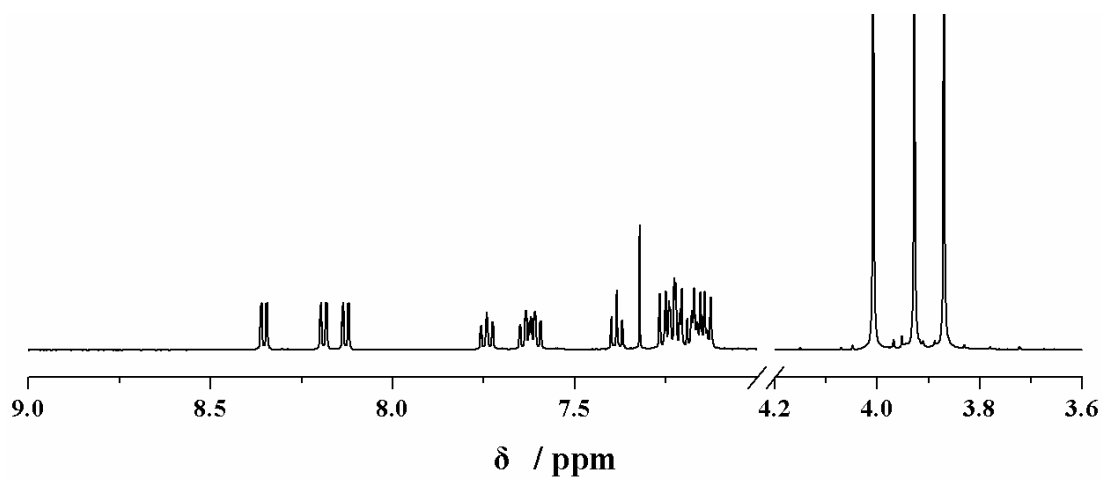
Figure 3-12 ^{1}H NMR spectra of **2d** in CD_2Cl_2.

3.4.2 X-ray Crystal Structure of SubPz 2c

Suitable crystals were obtained from slowly diffusion hexane into a toluene solution with a racemic mixture of **2c**. The crystal structure of **2c** exhibited C_3 symmetric arrangement of cyano and *p*-trifluoromethylphenyl substituents at the *β*-positions. Since subporphyrazine have a bowl-shaped molecular structure which clearly shown in the side view of the crystal structure. The racemic mixtures of both enantiomers with clockwise and anticlockwise arrangement of these substituents were also confirmed by X-ray crystal analysis.

Figure 3-13 X-ray crystal structure of **1a**, top view (up) and side view (bottom). The thermal elipsolids are scaled to the 50% probability level. Hydrogen atoms and solvent molecules are omitted for clarity. *β-p*-trifluoromethylphenyl and *β*-cyano units were omitted for clarity in the view side.
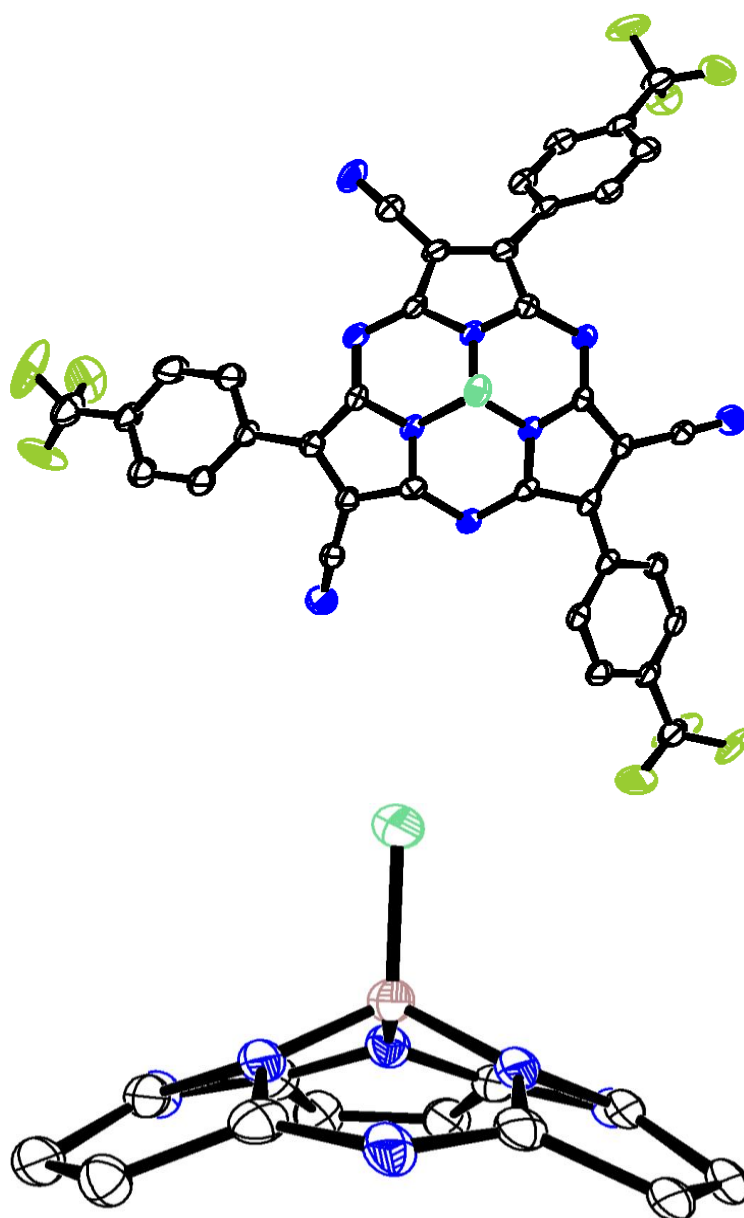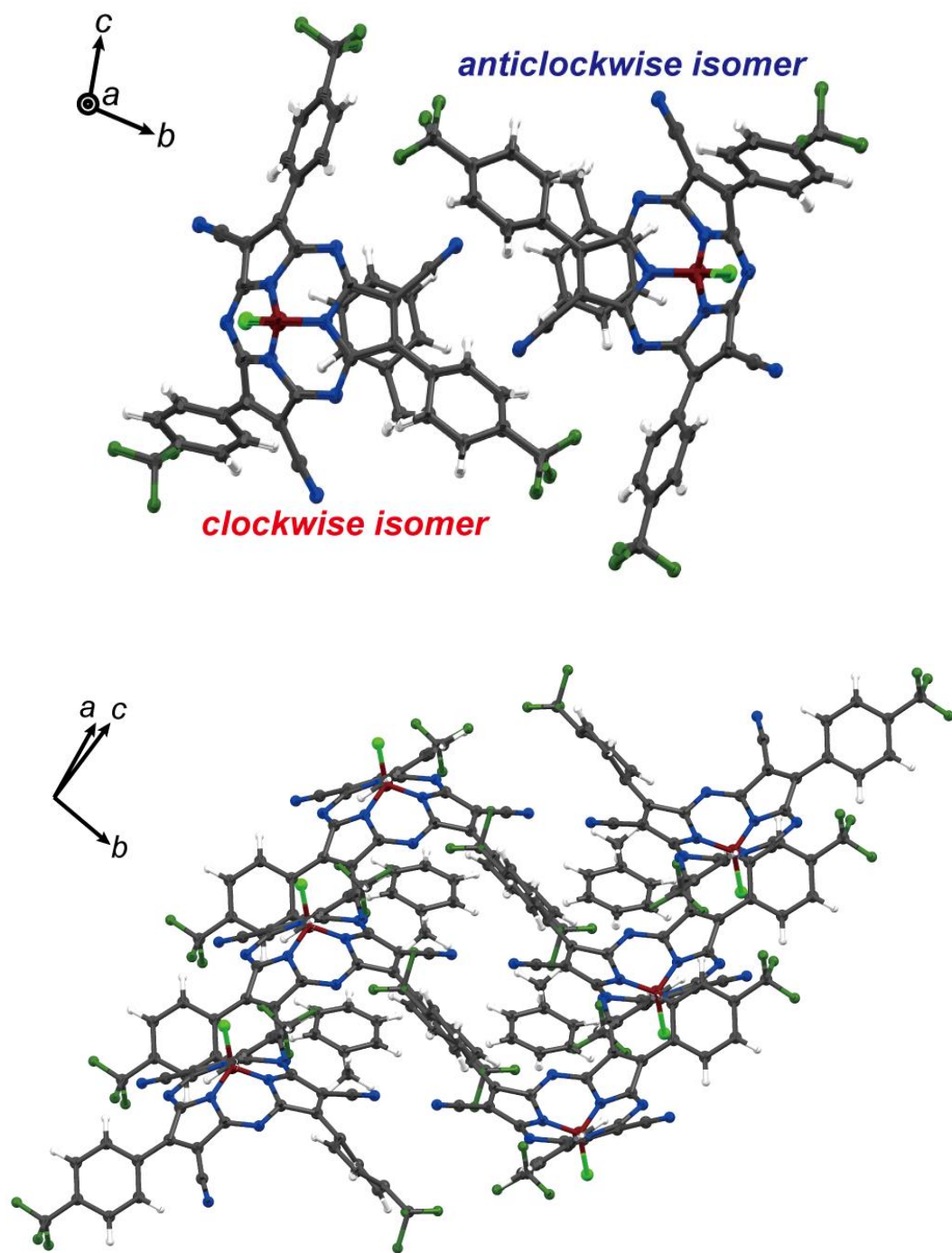
Figure 3-14. Crystal packing diagram of **2c**.

3.4.3 Spectroscopic Properties

3.4.3.1 Absorption and MCD spectra

The electronic absorption spectra of C_3 symmetry **2c** exhibits the main absorption band (Q-band) at 571 nm (**Figure 3-15** (bottom)), the soret band appears at 320 nm while an extra band appeared at 390 nm. **2b** and **2a** with increased electron donating abilities of push-substituents, exhibit similar shaped, but red-shift of the main absorption bands and the extra bands at 594, 419 nm for **2b**, and 633, 435 nm for **2a**. A significant red-shift of the main absorptions was observed in all these push-pull type subporphyrazines compared with the regular one (72 nm for **2c**, 95 nm for **2b**, and 134 nm for **2a**). Based on these results, we confirmed introduction of push-pull substituents to the subporphyrazine core is an effective strategy to control the red-shift of main absorptions. The broad absorption observed between the Q band and Soret band in the absorption spectra of **2a**–**2c**, is, therefore, considered to be composed of both intramolecular CT transitions from the HOMO-1 and HOMO-2 to the LUMO and p–p* transitions between the SubPz-centred HOMO-3 and LUMO. The peripherally aryl-substituted SubPzs also exhibit similar CT absorption in the similar region.[1]

Based on the same molecular symmetry of C_3, the MCD spectra of **2a**, **2b** and **2c** exhibited similar spectral shape and red-shift of the spectral resonance with negative to positive envelops which can be assigned as Faraday A term, at 580, 608 and 649 nm, respectively.[9] These MCD spectral features of **2a**, **2b** and **2c** in the Q band region indicate non-degenerate excited states. These entire compounds exhibit the negative-to-positive sequence of the MCD signals in ascending energy infers a greater energy difference between the first and second HOMOs (ΔHOMO) than that of the LUMOs (ΔLUMOs). Plots of position of the Q bands of the push-pull subporphyrazines versus Hammett σ_p parameters was shown in **Figure 3-16**, the extent of the red-shift is proportional to the donor ability of the push-substituent, which is broadly supported by a linear correlation between the position of the Q band absorptions and the Hammett σ_p parameters of the substituents of the aryl groups
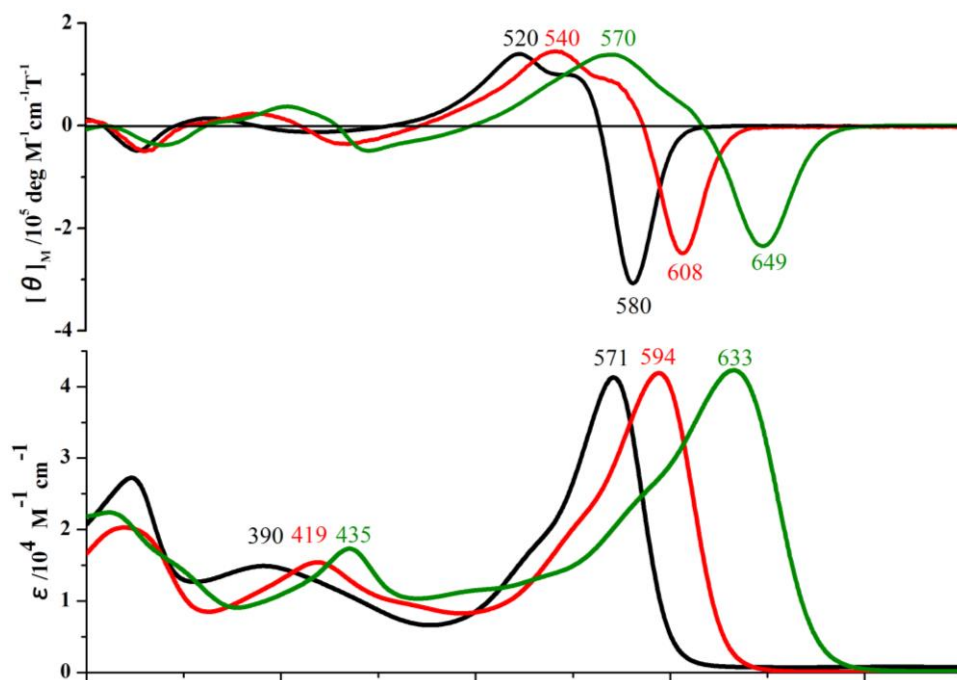
Figure 3-15 Magnetic circular dichlorism (up) spectra and absorption spectra

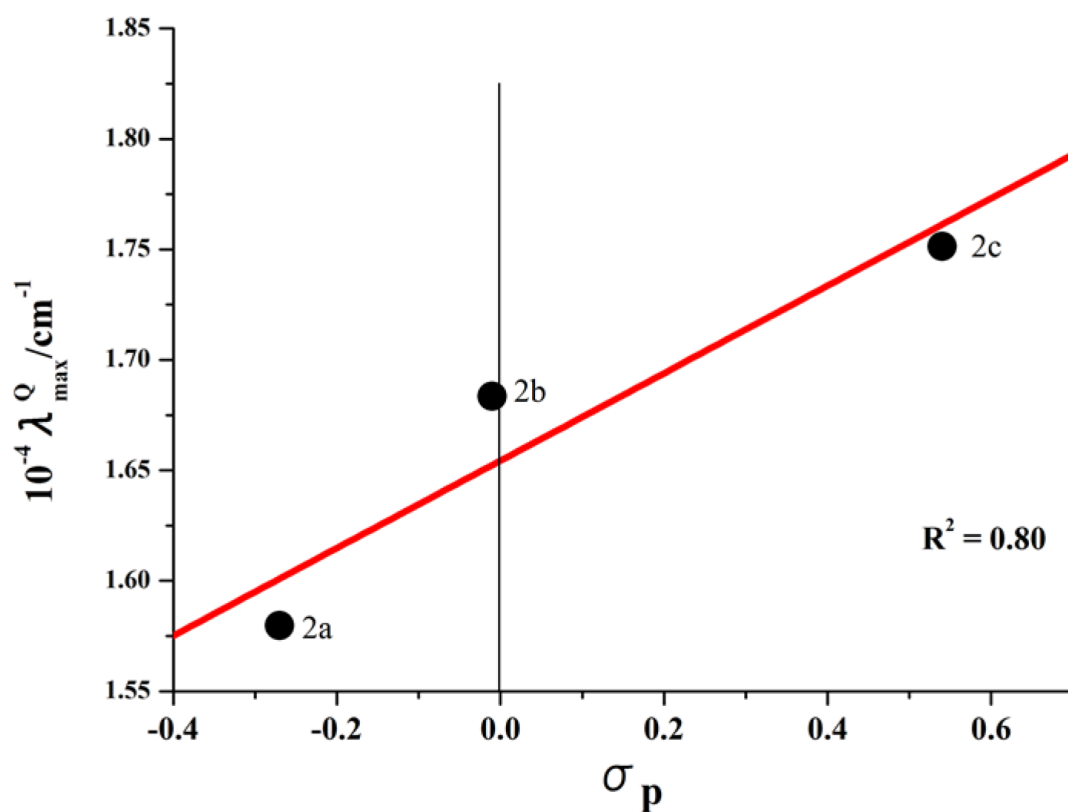(bottom) of compound **2a** (green) , **2b** (red) and **2c** (black).

Figure 3-16 Plots of position of the Q bands of the push-pull subporphyrazines versus

Hammett σ_p parameters.

In the case of **3a**, the C_1 symmetric isomer for that of **2a**, exhibits main absorption band at 626 nm and extended to the broader region of absorptions. The assigned pseudo Faraday A term of **3a** in the Q band region, broad shape at 643 nm, which is observed when two Faraday *B* terms lie close in energy, and the spectral feature of **3a** explain of non-degenerate excited states due to the molecular symmetry lower than C_3. The negative-to-positive sequence of the MCD signals of **2c** in ascending energy infers a greater energy difference between the first and second HOMOs (ΔHOMO) than that of the LUMOs (ΔLUMOs).

Figure 3-17 Magnetic circular dichlorism (up) spectra and absorption spectra (bottom) of compound **2a** (green), **3a** (blue).

3.4.3.2 Fluorescence spectra

These push-pull type subporphyrazines can also be emitted in the solution state. **2c** exhibits the intense fluorescence at 591 nm with stokes' shift of 649 cm^{-1}, which is larger that the common subphthalocyanines and subporphyrazines. Red-shift of the fluorescence peaks were observed for **2b** and **2a** with similar stokes shift and quantum

yield (705 cm^{-1}, 0.16 for **2b** and 692 cm^{-1}, 0.16 for **2a**). **3a** exhibits the fluorescence band at 696 nm, which has a similar quantum yield 0.18 but a larger stokes' shift, is 1004 nm^{-1}.
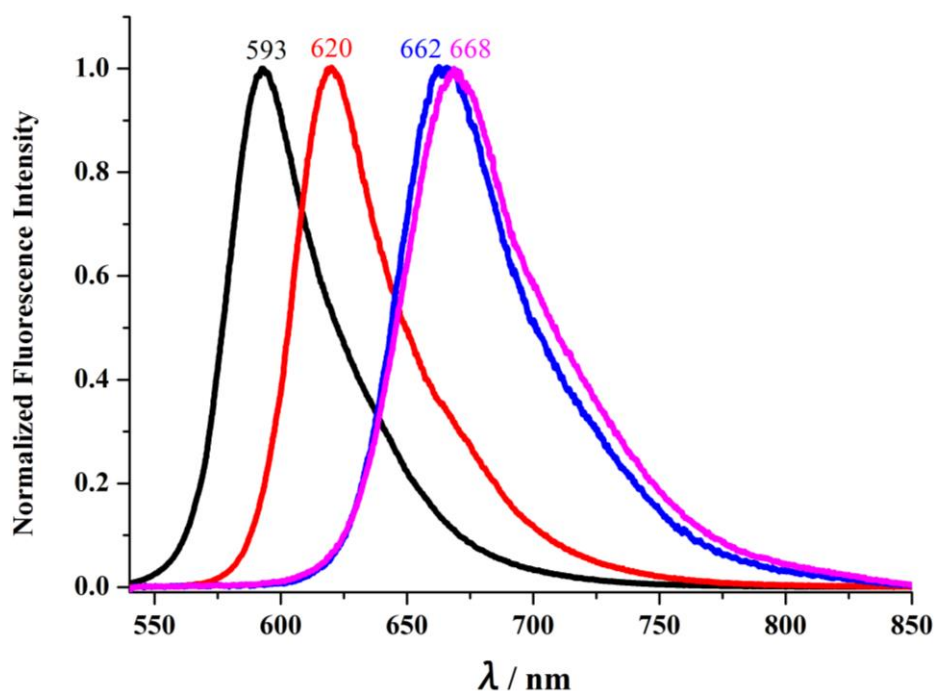
Figure 3-18 Fluorescence spectra of compound **2c** (purple), **2b** (red)**, 2c** (black), and and **3a** (blue) in toluene.

3.4.3.3 Spectroscopic properties of 2d and 3d

The spectroscopic properties of **2d** (**Figure 3-19**) including absorption, MCD and fluorescence spectra exhibits similar sharp, but blue-shift of the main absorption band at the shorter wavelength region. The smaller perturbation from the push-o-methoxylphenyl unit to the subporphyrazine core results the blue shift of the main absorption band at 582 nm. Based on the same molecular symmetry of C_3, the MCD spectra of **2d** exhibited similar spectral shape and red-shift of the spectral resonance with negative to positive envelops which can be assigned as Faraday A term, at 595 nm. This MCD spectral features of **2d** in the Q band region indicate non-degenerate excited states. These entire compounds exhibit the negative-to-positive sequence of the MCD signals in ascending energy infers a greater energy difference between the first and

second HOMOs (ΔHOMO) than that of the LUMOs (ΔLUMOs).

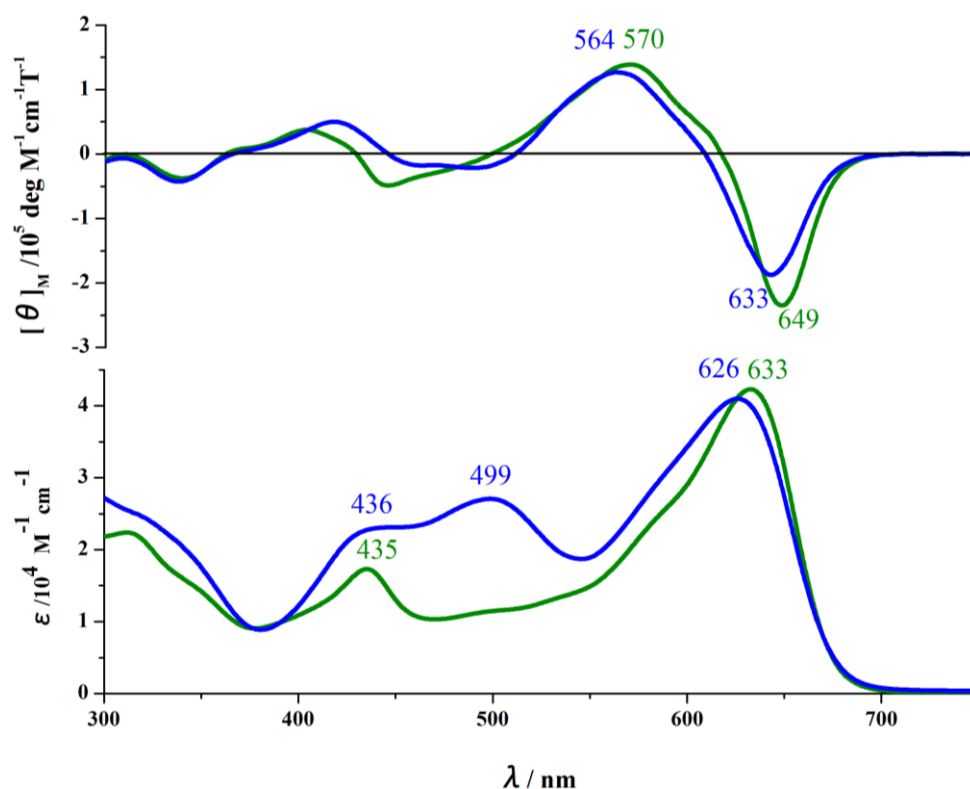**Figure 3-19** Magnetic circular dichlorism (up) spectra, absorption spectra (bottom, solid line) fluorescence spectra (bottom, solid line) of **2a** (green), **2d** (red) in toluene.

Similar blue shift of the main absorption band was also observed in the case of **3d**, the C_1 symmetric isomer for that of **2d**, exhibits main absorption band at 577 nm and extended to the broader region of absorptions.   The assigned pseudo Faraday A term of **3d** in the Q band region, broad shape at 593 nm, which is observed when two Faraday *B* terms lie close in energy, and the spectral feature of **3d** explain of non-degenerate excited states due to the molecular symmetry lower than C_3.   The negative-to-positive sequence of the MCD signals of **3d** in ascending energy infers a greater energy difference between the first and second HOMOs (ΔHOMO) than that of the LUMOs (ΔLUMOs).
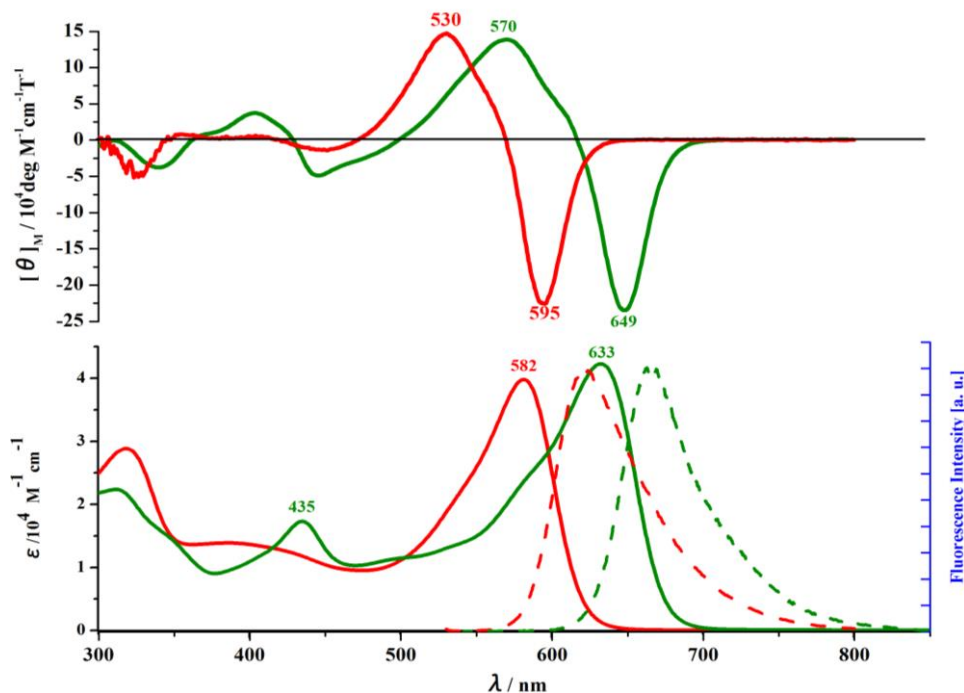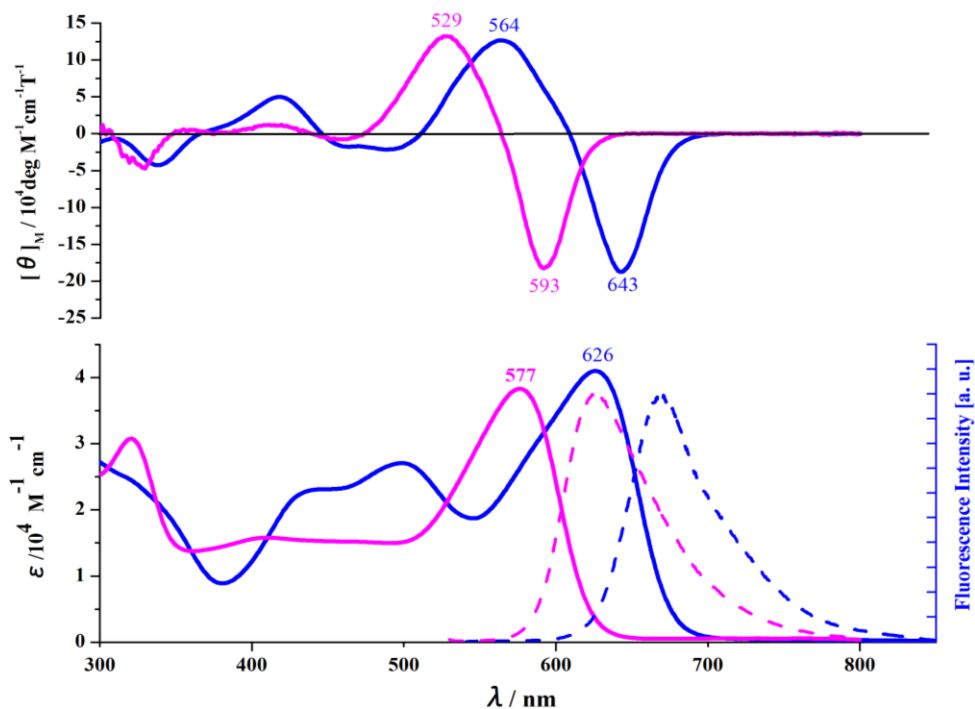
Figure 3-20 Magnetic circular dichlorism (up), absorption (bottom, solid line) fluorescence spectrums (bottom, dashed line) of **3a** (blue), **3d** (purple) in toluene.

3.4.4 Chiral Separation and CD Spectra of 2b

Optical resolution of **2b** was performed on an equipped with a chiral column using toluene to give us two main fractions (**2bFr1** and **2bFr2**) and the CD spectra was also measured in toluene. In the CD spectra (**Figure 3-21**), the first fraction **2bFr1** exhibits a negative-positive-negative-positive sign in the detection region from 750 nm to 300 nm, where the second fraction **2bFr2** exhibits a mirror-imaged positive and negative signs in the corresponding regions. The molecular chirality is originally come from the clockwise or anti clockwise arrangement of push-pull substituents at *β,β'*-positions of bowl shape subpz moieties which can be regarded as a kind of "bowl chirality".
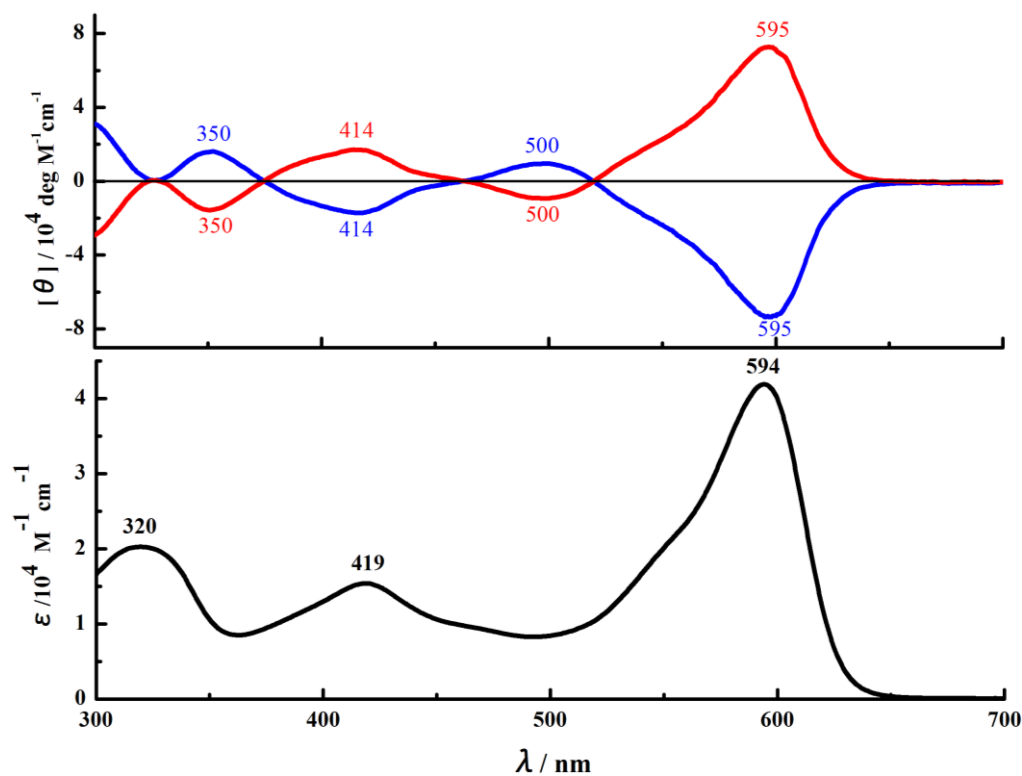
Figure 3-21 Cicular dichlorism (up) and absorption spectra (bottom) of enantiomers of **2b** in toluene.

3.5 Theoretical Calculations

In order to in-depth understand the electronic structures of these subporphyrazines compounds, theoretical calculations were successfully carried out. Structural optimization using **2a**, **2b**, **2c**, **3a**, and regular unsubstituted subporphyrazine **3** as the model compounds that were performed based on the DFT method at the B3LYP/63-1G(d) level. The time dependent (TD) DFT calculation was also carried out at the same level. In the frontier MOs (**Figure 3-22**) of **2c** and unsubstituted subPz **4**, similar electron density distribution pattern were observed, and the delocalization of electron density on the exterior β-trifluoromethylphenyl and β-cyano substituents were also confirmed. The non-degenerated LUMO and LUMO+1 orbitals of **2c** reproduced the observed Faraday A terms in the MCD spectra. Compared with SubPz **4**, the HOMO and the LUMO energy levels of **2c** was stabilized by introduction of pull-substituent at

83

pyrrole *β*-position, but the decrease of the LUMO is more significant.   Whereas the HOMO-1 and HOMO-2 localize on the push–pull substituents.   This finally results a decreased energy gap between the HOMO-LUMO orbital for **2c**, is -2.64 eV (-3.29 eV for **4**) and further suggested the red-shift of the main absorption band was caused by the introduction of the pull-substituents.
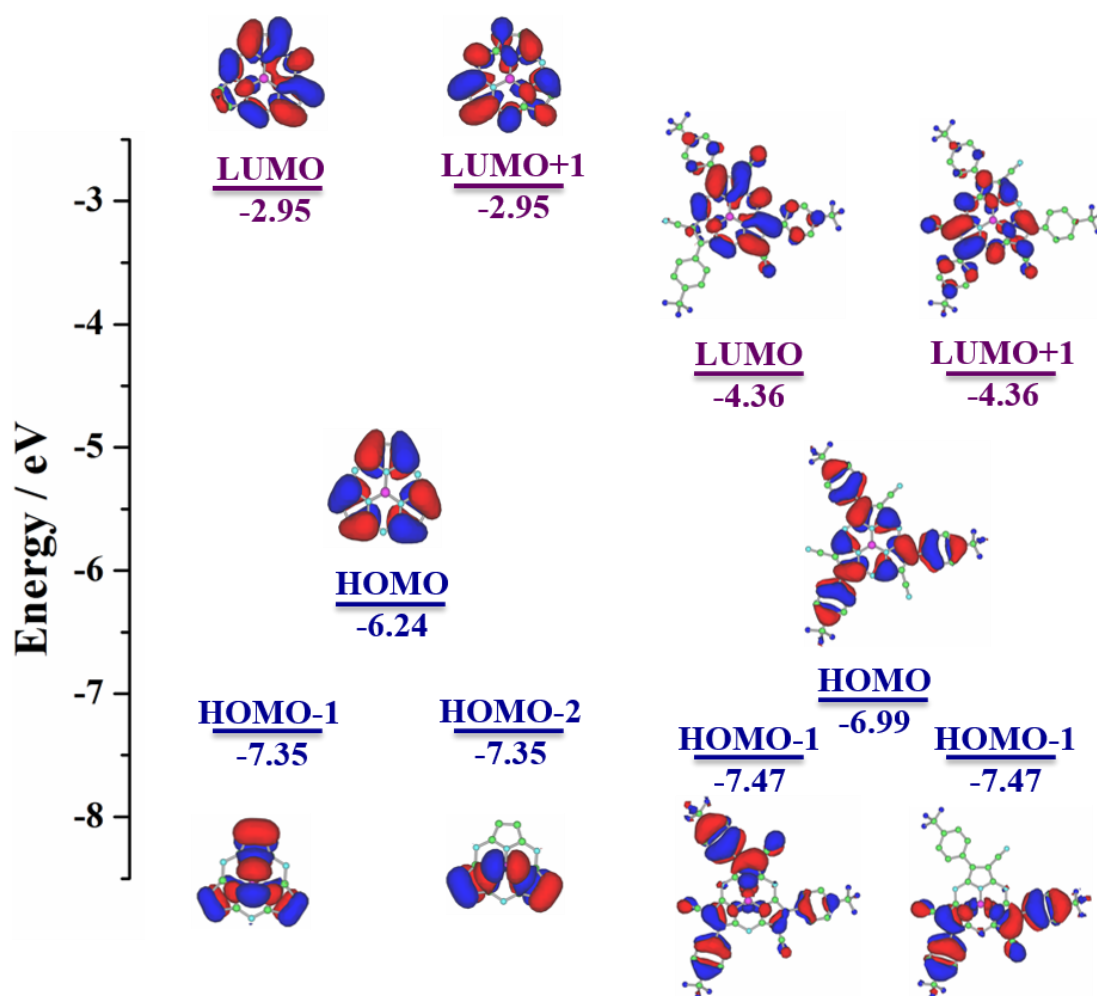
Figure 3-22 Partial MO diagrams of **2c** (left) and non-substituted SubPz **4** (right).

In the frontier MOs of **2a**, **2b** and **2c** (**Figure 3-23**), similar electron density distribution pattern and the delocalization of electron density on the exterior β-aryl and β-cyano substituents were confirmed. The non-degenerated LUMO and LUMO+1 orbitals of **2a**, **2b** and **2c** were also reproduced the observed Faraday A terms in the MCD spectra. With the increase of the electro donating ability of β-aryl (Push-) substituent, the HOMO and the LUMO energy levels were destabilized, and the destabilization of the LUMO is more significant. The selected transitions of **2a**, **2b** and **2c** were shown in **Figure 3-24**, the lowest energy transitions are mainly from the HOMO orbitals to the LUMO and the LUMO+1 orbitals. The significant red-shift of the
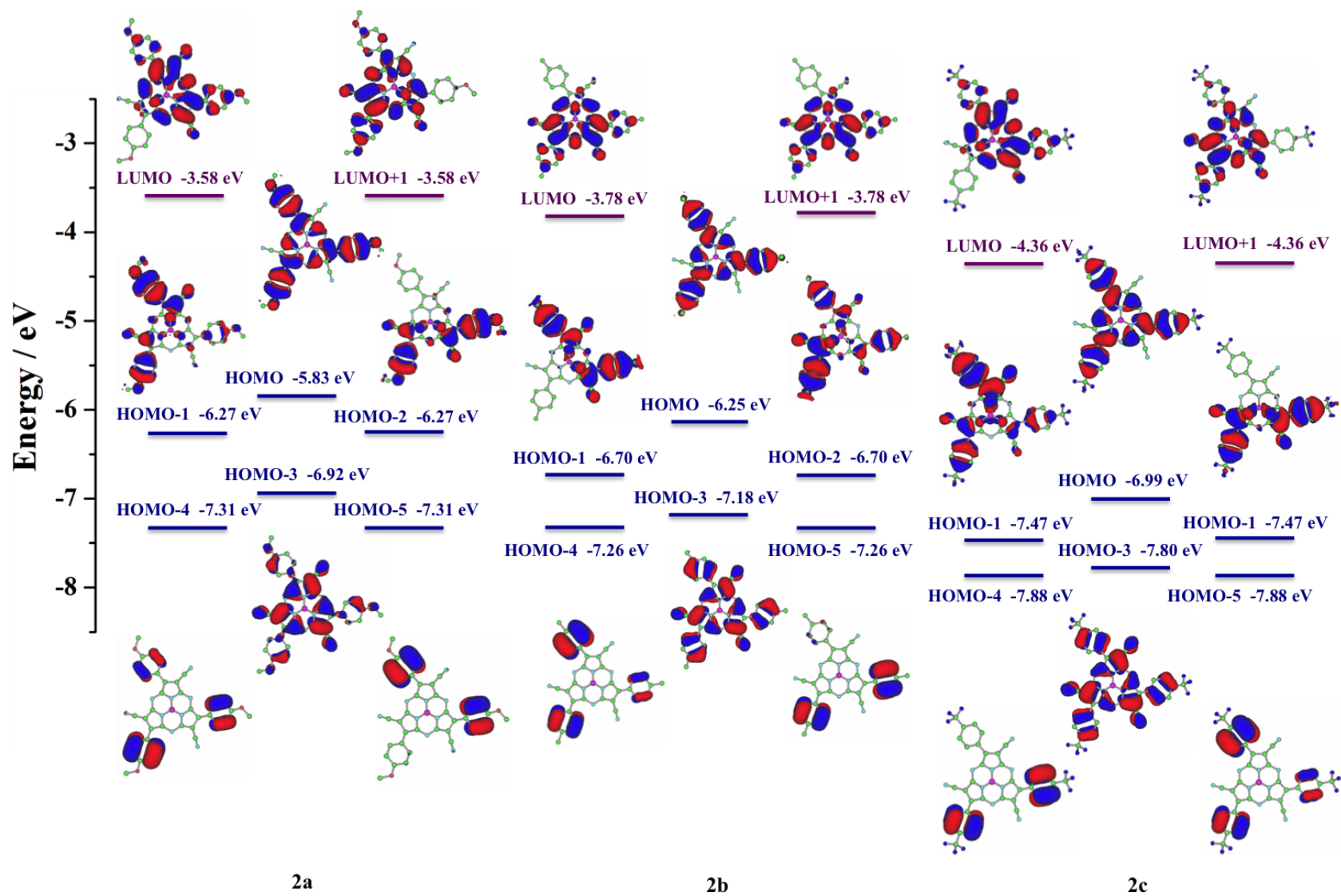
Figure 3-23 Partial MO diagrams of **2a** (left), **2b** (middle) and **2c** (right).
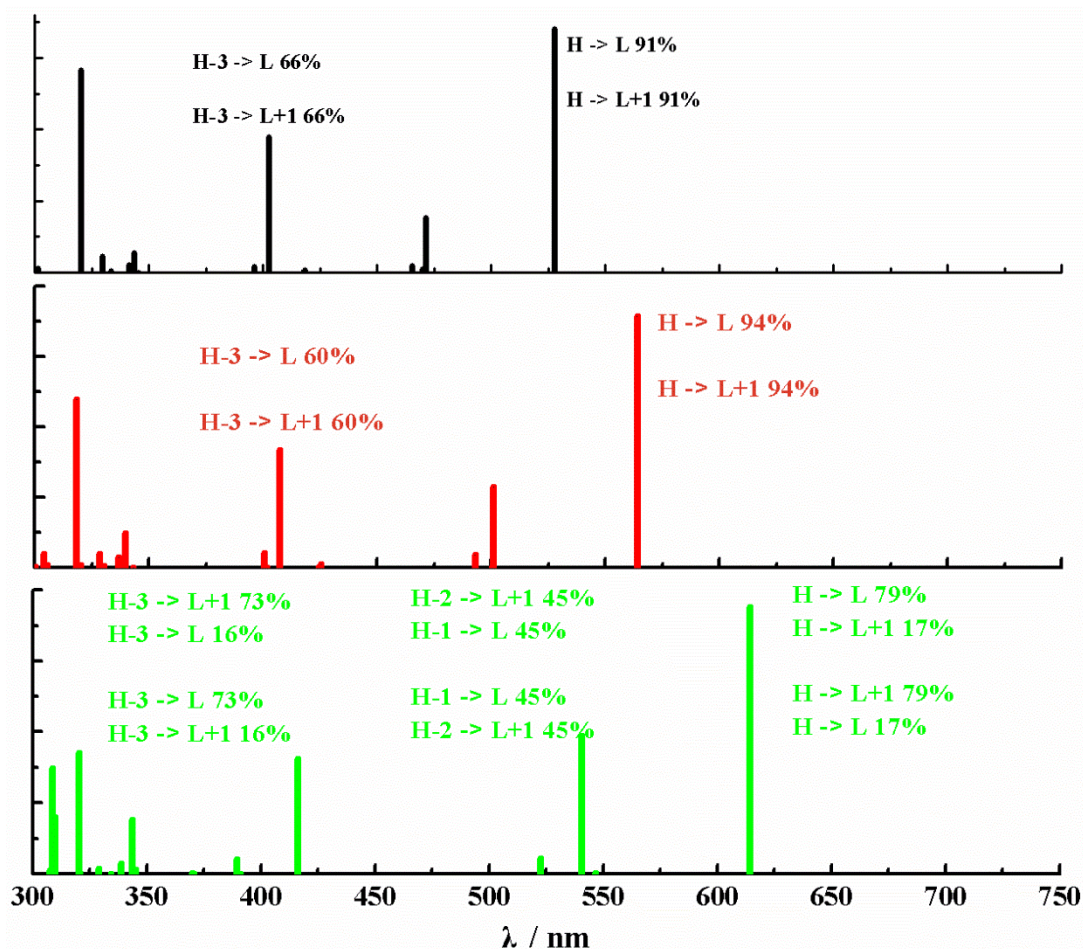
Figure 3-24 Selected transitions of **2a** (bottom), **2b** (middle) and **2c** (top)**.**

The partial MO diagrams of C_3 symmetry **2a** and C_1 symmetry **3a** were shown in **Figure 3-25**, the LUMO and LUMO+1 orbitals of **3a** were non-degenerated that reproduced pseudo-Faraday A term on the MCD spectra. The energy spilt of molecular orbitals HOMO-1 and HOMO-2 was only observed in the case of **3a**. All these difference is due to transitions between these non-degenerated orbitals extended the electronic absorptions across the broader region compared with **3a**.

Figure 3-25 Partial MO diagrams of **2a** (left), **3a** (right).

Table 3-1 Selected transition energies and wave functions of **1a** and **2a** calculated by the TDDFT method (B3LYP/6-31G(d)).

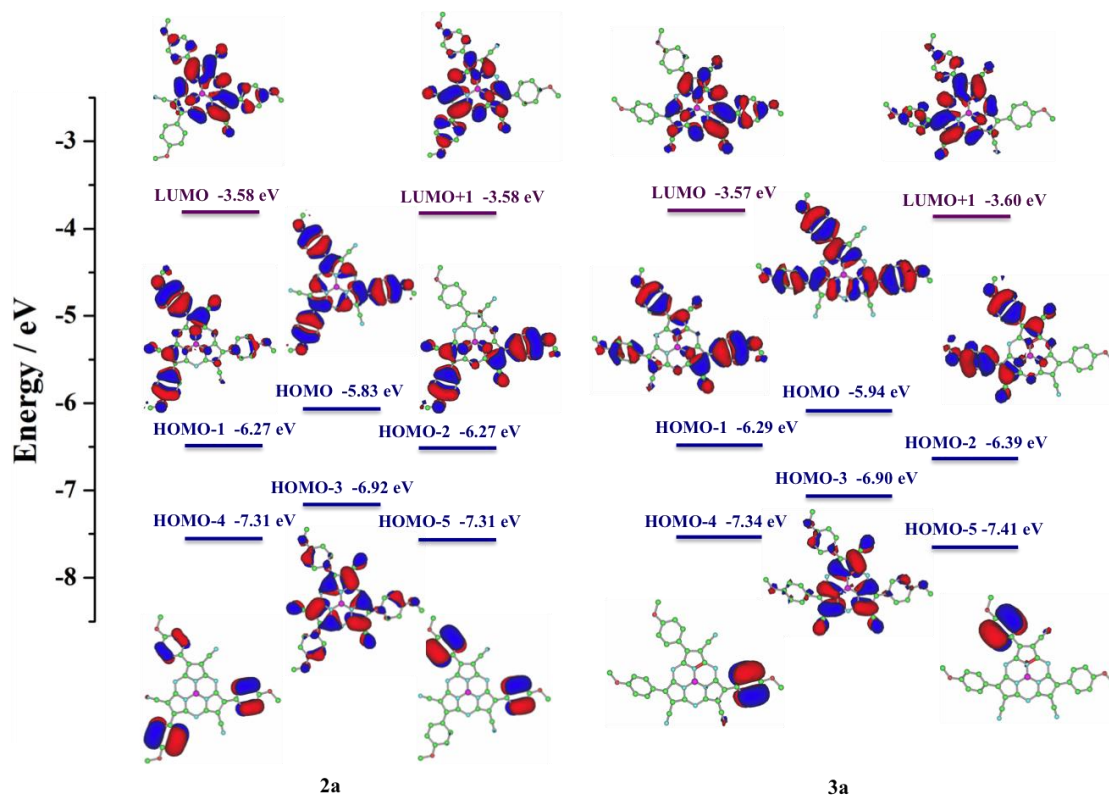| No.	Energy [nm]	f [a]	Wave function[b]
2a	614	0.376	$+0.629\|L \leftarrow H> + 0.290\|L+1 \leftarrow H> + \ldots$
	614	0.376	$+0.629\|L+1 \leftarrow H> + 0.290\|L \leftarrow H> + \ldots$
	547	0.195	$+0.472\|L+1 \leftarrow H–2> + 0.472\|L \leftarrow H–1> – 0.142\|L \leftarrow H–2> + 0.142\|L+1 \leftarrow H–1> + \ldots$
	547	0.195	$+0.472\|L+1 \leftarrow H–1> – 0.472\|L \leftarrow H–2> – 0.142\|L+1 \leftarrow H–2> – 0.142\|L \leftarrow H–1> + \ldots$
	416	0.162	$+0.606\|L+1 \leftarrow H–3> + 0.280\|L \leftarrow H–3> – 0.132\|L \leftarrow H–9> + \ldots$
	416	0.162	$+0.606\|L \leftarrow H–3> – 0.280\|L+1 \leftarrow H–3> + 0.132\|L+1 \leftarrow H–9> + \ldots$
2b	564	0.356	$+0.687\|L \leftarrow H> \; + \ldots$
	564	0.356	$+0.687\|L+1 \leftarrow H> \; + \ldots$
	501	0.115	$+0.357\|L+1 \leftarrow H–2> – 0.357\|L \leftarrow H–1> + 0.344\|L \leftarrow H–2> \; + 0.344\|L+1 \leftarrow H–1> + \ldots$
	501	0.115	$+0.357\|L \leftarrow H–2> + 0.357\|L+1 \leftarrow H–1> – 0.344\|L+1 \leftarrow H–2> + 0.344\|L \leftarrow H–1> + \ldots$
	407	0.167	$+0.550\|L+1 \leftarrow H–3> + 0.199\|L+1 \leftarrow H–6> \; – 0.168\|L \leftarrow H–5> – 0.168\|L+1 \leftarrow H–4>$
	407	0.167	$+0.148\|L+1 \leftarrow H–5> – 0.148\|L \leftarrow H–4> \; – 0.130\|L \leftarrow H–8> \; – 0.122\|L \leftarrow H–3> + \ldots$ $+0.550\|L \leftarrow H–3> + 0.199\|L \leftarrow H–6> \; – 0.168\|L+1 \leftarrow H–5> + 0.168\|L \leftarrow H–4> –$ $0.148\|L \leftarrow H–5> – 0.148\|L+1 \leftarrow H–4> + 0.130\|L+1 \leftarrow H–8> + 0.122\|L+1 \leftarrow H–3> + \ldots$

2c	528	0.341	$+0.677|L \leftarrow H> - 0.122|L+1 \leftarrow H–3> + 0.109|L+1 \leftarrow H> + \ldots$
	528	0.341	$+0.677|L+1 \leftarrow H> + 0.122|L \leftarrow H–3> - 0.109|L \leftarrow H> + \ldots$
	403	0.190	$+0.574|L+1 \leftarrow H–3> - 0.118|L \leftarrow H–9> - 0.127|L+1 \leftarrow H–9> - 0.219|L+1 \leftarrow H–6> +$
	403	0.190	$0.153|L+1 \leftarrow H–5> + 0.153|L \leftarrow H–4> - 0.114|L \leftarrow H–3> + 0.112|L \leftarrow H> + \ldots$
			$+0.574|L \leftarrow H–3> - 0.153|L \leftarrow H–5> + 0.153|L+1 \leftarrow H–4> - 0.127|L \leftarrow H–9> +$
			$0.118|L+1 \leftarrow H–9> - 0.219|L \leftarrow H–6> + 0.114|L+1 \leftarrow H–3> - 0.112|L+1 \leftarrow H> + \ldots$
	610	0.223	
3a	594	0.252	$+0.521|L \leftarrow H> + 0.437|L+1 \leftarrow H> + \ldots$
	496	0.283	$+0.535|L+1 \leftarrow H> - 0.445|L \leftarrow H> + \ldots$
	423	0.117	$+0.657|L+1 \leftarrow H–2> - 0.206|L \leftarrow H–1> - 0.107|L \leftarrow H–3> + \ldots$
	422	0.229	$+0.472|L+1 \leftarrow H–3> - 0.458|L \leftarrow H–3> - 0.125|L \leftarrow H–9> + \ldots$
			$+0.487|L \leftarrow H–3> + 0.456|L+1 \leftarrow H–3> - 0.107|L \leftarrow H–9> + 0.107|L+1 \leftarrow H–9> + \ldots$

3.6 Electrochemistry

Electrochemistry of the synthetic subporphyrazines were measured in *o*-dichlorobenzene. Due to the poor stability of push-pull porphyrazines in the solution state, the measurements were not proceeded well and CV curves of **2a**, **2b** and **2c** were shown in **Figure 3-26~3-28**.

Table 3-2. Electrochemical reduction potentials of **2a**, **2b** and **2c**, $E_{1/2}^{Red}$ versus Fc/Fc+ (in V) for the SubPzs studied in this work.

Sample name	$E_{1/2}^{Red1}$	$E_{1/2}^{Red2}$	$E_{1/2}^{Red3}$
2a[a]	-1.32 V	-1.70 V	-1.90 V
2b[a]	-1.27 V	-1.66 V	-1.80 V
2c[b]	-1.49 V	-	-

[a] Irreversible process of the oxidation parts (potential corresponds to the peak potential). [b] The compound **3c** decomposed soon during the measurement.

Figure 3-26 Cyclic voltammetry data for **2a**. Cyclic voltammograms were acquired from 1.0 mM solutions of analyte in 0.1M nBu₄NClO₄/**o**-DCB. Ferrocene was used as an internal standard and set to 0 V.

Figure 3-27 Cyclic voltammetry data for **2b**. Cyclic voltammograms were acquired from 1.0 mM solutions of analyte in 0.1M nBu₄NClO₄/**o**-DCB. Ferrocene was used as an internal standard and set to 0 V.
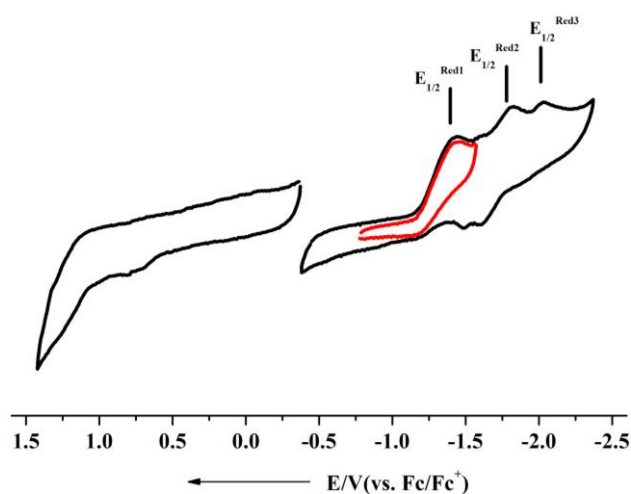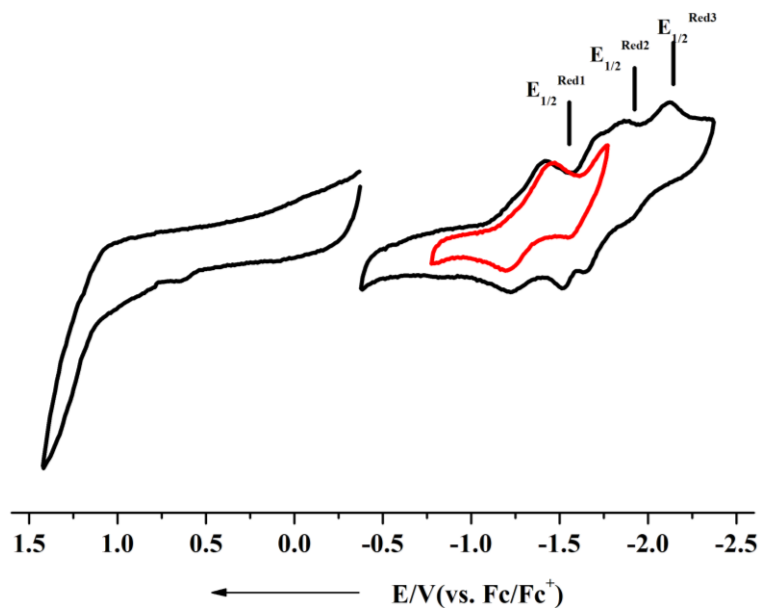

Figure 3-28 Cyclic voltammetry data for **2c**. Cyclic voltammograms were acquired from 1.0 mM solutions of analyte in 0.1M nBu₄NClO₄/**o**-DCB. Ferrocene was used as an internal standard and set to 0 V.
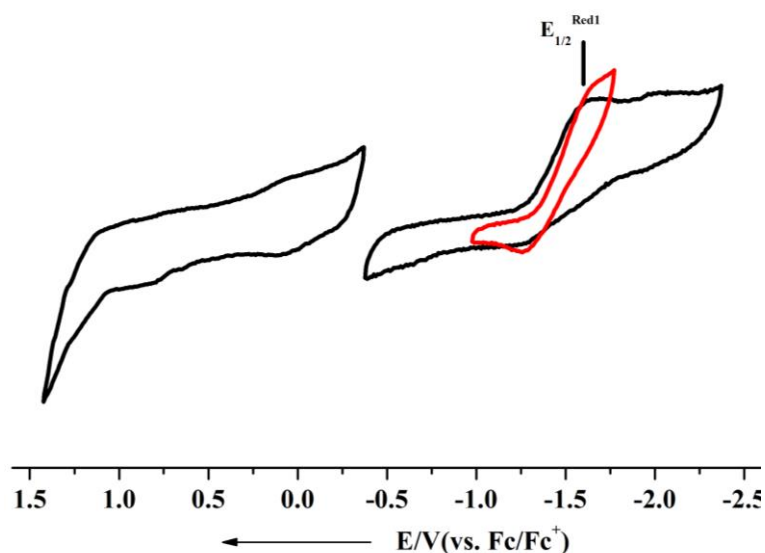
3.7 Summary

In this chapter, First examples of asymmetric push–pull SubPzs were successfully obtained via facile synthesis, and their diastereomers and enantiomers based on the arrangement of the peripheral substituents were also successfully separated.   Push-pull SubPz **2c** with strong electron withdrawing pull substituents exhibits main absorption band at the longer wavelength region at 571 nm (496 nm for regular SubPz).   Further introduction of electron donating push-substituent to subporphyrazine **2a** causes a further red-shift of the main absorption band, to 633 nm, due to the large perturbation of push-pull substituents.   The red-shift and broad range of the absorptions push-pull SubPzs can be controlled by electronic donating ability of peripheral push-substituents.

3.8 Reference

[1] a) Claessens, C. G.; Gonzlez-Rodrguez, D.; Torres, T.; *Chem. Rev.* **2002**, *102*, 835-853. b) Rio, Y.; Rodrguez-Morgade, M. S.; Torres, T.; *Org. Biomol. Chem.* **2008**, *6*, 1877-1894. c) Rahman, G. M. D. A.; Rodrguez-Morgade, M. S.; Caballero, E.; Torres, T.; Guldi, D. M. *ChemSusChem* **2009**, *2*, 330-335. d) Fukuda, T.; Kobayashi, N. *in handbook of porphyrin science,* Vol. 9 (Eds.: K. M. Kadishi, K. M. Smith, R. Guilard). e) Kobayashi, N. *in The Porphyrin Handbook*, Vol. 15: Synthesis and Spectroscopic Properties of Phthalocyanine Analogs (Eds.: K. M. Kadish, K. M. Smith, R. Guillard), Academic Press, San Diego, 2003, pp. 161-262;

[2] a) Rodrguez-Morgade, M. S.; Esperanza, S.; Torres, T.; Barber, J. *Chem. Eur. J.* **2005**, *11*, 354-360. b) Rodríguez-Morgade, M. S.; Claessens, C. G.; Medina, A.; González-Rodríguez, D.; Gutiérrez-Puebla, E.; Monge, A.; Alkorta, I.; Elguero, J.; Torres, T.; *Chem. Euro. J.* **2008**, *14*, 1342-1350. c) Higashino, T.; Rodrguez-Morgade, M. S.; Osuka, A.; Torres, T. *Chem. Eur. J.* **2013**, *19*, 10353-10359.

[3] Shimizu, S.; Otaki, T.; Yamazaki, Y.; Kobayashi, N. *Chem. Commun.* **2012**, *48*, 4100-4102.

[4] a) R. Stork, J. J. Brewer, T. Fukuda, J. P. Fitzgerald, G. T. Yee, A. Y. Nazarenko, N. Kobayashi, W. S. Durfee, *Inorg. Chem.* **2006**, *45*, 6148-6151. b) M. Hanack, *Tetrahedron Lett.*, **1995**, *36*, 1629. c) Kobayashi, N. *J. Am. Chem. Soc.*, **1999**, *121*, 9096

[5] a) Claessens, C. G.; Torres, T. *Tetrahedron Lett.* **2000**, 41, 6361-6365. b) Claessens, C. G.; Torres, T. *Chem. Eur. J.* **2000**, *6*, 2168-2172. c) Claessens, C. G.; Torres, T. *Eur. J. Org. Chem.* **2000**, *8*, 1603-1607.

[6] a) Shimizu, S.; Miura, A.; Khene, S.; Nyokong, T.; N. Kobayashi, *J. Am. Chem. Soc.* **2011**, *133*, 17322-17328; b) Higashibayashi, S.; Sakurai, H. *J. Am. Chem. Soc.* **2008**, *130*, 8592-8593.

[7] Sheldrick, G. M. SHELXL-97, Program for the Solution and Refinement of Crystal Structures, University of Göttingen, Göttingen, Germany, 1997.

[8] Gaussian 09, Revision A.02, Frisch, M. J.; Trucks, G. W.; Schlegel, H. B.; Scuseria, G. E.; Robb, M. A.; Cheeseman, J. R.; Scalmani, G.; Barone, V.; Mennucci, B.;

Petersson, G. A.; Nakatsuji, H.; Caricato, M.; Li, X.; Hratchian, H. P.; Izmaylov, A. F.; Bloino, J.; Zheng, G.; Sonnenberg, J. L.; Hada, M.; Ehara, M.; Toyota, K.; Fukuda, R.; Hasegawa, J.; Ishida, M.; Nakajima, T.; Honda, Y.; Kitao, O.; Nakai, H.; Vreven, T.; Montgomery, Jr., J. A.; Peralta, J. E.; Ogliaro, F.; Bearpark, M.; Heyd, J. J.; Brothers, E.; Kudin, K. N.; Staroverov, V. N.; Kobayashi, R.; Normand, J.; Raghavachari, K.; Rendell, A.; C. Burant, J.; Iyengar, S. S.; Tomasi, J.; Cossi, M.; Rega, N.; Millam, J. M.; Klene, M.; Knox, J. E.; Cross, J. B.; Bakken, V.; Adamo, C.; Jaramillo, J.; Gomperts, R.; Stratmann, R. E.; Yazyev, O.; Austin, A. J.; Cammi, R.; Pomelli, C.; Ochterski, J. W.; Martin, R. L.; Morokuma, K.; Zakrzewski, V. G.; Voth, G. A.; Salvador, P.; Dannenberg, J. J.; Dapprich, S.; Daniels, A. D.; Farkas, O.; Foresman, J. B.; Ortiz, J. V.; Cioslowski, J.; Fox, D. J. Gaussian, Inc., Wallingford CT, 2009.

[9] a) Mack, J.; Stillman, M. J.; Kobayashi, N. *Coord. Chem. Rev.* **2007**, *251*, 429–453. b) P. J. Stephens, *Adv. Chem. Phys.* **1976**, *35*, 197-264. c) Piepho, S. B.; Schatz, P. N. *Group Theory in Spectroscopy with Applications to Magnetic Circular Dichroism*, Wiley, New York, 1983. d) Kobayashi, N.; Muranaka, A.; Mack, J. *Circular Dichroism and Magnetic Circular Dichroism Spectroscopy for Organic Chemists*, RSC Publishing, 2012. e) Kobayashi, N.; Nakai K. *Chem. Commun.*, **2007**, 4077–4092.

Chapter IV

Synthesis and Properties of Push-Pull Type Porhyrazines

4.1 Introduction

Porphyrazine, the 18π aromatic compound which removal of four benzene rings from phthalocyanine (Pzs) which comprising for isoindole units bridged by imino-nitrogen atoms, the lower homologue of phthalocyanine. The benzo-abstraction of porphyrazine generally exhibits main absorption band at about 100 nm shorter wavelength region compared with regular phthalocyanine, at around 600 nm. In order to promote the chemistry of porphyrazine, control the spectroscopic properties of porphyrazine analogues are interesting, but structure modification of porphyrazines turned to be difficult.[1]

In 2014, A series of tetraazaporphyrin phosphorus(V) complexes with control the electronic structures by substituents effect has been published by N. Kobayashi in 2014. The strong electron-withdrawing phosphorus(V) ion perturbs the electronic absorption properties of TAP, while the absorption properties of the phthalocyanine phosphorus(V) complexes resemble those of metallated Pcs. Various peripheral substituents with different electron donating ablities can alter the position and intensity of the intense CT band lying between the Soret and Q bands.[2]
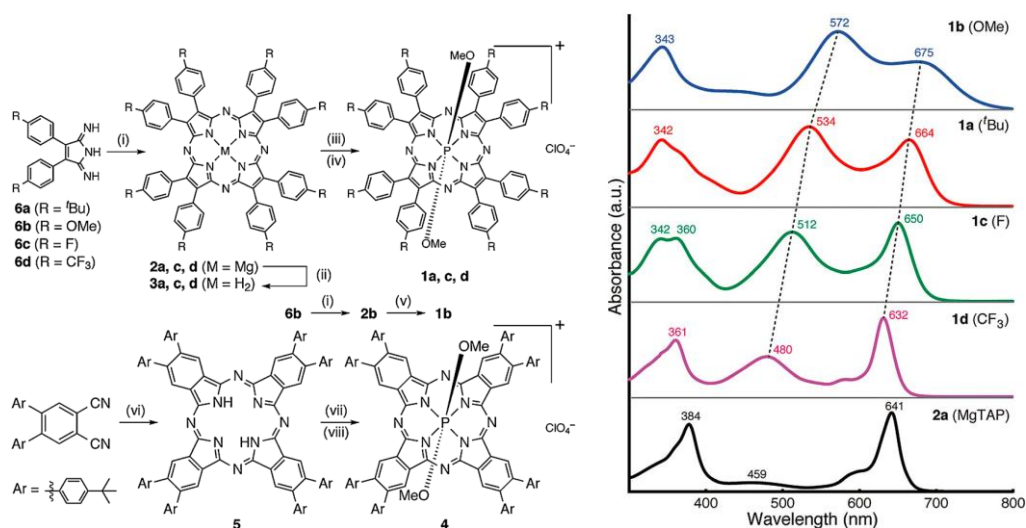

Figure 4-1 Synthesis and absorption spectra of P(V)porphyrazine

Considering introduction of electron donating (push-) and electron withdrawing (pull-) substituents have large contribution on the decrease of the gap between the HOMOs and the LUMOs, introduction of electron donating (push-) and electron

withdrawing (pull-) substituents to the porphyrazine core causes a significant red-shift of the main absorption band at 713 nm for C_{4h} push-pull type porphyrazine. As it is also described in the introduction part of this thesis, the control of porphyrinoid chromophore symmetry based on the positional isomerism of peripheral substituents has been achieved by preparing tetraazaporphyrins (TAPs) with C_{4h}, D_{2h}, C_{2v}, and C_s symmetry due to the relative arrangement of peripheral tert-butylamino and cyano groups as push and pull substituents, respectively.[3]
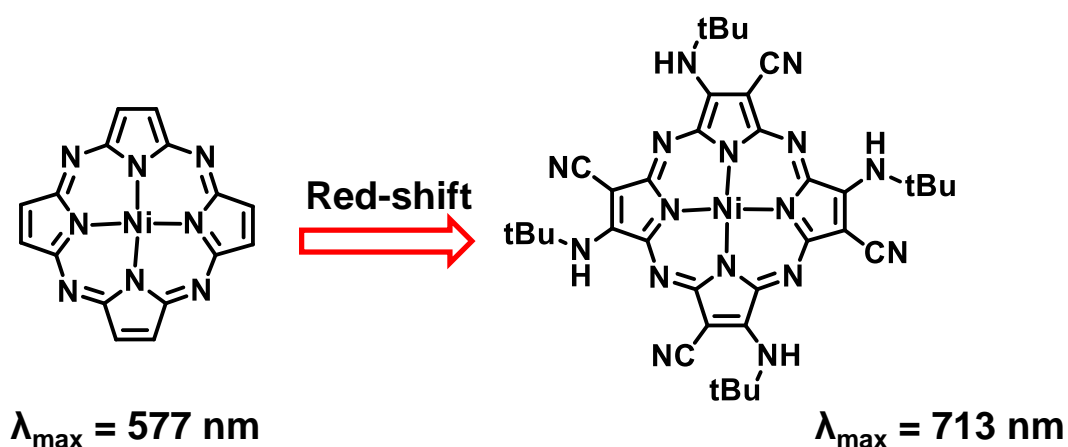

λ_max = 577 nm   **Red-shift**   **λ_max = 713 nm**

Figure 4-1 Molecular structure and spectroscopic data of regular Ni(II)porphyrazine and push-pull type Ni(II)porphyrazine.

4.2 Propose of This Research

Porphyrazine, an important conjugation decrease analogue derived from phthalocyanine, have been reported previously. The research interests on the design, synthesis, and investigations on the spectroscopic properties of porphyrazines are still growing. It is because of the porphyrazine analogues generally exhibit larger substituents induced tunable electronic structure. In addition to consider the introduction of electron donating (push-) and electron withdrawing (pull-) substituents have large contribution on the decrease of the gap between the HOMOs and the LUMOs, and research on the push-pull type diyprrins and subporphyrazines have been succeeded in this doctor thesis. In this chapter, the push-pull effect will be tested for porphyrazine analogues, and design, synthesis, properties will be described.
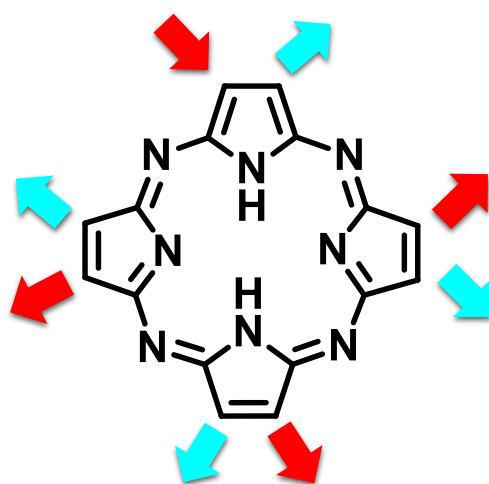
Push-Pull porphyrazine

**Push substituents**

Pull substituents

4.3 Experimental Section

4.3.1 Chemicals and Instruments

Electronic absorption spectra were recorded on a JASCO V-570 spectrophotometer. ^{1}H NMR spectra were recorded on a Bruker AVANCE 500 spectrometer (operating at 500.13 MHz) using the residual solvent as an internal reference for ^{1}H ($\delta = 7.26$ ppm for CDCl$_3$, $\delta = 5.32$ ppm for CD$_2$Cl$_2$). High resolution mass spectra were recorded on a Bruker Daltonics solariX 9.4T spectrometer. Preparative separations were performed by silica gel column chromatography (Merck Kieselegel 60H) and recycling preparative GPC-HPLC (JAI LC-9201 with preparative JAIGEL-2H, 2.5H, and 3.0H columns). All chemical reagents and solvents were of commercial reagent grade and were used without further purification except where noted.

4.3.2 Synthesis of 1-α-C$_8$H$_{17}$-bithiophene-1,2,2-tricyanoethylene

Regular porphyrazines generally exhibit the poor solubility similar like that of unsubstituted phthalocyanines, this is the limit of the synthesis and purification of porphyrazine analogues. In addition to introduce electron-rich substituents like thiophene and its derivatives, rationally design and synthesis a new aryl-tricyanoethylene as the key precursor of push-pull type porphyrazine synthesis.
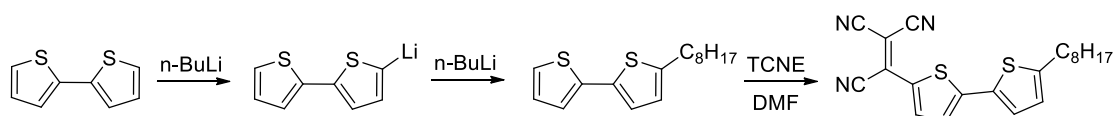
Scheme 4-1 Synthesis of 1-α-C$_8$H$_{17}$-bithiophene-1,2,2-tricyanoethylene

246 mg bithiophene was dissolved in 10 mL dehydrous THF and 0.7 mL n-BuLi solution was slowly added under N$_2$ at -78°C. The mixture was kept at -78oC for 30 min and moved to RT for 1h. 2 mL 1-bromooctane (over excess) was added at 0°C and stirred at RT overnight, the target compound was isolated from silica gel column using hexane to give the target compound. The freshly isolated n-C$_8$H$_{17}$-bithiophene was mixed with 2.0 eq of TCNE in a DMF solution, stirred at room

temperature for 2 days with absence of light. The mixture extracted from water and CHCl$_3$, washed by brine and further purification passed silica gel column to give the target compound. ^{1}H NMR (500 MHz, CDCl$_3$): δ = 7.96 (d, J = 5.0Hz, 1H), 7.36 (d, J = 5.0 Hz, 1H), 7.26 (d, J = 5.0Hz, 1H), 6.82 (d, J = 5.0 Hz, 1H), 2.84 (t, 2H), 1.70~1.66 (m, 2H), 1.36~1.26 (m, 10H), 0.86 (t, 3H); UV/vis (CHCl$_3$): λ_{max} [nm] (ε) = 527; MALDI-TOF-mass: m/z = 380.63 (Calcd. [M+H]$^+$ = 380.54).

4.3.3 Synthesis of push-pull type β-1-α-C$_8$H$_{17}$-bithiophene-β-cyano porphyrazine

Magnesium powder (24 mg, 1.0 mmol) was added to 1.5 mL freshly distilled 1-butanol, and a small piece of iodine was also added to clean the surface of magnesium. The mixture was stirred and heated at 150°C till the magnesium was completely dissolved in the 1-butanol, 1-α-C$_8$H$_{17}$-bithiophene-1,2,2-tricyanoethylene (190 mg, 0.5 mmol, 0.125 eq) was added. The mixture was heated again at 150°C for 3h longer with absence of light, after removal of solvent under vacuum, the black residue was obtained. The purification passed silica gel column chromatography (CH$_2$Cl$_2$), Bio-beads column (SX-1, CHCl$_3$) and finally purified by GPC-HPLC (CHCl$_3$). MALDI-TOF-mass: m/z = 1542.46 (Calcd. [M$^-$] = 1542.55); UV/vis (CHCl$_3$): λ_{max} [nm] (ε) = 755, 565, 340.
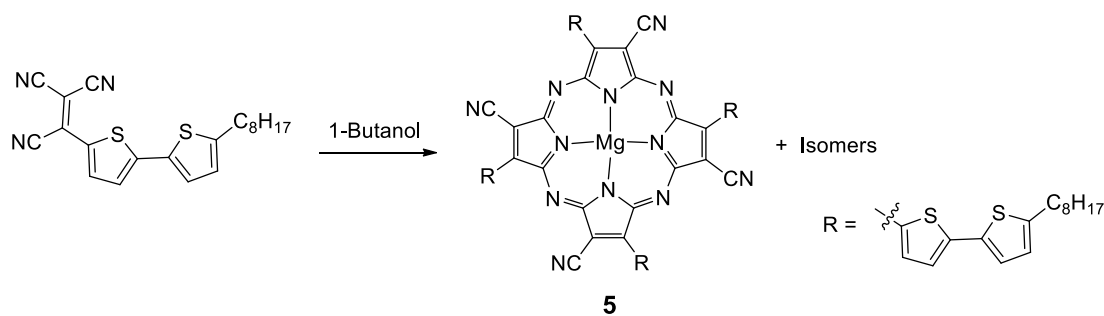
Scheme 4-2 Synthesis of push-pull type β-1-α-C$_8$H$_{17}$-bithiophene-β-cyano porphyrazine

4.4 Results and Discussions

4.4.1 Structural characterizations

The key precursor 1-α-C_8H_{17}-bithiophene-1,2,2-tricyanoethylene was characterized by both MALDI-TOF-mass and ^{1}HNMR spectra, but the measurement of push-pull porphyrazine was only succeeded in the case of MALDI-TOF-mass spectra measurement due to the difficulties in the purification.

In the case of key precursor 1-α-C_8H_{17}-bithiophene-1,2,2-tricyanoethylene, MALDI-TOF-mass spectra exhibits target peak at the m/z = 380.63 (Calcd. $[M+H]^+$ = 380.54) indicates the target compound was obtained. ^{1}HNMR spectra reveals for doublet peaks at δ = 7.96, 7.36, 7.26, 6.82 ppm indicates the di-substituted molecular structure.
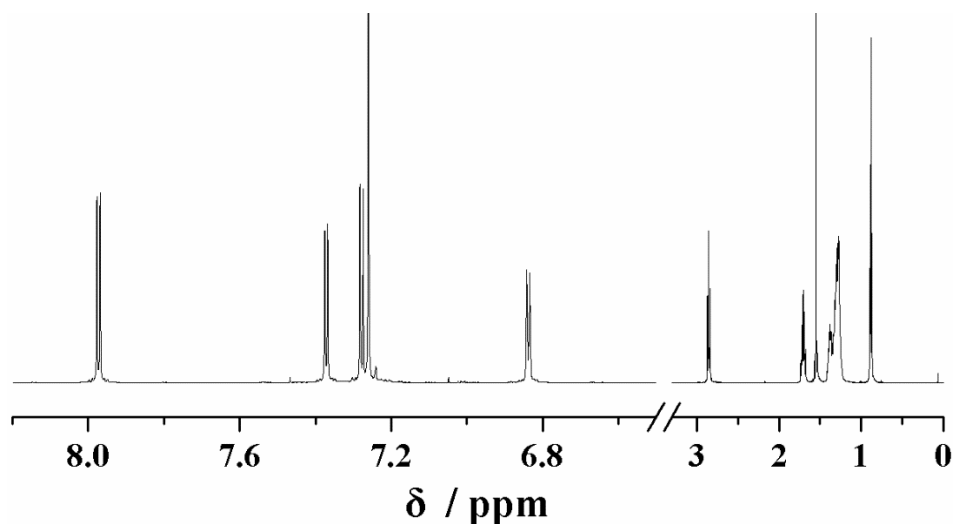

Figure 4-3 ^{1}HNMR spectra of 1-α-C_8H_{17}-bithiophene-1,2,2-tricyanoethylene in CDCl$_3$.

On the other hand, the MALDI-TOF-mass spectra of β-1-α-C_8H_{17}-bithiophene-β-cyano-porphyrazine 5 clearly revealed an intense anion peak at m/z = 1542.46 (Calcd. $[M^-]$ = 1542.55) indicates the target compound was obtained. Although the research on this topic was not succeeded on the NMR measurement, but MS result is the specific evidence that target compound was obtained.
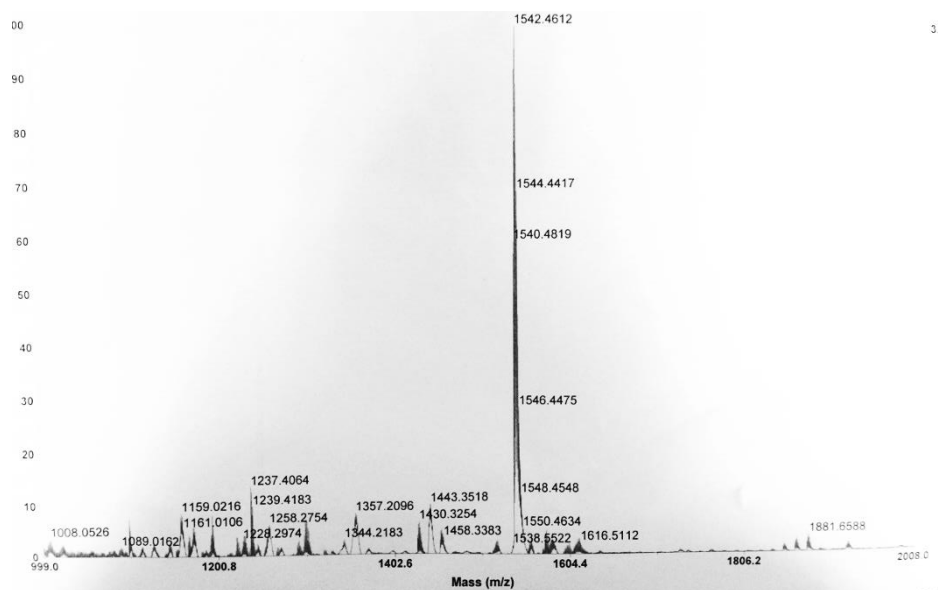
Figure 4-4 MALDI-TOF-mass spectra of push-pull porphyrazine.

4.4.2 Spectroscopic properties

The absorption spectra of key precursor 1-α-C_8H_{17}-bithiophene-1,2,2-tricyanoethylene with strong electron withdrawing tricyanoethylene unit exhibits the red-shift of main absorption band at λ_{max} = 527 nm compared with the regular bi-thiophene derivatives without this strong electron withdrawing unit.[4]
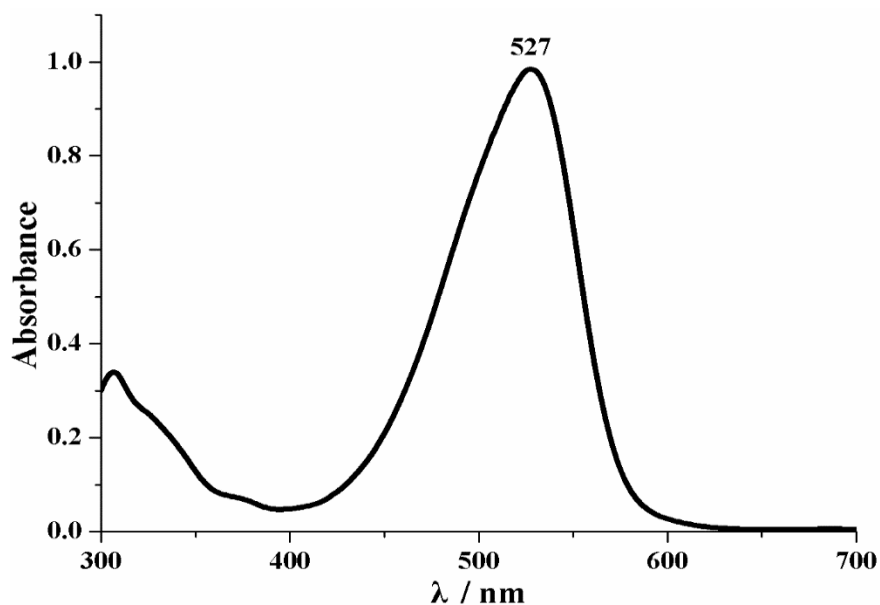

Figure 4-5 Absorption Spectra of 1-α-C_8H_{17}-bithiophene-1,2,2-tricyanoethylene.

In addition to investigate the spectroscopic properties of push-pull porphyrazine **5** by UV-vis absorption spectra, the main absorption band (Q-band) was appeared at 755 nm, soret band appears at 340 nm and an additional band appears at 565 nm. Compared with the regular porphyrazine (λ_{max} [nm] = 600), the significant red-shift of the main absorption band of push-pull type porphyrazine **5** (around 150 nm) can be explained as the large perturbation of push-pull substituents to the porphyrinic chromophores, and push-pull effect is one of the most effective strategies for the porphyrazine having main absorption band at the longer wavelength region.
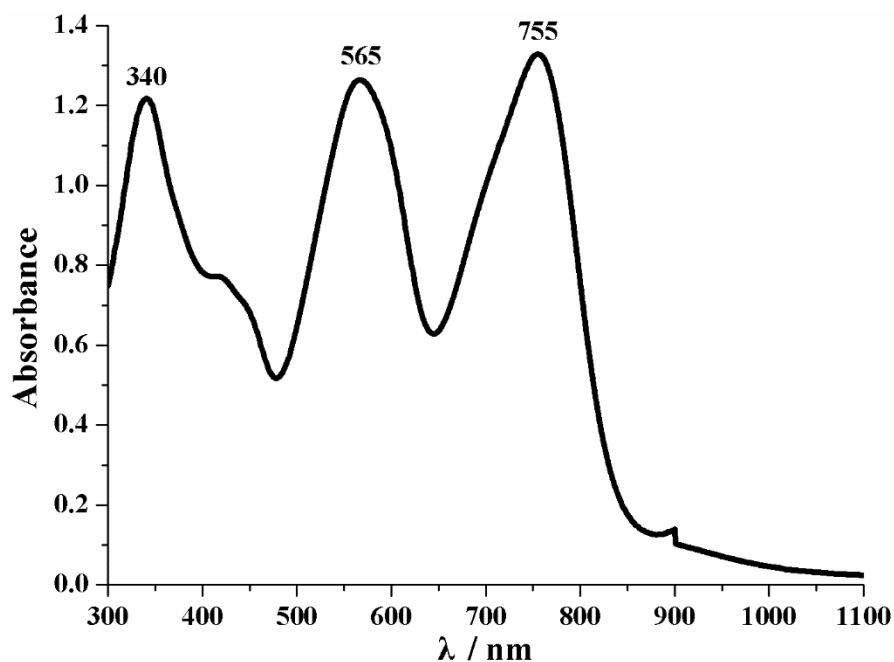
Figure 4-6 Absorption Spectra of push-pull porphyrazine.

4.5 Summary

In this chapter, the synthesis, purification, structural characterization, spectroscopic investigations of both push-pull type β-1-α-C_8H_{17}-bithiophene-β-cyano porphyrazine **5** and its key precursor 1-α-C_8H_{17}-bithiophene-1,2,2-tricyanoethylene were described.   The significant red-shift of the main absorption band appeared at 755 nm, and the broad range of the absorptions of push-pull porphyrazine **5** were observed. This result indicate the introduction of push-pull substituents to the porphyrazine core is an effective method for the red-shift of the main absorption band.

4.6 Reference

[1] a) Fukuda, T.; Kobayashi, N. *in handbook of porphyrin science,* Vol. 9 (Eds.: K. M. Kadishi, K. M. Smith, R. Guilard). b) Kobayashi, N. *in The Porphyrin Handbook*, Vol. 15: Synthesis and Spectroscopic Properties of Phthalocyanine Analogs (Eds.: K. M. Kadish, K. M. Smith, R. Guillard), Academic Press, San Diego, 2003. c) *Phthalocyanines: properties and applications*, Vol. 1 − 4 (Eds.: C. C. Leznoff, A. B. P. Lever), Wiley-VCH, New York, 1989–1996.

[2] Furuyama, T.; Yoshida, T.; Hashizume, D.; Kobayashi, N. *Chem. Sci.* **2014**, *5*, 2466-2474.

[3] a) Shimizu, S.; Haseba, Y.; Yamazaki, M.; Kumazawa, G.; Kobayashi, N. *Chem. Eur. J.* **2014**, *20*, 4822-4828**.** b) Kopranenkov, V. N.; Goncharova, L. S.; Luk'yanets, E. A. *Zh. Obshch. Khim.* **1979**, *49*, 1408 −1412.

Chapter V   Conclusion

This doctor thesis is focused on the design, synthesis and properties studies of new small conjugated push-pull chromophores including push-pull type dipyrrins, subporphyrazines, and porphyrazines. The electronic structures were studied by spectroscopy and further in-depth investigated by theoretical calculations. The main summarization of this thesis will be described in the following.

In the chapter II, push-pull type dipyrrins were successfully obtained via facile synthesis through dipyrromethane and tetracyanoethylene for the first time, and the electronic structures were studied by spectroscopic investigations and theoretical calculations. α-Tricyanovinyl-α-dicyanovinyl-dipyrrins **1** with expanded dipyrrin molecular structure, exhibits the marked red-shift and broad range of absorption, which tails beyond 640 nm. **1f** with a strong electron donating substituent N,N-dimethylaminophenyl unit at *meso*-position also exhibits an additional band at 476 nm, resulting the absorption band covered the whole visible region. α-Tricyanovinyl-dipyrrins **2** exhibit the size red-shift of main absorption band. **2f** with a strong electron donating substituent N,N-dimethylaminophenyl unit at *meso*-position exhibits the significant red-shift of the main absorption band to 655 nm.

In this chapter, First examples of asymmetric push–pull SubPzs were successfully obtained via facile synthesis by using aryl-tricyanoethylene as the key precursor Both diastereomers and enantiomers based on the asymmetric arrangement of the peripheral substituents were also successfully separated. Push-pull SubPz **2c** with strong electron withdrawing pull substituents exhibits main absorption band at the longer wavelength region at 571 nm (496 nm for regular SubPz). Further introduction of electron donating push-substituent to subporphyrazine **2a** causes a further red-shift of the main absorption band, to 633 nm, due to the large perturbation of push-pull substituents. The red-shift and broad range of the absorptions push-pull SubPzs can be controlled by electronic donating ability of peripheral push-substituents.

In this chapter, the synthesis, purification, structural characterization, spectroscopic investigations of both push-pull type β-1-α-C_8H_{17}-bithiophene-β-cyano porphyrazine **5** and its key precursor 1-α-C_8H_{17}-bithiophene-1,2,2-tricyanoethylene were described. The significant red-shift of the main absorption band appeared at 755

nm, and the broad range of the absorptions of push-pull porphyrazine **5** were observed. This result indicate the introduction of push-pull substituents to the porphyrazine core is an effective method for the red-shift of the main absorption band.

In summary, this doctor thesis described the synthesis, properties, theoretical calculations of a series of push-pull type porphyrinic chromophores, including push-pull type dipyrrins, subporphyrazines and porphyrazines. Electronic structures were studied by the spectroscopic investigations and theoretical calculations. Considering small conjugated molecule with red-shift and broader range of the absorptions have potential applications in various fields, the chromophores studied in this thesis may offer useful information for future molecular design, electronic studies and even their applications in various high-tech fields.

Acknowledgements

I herein show my heartfelt gratitude and warm appreciation to all of the people who encouraged me and provided kindness in the completion of this doctor thesis, and throughout my life in Japan during past five years, especially after the Tohoku great earthquake in 2011. All of experience including my academic attitude, basic chemistry theories, experimental skills and manuscripts preparation, that will play essential roles in my future academic research.

Firstly, I would like to express my thanks to my kind supervisor, Prof. Dr. Nagao Kobayashi. He gave me a lot of useful suggestions during the period of application and examination. He bring me to the phthalocyanine chemistry world and introduce several important things from beginning. It has been a great privilege and honor to study under his guidance and supervision. Since Prof. Dr. Nagao Kobayashi will retire from 2015, this doctor thesis also dedicates on his 65th years birthday and happy retirement.

Secondly, I would like thank Associate Prof. Dr. Soji Shimuzu. He gave me a lot of personal instruction for improving my basic theories and experimental skills, which played a significant role in the past years study in Tohoku University. His suggestions were always fruitful and accurate. He also helped me a lot in my daily life from the first day I met him at Sendai airport. It is my pleasure that I can finish my experiments and master and doctor thesis under his direction.

The third but no less appreciation is dedicated to Prof. Dr. Li-Min Zheng from NanJing University. Her suggestions and encouragements also played an essential role in the period of my study and life in Japan. I especially thank her for their help in my application to the Tohoku University master&doctor program, and the time I carried out some experiments at NanJing University after the Tohoku great earthquake in 2011.

Also, I would like thank Prof. Dr. Wei-Hua Zhu in JiangSu University. Thank you very much for inviting me join your group for my future scientific research. I hope we can produce very nice results in the future scientific research.

Finally, I would like thank Prof. Dr. Zhen Shen (Nanjing University, China), Prof. Dr. Fu-you Li (Fudan University, China), Prof. Tebello Nayokon (Rhodes University,

South Africa) for their kind collaboration.

I would also like to express my best wishes to other previous and current staffs in our laboratory, including associate Prof. Dr. Hua Lu (Hanzhou Nomal University, China), Dr. John Mack (Rhodes University, South Afirca), Dr. Taniyuki Furuyama, and the secretaries in our laboratory Ms. Shono Naomi and Suzuki Madoka. Thanks to all students in Kobayashi's laboratory, including: Dr. Hashimoto Naoaki, Dr. Matsushita Osamu, Dr. Zhu hua, Dr. Kikukawa Yu, Dr. Sugita Ippei, Ito Yuki, Uemura Kaoru, Takaishi Shiori, Oniwa kazuaki, Miura Yoshiaki, Miura Akito, Thiago Teixeira Tasso, Abe Koji, Endo Takahiro, Otaki Tatsuya, Sato Koh, Sato Yuta, Nakano Shota, Iino Taku, Emura Natsuko, Ogura Yosuke, Kushiya Tomohumi, Murata Agato, Yamazaki Yoko, Kojima Ayaka, Sugiya Yusuke, Noguti Daiki, Haryyama Takuya, Harako Ryosuke, Hirokawa Shoma, Murayama Ai, Yosida Takuya, Asai Mitsuo, Kuronuma Makoto, Shiina Yuta, Shitanda Sho, Suzuki Yuta, Takahasgi Yuichi, Iizuka humiya, Sato Takehiko, Shimooka Chihiro, Tamada, Masamichi, Wada kousuke, Nakamura Ryo, Hukuda Shintaro.

I also want to express my best wishes to Dr. Quan Liu, Dr. Han-zhuang Liu, and Dr. Yong-chao Yang, Dr. Xing-Yu Qu from NanJing University, China, who were staying in Tohoku University during the period of my study in Tohoku University.

Finally, I would like to express my sincere thanks and appreciation to my parents and wife for their encouragement and support from all of my living in Japan during the past years. Their suggestions covered all of my study periods, which allow me to remain optimistic for the upcoming Doctor course.

<div align="right">Xu LIANG

Feb., 2015; Sendai, Japan</div>